- 1 Caulobacter lipid A is conditionally dispensable in the absence of fur and the
- 2 presence of a novel anionic sphingolipid

3

- 4 Justin J. Zik<sup>1,12</sup>, Sung Hwan Yoon<sup>2,13</sup>, Ziqiang Guan<sup>3</sup>, Gabriele Stankeviciute Skidmore<sup>4,11</sup>, Ridhi
- 5 R. Gudoor<sup>5,6</sup>, Karen M. Davies<sup>5,6,14</sup>, Adam M. Deutschbauer<sup>7</sup>, David R. Goodlett<sup>2,8,9</sup>, Eric A.
- 6 Klein<sup>4,10,11</sup> and Kathleen R. Ryan<sup>1,7,\*</sup>

7

- <sup>1</sup>Department of Plant & Microbial Biology, University of California, Berkeley, Berkeley, CA 94720
- 9 USA
- <sup>2</sup>Department of Microbial Pathogenesis, University of Maryland School of Dentistry, Baltimore,
- 11 MD 21201 USA
- <sup>3</sup>Department of Biochemistry, Duke University Medical Center, Durham, NC 27710
- 13 <sup>4</sup>Center for Computational and Integrative Biology, Rutgers University-Camden, Camden, NJ
- 14 08102 USA
- 15 Molecular Biosciences and Integrated Bioimaging Division, Lawrence Berkeley National
- 16 Laboratory, Berkeley, CA 94720 USA
- 17 <sup>6</sup>Department of Molecular and Cell Biology, University of California, Berkeley, Berkeley, CA
- 18 94720 USA
- <sup>7</sup>Environmental Genomics & Systems Biology Division, Lawrence Berkeley National Laboratory,
- 20 Berkeley, CA 94720 USA
- <sup>8</sup>Department of Biochemistry & Microbiology, University of Victoria, Victoria, BC V8W 2Y2
- 22 Canada
- <sup>9</sup>University of Victoria-Genome BC Proteomics Centre, Victoria, BC V8Z 7X8 Canada
- <sup>10</sup>Biology Department, Rutgers University-Camden, Camden, NJ 08102 USA
- <sup>11</sup>Rutgers Center for Lipid Research, Rutgers University, New Brunswick, NJ 08901 USA
- 26 <sup>12</sup>present address: Infectious Diseases Translational Research Programme, Department of
- 27 Microbiology and Immunology, Yong Loo Lin School of Medicine, National University of
- 28 Singapore, Singapore 117545, Singapore
- 29 <sup>13</sup>present address: National Institute of Allergy and Infectious Diseases, Bethesda, MD 20892-
- 30 0421 USA
- 31 <sup>14</sup>present address: Diamond Light Source Ltd. Harwell Science & Innovation Campus, Didcot,
- 32 Oxfordshire, OX11 0DE, UK

33

\*Correspondence: krr@berkeley.edu

- 36 ORCID: Kathleen R. Ryan, 0000-0003-3657-8069; Justin J. Zik, 0000-0003-0260-2446; Eric A.
- 37 Klein, 0000-0003-3941-6233, Karen M. Davies, 0000-0002-3207-9337; David R. Goodlett,
- 38 0000-0002-8045-8200

## Summary

Lipid A, the membrane-anchored portion of lipopolysaccharide (LPS), is an essential component of the outer membrane (OM) of nearly all Gram-negative bacteria. Here, we identify regulatory and structural factors that together render lipid A nonessential in *Caulobacter crescentus*. Mutations in the ferric uptake regulator *fur* allow *Caulobacter* to survive in the absence of either LpxC, which catalyzes an early step of lipid A synthesis, or CtpA, a tyrosine phosphatase homolog which we find is needed for wild-type lipid A structure and abundance. Alterations in Fur-regulated processes, rather than iron status *per se*, underlie the ability to survive when lipid A synthesis is blocked. Fitness of lipid A-deficient *Caulobacter* requires a previously uncharacterized anionic sphingolipid, ceramide phosphoglycerate (CPG), which also mediates sensitivity to the antibiotic colistin. Our results demonstrate that, in an altered regulatory landscape, anionic sphingolipids can support the integrity of a lipid A-deficient OM.

## Introduction

Gram-negative bacteria are enclosed in a three-layer envelope, composed of the inner or cytoplasmic membrane (IM), a thin layer of peptidoglycan (PG), and an outer membrane (OM). The OM is an asymmetric bilayer, with phospholipids populating the inner leaflet and lipopolysaccharide (LPS) predominating in the outer leaflet. The canonical LPS structure, first described in *Escherichia coli*, consists of three segments: 1) lipid A, a hexa-acylated, phosphorylated glucosamine disaccharide anchored in the membrane; 2) a core oligosaccharide usually shared by members of the same species; and 3) a repeating polysaccharide (O-antigen) which can vary highly among strains of the same species (Whitfield and Trent, 2014). LPS confers robust barrier function upon the OM, making it inherently less permeable than the IM to small hydrophobic compounds (Nikaido, 2003).

Although the O-antigen and core polysaccharide are nearly always dispensable, it is widely accepted that the lipid A portion of LPS is essential for the viability of Gram-negative bacteria. Some exceptions to this rule are species that possess a dual membrane system but naturally lack lipid A, such as *Sphingomonas spp.* and the spirochetes *Borrelia burgdorferi* and *Treponema pallidum* (Kawahara et al., 1991; Kawasaki et al., 1994; Radolf and Kumar, 2018). Efforts to eliminate lipid A from *E. coli* strains have demonstrated that the intermediate molecule lipid IV<sub>A</sub> is sufficient for viability, but only if the strain also has compensatory mutations that promote the export of this species across the IM (Mamat et al., 2008; Meredith et al., 2006). To

date, lipid A-deficient mutants have been recovered in *Neisseria meningitidis*, *Moraxella catarrhalis*, and *Acinetobacter baumannii* (Moffatt et al., 2010; Peng et al., 2005; Steeghs et al., 1998). It remains unclear why at least a minimal lipid A structure is essential in some Gramnegative bacteria but not others.

Lipid A is synthesized by the highly conserved Raetz pathway (Whitfield and Trent, 2014), yet significant variation exists in lipid A structures. In many species, mechanisms exist to modify the 1- and 4'-phosphates of lipid A to decrease its negative charge and reduce susceptibility to cationic antimicrobial peptides (Moffatt et al., 2019). In a few species, replacement of the 1- and/or 4'-phosphates of lipid A with sugars is constitutive (De Castro et al., 2008; Plötz et al., 2000). The predominant lipid A species in the alphaproteobacterium *Caulobacter crescentus* (Smit et al., 2008) varies from that of *E. coli* (Qureshi et al., 1988) in that the central glucosamine disaccharide is replaced by two 2,3-diamino-2,3-dideoxy-D-glucopyranose (GlcN3N) residues, and the 1- and 4'-phosphates are replaced by galactopyranuronic acid (GalpA) residues.

The tyrosine phosphatase homolog ctpA (for  $\underline{C}$  aulobacter  $\underline{t}$  yrosine  $\underline{p}$  hosphatase  $\underline{A}$ ) is essential for viability and is implicated in cell envelope maintenance, but its molecular function remains unknown (Shapland et al., 2011). Depletion of ctpA causes extensive OM blebbing, failure to resolve PG at the division site, and cell death. Here, we show that ctpA is required for the wild-type structure and abundance of lipid A. A screen for suppressors of ctpA essentiality recovered strains with null mutations in the O-antigen biosynthetic pathway or in the ferric uptake regulator fur. Surprisingly, mutations in fur also permitted the deletion of lpxC, which encodes an otherwise essential enzyme catalyzing the first committed step in lipid A synthesis.  $\Delta ctpA$  and  $\Delta lpxC$  strains containing suppressor mutations have significantly reduced or undetectable levels of lipid A, respectively.

To identify mechanisms that promote survival in the absence of lipid A, we used random barcode-transposon site sequencing (RB-Tnseq) to identify genes important for fitness when lipid A synthesis is chemically inhibited. Interestingly, we obtained several hits in genes required for sphingolipid synthesis in *Caulobacter* (Stankeviciute et al., 2019, 2021). Since *Sphingomonads* naturally lack LPS and bear anionic sphingolipids on the cell surface (Kawasaki et al., 1994), we hypothesized that anionic sphingolipids could support viability in the *Caulobacter ΔlpxC* strain. Indeed, we identified a previously unknown sphingolipid species, ceramide phosphoglycerate, which is produced in wild-type cells and is a critical fitness factor in the absence of lipid A. Further, we found that ceramide phosphoglycerate, rather than LPS, underlies *Caulobacter*'s sensitivity to the cationic antimicrobial peptide colistin.

#### Results

Suppressor mutations affecting fur or O-antigen synthesis permit the loss of ctpA

We used a CtpA depletion strain developed in a prior study to identify mutations that would support *Caulobacter* viability in the absence of CtpA (Shapland et al., 2011). Regulated depletion of CtpA in KR3906 is achieved by expressing *ctpA::3xFLAG::ssrA* from a xylose-inducible promoter (Meisenzahl et al., 1997) on a high-copy plasmid in a Δ*ctpA* strain also lacking the proteolytic adaptor *sspB* (Levchenko et al., 2000). The native CtpA protein could not be depleted without an ssrA tag to target it for proteolysis. However, addition of this tag made CtpA proteolysis so rapid that xylose-dependent expression of CtpA-3xFLAG-ssrA did not support viability. Further deleting *sspB*, which encodes a proteolytic adaptor for ssrA-tagged substrates, reduced the basal rate of CtpA-3xFLAG-ssrA degradation enough to permit complementation in xylose-supplemented PYE medium (PYEX).

When depleting CtpA by transferring cells from PYEX to dextrose-supplemented PYE medium (PYED), KR3906 exhibits division defects, significant OM blebbing, and death (**Fig. 1**). We UV-mutagenized KR3906, plated on solid PYED medium to deplete CtpA, and grew the recovered colonies in PYED liquid medium to allow loss of the plasmid bearing *ctpA*. Isolates cured of the plasmid were identified via chloramphenicol sensitivity and the inability to PCR-amplify *ctpA* (**Fig. 1A**). Genome resequencing of 17 confirmed suppressors yielded 15 strains with mutations in nine genes predicted to participate in O-antigen biosynthesis, one strain with a single mutation in *fur*, encoding the ferric uptake regulator, and one strain harboring a mutation in *fur* along with a mutation in an O-antigen biosynthetic gene (**Table S1**). Although individual strains sometimes contained point mutations in other genes, every suppressor strain harbored a mutation predicted to affect either O-antigen synthesis or Fur. Due to the frequent occurrence of frameshift or nonsense mutations, we assumed that each mutation disrupted the function of the affected gene.

We chose for further analysis candidate suppressor genes whose functions were well-established in *Caulobacter* or other bacteria. *CCNA\_00497* encodes a predicted glycosyltransferase transferase necessary for wild-type levels of smooth LPS (S-LPS) containing the O-antigen in *Caulobacter* (Hershey et al., 2019). *CCNA\_01553* encodes a glycosyltransferase which initiates O-antigen synthesis on undecaprenyl-phosphate (Toh et al., 2008). *CCNA\_03733* encodes a homolog of *manC* involved in synthesizing the activated sugar GDP-D-mannose (Samuel and Reeves, 2003), which is present in the core oligosaccharide and O-antigen of *Caulobacter* S-LPS (Jones et al., 2015). *CCNA\_00055* encodes the iron-

responsive transcriptional regulator Fur (da Silva Neto et al., 2009) and is predicted to be functionally distinct among the genes harboring suppressor mutations. We deleted each gene in the wild-type background (NA1000) or in combination with  $\Delta sspB$ , but we were unable to subsequently delete ctpA in these strains by double homologous recombination. Therefore, we individually deleted these genes in the CtpA depletion strain KR3906 while propagating the strains on PYEX to supply CtpA.

To determine how each deletion affects cells during acute CtpA depletion, we shifted each mutant onto liquid or solid PYED medium and observed cell morphology and viability (**Fig. 1**). Compared to CtpA depletion in KR3906, depletion of CtpA in the Δ*fur* mutant caused much less OM blebbing, but still yielded elongated cells indicative of a division defect (**Fig. 1C**). Surprisingly, neither OM blebbing nor cell chaining/elongation was markedly improved when CtpA was depleted from the strains lacking *CCNA\_00497*, *CCNA\_01553*, or *CCNA\_03733*. Despite the persistence of one or more morphological defects, deletion of *fur*, *CCNA\_01553*, or *CCNA\_03733* significantly improved cell viability during CtpA depletion on solid PYED (**Fig. 1B**). The deletion of *CCNA\_00497* improved survival on PYED to a lesser extent, despite the fact that two independent strains with point mutations in *CCNA\_00497* were isolated in the suppressor screen. Notably, each strain with a mutation in *CCNA\_00497* also harbored 1-2 other mutations (**Table S1**), which may have augmented the fitness of the original isolates.

We acquired stable, suppressed  $\Delta ctpA$  mutants by passaging each modified CtpA depletion strain (above) in PYED medium, plating on solid PYED medium, and screening viable colonies for loss of the ctpA-bearing plasmid. The OM of each stable  $\Delta ctpA$  strain was smooth with minimal blebbing, but chains of cells were still prevalent in the  $\Delta ctpA$   $\Delta sspB$   $\Delta CCNA\_01553$  and  $\Delta ctpA$   $\Delta sspB$   $\Delta fur$  mutants (**Fig. 1D**). The reconstituted suppressor strains were morphologically similar to the original isolates containing point mutations in the same genes (**Fig. S1A**). Suppressed  $\Delta ctpA$  mutants grew more slowly than the wild-type strain NA1000 and the corresponding  $ctpA^+$  strains, but all achieved similar stationary phase densities in PYE medium (**Fig. S1B**). As expected, restoring the expression of fur,  $CCNA\_00497$ , or  $CCNA\_03733$  using a xylose-inducible promoter reduced the viability of each corresponding stable  $\Delta ctpA$  strain (**Fig. S1C**). Thus, null mutations affecting fur or O-antigen biosynthesis allow Caulobacter to survive in the absence of ctpA.

It was puzzling that we could not obtain the strains  $\triangle ctpA$   $\triangle CCNA\_00497$ ,  $\triangle ctpA$   $\triangle CCNA\_1553$ ,  $\triangle ctpA$   $\triangle CCNA\_03733$ , or  $\triangle ctpA$   $\triangle fur$  (with or without  $\triangle sspB$ ) by double homologous recombination, yet they were accessible by depleting CtpA and curing the ctpA covering plasmid. A key difference between these two procedures is that double homologous

recombination relies on sacB counterselection, where the desired mutants must survive on medium containing 3% sucrose. Unlike the parent  $\Delta fur \Delta sspB$  strain, the  $\Delta ctpA \Delta fur \Delta sspB$  strain displayed a growth defect on PYE medium containing sucrose (**Fig. S1D**), indicating that  $\Delta ctpA$  confers susceptibility to sucrose, which likely accounts for the discrepancy between the two genetic methods.

To confirm the functions of CCNA 00497, ΔCCNA 01553, and CCNA 03733 in Oantigen synthesis, we deleted individual genes in a strain lacking sspB. Whole-cell lysates treated with proteinase K were probed with antibodies recognizing S-LPS (Fig. S2A) or stained with Pro-Q Emerald 300 to detect carbohydrates (Fig. S2B). As previously observed, strains lacking CCNA 01068 (wbgA) or CCNA 01553 lacked S-LPS, while ΔCCNA 000497 contained reduced amounts of S-LPS, which migrates as a single high-molecular weight species in Caulobacter (Walker et al., 1994; Awram and Smit, 2001; Hershey et al., 2019). Deletion of CCNA 03733 (manC) eliminated S-LPS and reduced the size of a species that we propose to be lipid A + core polysaccharide (Fig. S2B-C, \*\*). The core oligosaccharide of Caulobacter LPS contains a single penultimate mannose residue (Jones et al., 2015); thus, the reduced size of the indicated band for ΔCCNA\_03733 (Fig. S2B and S2C, \*) may arise from an incomplete core oligosaccharide. S-LPS was restored to each mutant by xylose-driven complementation of the respective genes (Fig. S2C). In contrast to strains with mutations in CCNA 00497, CCNA 01553, or CCNA 03733, the Δfur ΔsspB mutant contained wild-type levels of S-LPS (Fig. S2A-B), indicating that fur mutations do not suppress the lethality of  $\Delta ctpA$  by eliminating the O-antigen.

 $\Delta$ ctpA and  $\Delta$ lpxC strains containing suppressor mutations contain little or no lipid A

ctpA is transcribed divergently from an operon containing msbA, lpxJ, kdtA, and lpxK (Zhou et al., 2015), which in other bacteria participate in the synthesis and export of lipid A + core polysaccharide (Whitfield and Trent, 2014). Like ctpA, these genes are essential for Caulobacter viability (Christen et al., 2011). Since CtpA depletion results in OM defects, and suppressor mutations were identified in O-antigen biosynthetic genes, we hypothesized that ctpA is required for some aspect of LPS synthesis or export.

We performed hot aqueous-phenol extraction of LPS from suppressor mutants lacking ctpA, along with their  $ctpA^+$  counterparts, and analyzed them by PAGE and Pro-Q Emerald 300 staining. As expected, full-length S-LPS was recovered from NA1000,  $\Delta sspB$ , and  $\Delta fur \Delta sspB$  (**Fig. 2B**, \*\*\*), but was absent from  $\Delta sspB$  strains lacking  $CCNA\_00497$ ,  $CCNA\_01553$ , or  $CCNA\_03733$ . Interestingly, all  $\Delta ctpA$  strains were deficient in low-molecular weight species

that could represent lipid A +/- core oligosaccharide (**Fig. 2B**). We therefore used the Limulus Amebocyte Lysate (LAL) assay to measure lipid A abundance in live *Caulobacter* strains. All  $\Delta ctpA$  mutants contained ~1,000-fold less lipid A than strains encoding this gene (**Fig. 2A**).

Since Δ*ctpA* suppressor mutants could survive with drastically reduced amounts of lipid A, we asked if mutations in *fur* or O-antigen synthesis could render lipid A completely dispensable. LpxC catalyzes the first committed step in lipid A synthesis, removal of the 2-acetyl group from acylated UDP-GlcNAc (Whitfield and Trent, 2014). The *lpxC* homolog *CCNA\_02064* is essential for viability in wild-type *Caulobacter* (Christen et al., 2011). We constructed an LpxC depletion strain (KR4007) analogous to the CtpA depletion strain. We subsequently deleted *fur*, *CCNA\_00497*, *CCNA\_01553*, or *CCNA\_03733* in this strain and examined the effects of acute LpxC depletion during growth in PYED. When these O-antigen synthesis genes and *fur* were intact, LpxC depletion yielded chains of cells with extensive membrane blebs. Cells lacking a gene for O-antigen synthesis still showed OM blebs and chaining when LpxC was depleted (**Fig. 3A**). Cells lacking *fur* had far fewer OM blebs upon LpxC depletion but were still frequently elongated or chained (**Fig. 3A**). These morphologies are generally similar to those seen during CtpA depletion, but unlike CtpA, only Δ*fur* allowed significant growth of the LpxC depletion strain on solid PYED medium (**Fig. 3B**).

When we attempted to isolate stable  $\Delta lpxC$  mutants by depleting LpxC and curing the covering plasmid, only the strain harboring a  $\Delta fur$  mutation permitted complete loss of lpxC (KR4103). Importantly, we recovered two stable  $\Delta lpxC$  isolates (KR4224 and 4225) from an LpxC depletion strain harboring only  $\Delta CCNA\_00497$  and not  $\Delta sspB$  (KR4223), but genome resequencing revealed that they had acquired additional point mutations in fur (**Table S2**). Together, these results indicate that fur mutations are necessary to render  $\Delta lpxC$  inessential, and that deletion of sspB is not required for the viability of  $\Delta lpxC$  cells. As in  $\Delta ctpA$   $\Delta fur$   $\Delta sspB$ , the stable  $\Delta lpxC$   $\Delta fur$   $\Delta sspB$  mutant still formed chains (**Fig. 1D**), and xylose-driven fur expression induced lethality in this strain (**Fig. 3C**).

Background levels of lipid A were detected in  $\Delta lpxC$   $\Delta fur$   $\Delta sspB$  cells in the LAL assay (**Fig. 2A**), strongly suggesting that lipid A is absent. To corroborate this result, we extracted LPS species by three distinct methods, separated them by PAGE, and stained with Pro-Q Emerald 300. Hot aqueous-phenol extracts of  $\Delta lpxC$   $\Delta fur$   $\Delta sspB$  cells were deficient in S-LPS and putative lipid A +/- core species (**Fig. 2B**). However, unknown carbohydrate-containing species were extracted by this method. Extraction of free lipid A (El Hamidi et al., 2005) revealed that a species of ~1800 Da, consistent with the mass of *Caulobacter* lipid A (Smit et al., 2008), is present in NA1000 but absent from  $\Delta lpxC$   $\Delta fur$   $\Delta sspB$  (**Fig. 2C, left**). Again, however,

unidentified carbohydrate species were present in these extracts. Lastly, the method of Darveau and Hancock (Darveau and Hancock, 1983) yielded a single rough LPS species which was present in NA1000 and absent from  $\Delta lpxC$   $\Delta fur$   $\Delta sspB$  (**Fig. 2C, right**); this method resulted in no unidentified contaminants. Although some *Caulobacter* extracts contain unidentified lipids, these assays together strongly imply that lipid A is absent from the  $\Delta lpxC$   $\Delta fur$   $\Delta sspB$  mutant. Xylose-driven expression of lpxC or ctpA restored the production of lipid A-containing species to  $\Delta lpxC$   $\Delta fur$   $\Delta sspB$  or  $\Delta ctpA$   $\Delta CCNA$  03733  $\Delta sspB$ , respectively (**Fig. 2D**).

Lipid A extracts from Δ*ctpA* Δ*fur* Δ*sspB*, Δ*lpxC* Δ*fur* Δ*sspB*, and control strains were further analyzed by matrix-assisted laser desorption/ionization tandem mass spectrometry (MALDI-MS/MS). Wild-type NA1000, Δ*sspB*, and Δ*fur* Δ*sspB* extracts contained predominantly the full-length lipid A (*m*/*z* 1874, (Smit et al., 2008) and lesser amounts of an ion at *m*/*z* 1858 that differs from 1874 by 16 *m*/*z*, consistent with the absence of one hydroxyl group (**Fig. S3A-C**). MALDI-MS analyses of lipid A extracts from Δ*ctpA* Δ*fur* Δ*sspB* cells revealed no ions consistent with full-length *Caulobacter* lipid A, but identified ions at *m*/*z* 1682 and *m*/*z* 1486 (**Fig. S3D**) that appeared to be missing the Gal*p*A residues at the 1 and 4' positions. Tandem MS analysis of these ions revealed losses of mass consistent with the loss of phosphates, as would be expected for the dissociation of canonical, phosphate-bearing lipid A structures. Although additional characterization is needed, our results suggest that *Caulobacter* mutants lacking CtpA produce a lipid A species which retains phosphate at the 1 and 4' positions, and which lacks one or more of the secondary fatty acids. While these lipid A species were detectable by mass spectrometry, gel electrophoresis and LAL assays indicate that they are much less abundant than the lipid A in wild-type strains.

Lipid A extracts from the  $\Delta lpxC$   $\Delta fur$   $\Delta sspB$  mutant yielded no ions consistent with wild-type lipid A and instead contained an unknown lipid (**Fig. S3E**, m/z 1412). Numerous attempts to interpret the structure of this ion using the same type of tandem MS data as used in Fig. S3A-D failed to generate a structural hypothesis resembling lipid A derivatives or other known lipids. Again, it is important to note that while this unknown ion was detected by mass spectrometry, gel electrophoresis and LAL assays together indicate that lipid A is absent from  $\Delta lpxC$   $\Delta fur$   $\Delta sspB$  cells.

Lipid A-deficient Caulobacter mutants produce a three-layer cell envelope

We analyzed NA1000,  $\Delta ctpA$   $\Delta fur$   $\Delta sspB$  and  $\Delta lpxC$   $\Delta fur$   $\Delta sspB$  strains via electron cryotomography to assess the effects of mutations on cell envelope structure (**Movies S1-S4**). As expected, the S-layer is absent from both mutants due to the loss of its O-antigen

attachment site (Walker et al., 1994). Despite drastic reductions in lipid A levels, the  $\Delta ctpA$   $\Delta fur$   $\Delta sspB$  and  $\Delta lpxC$   $\Delta fur$   $\Delta sspB$  mutants still generate a three-layer cell envelope, including an OM (**Fig. 2E**). Although much less severe than during acute CtpA depletion (**Movie S4**), membrane blebs were often observed at the cell poles or division sites in  $\Delta ctpA$   $\Delta fur$   $\Delta sspB$  and  $\Delta lpxC$   $\Delta fur$   $\Delta sspB$  cells (**Fig. 2E**). A large fraction of ctpA and lpxC mutant cells exhibited defects in stalk structure or internal membrane folds at the pole or midcell (N = 100;  $\Delta ctpA$   $\Delta fur$  s4

The ability to produce an outer membrane in the absence of LPS, along with excess membrane folds visible in the cytoplasm, suggest that  $\Delta fur$  could suppress  $\Delta ctpA$  and  $\Delta lpxC$  by increasing the synthesis of other lipids. We examined published transcriptomic data (Leaden et al., 2018; da Silva Neto et al., 2013) for a group of 22 genes predicted to participate in fatty acid or phospholipid synthesis. For 19 of these genes, expression was not altered in a  $\Delta fur$  mutant or in wild-type *Caulobacter* treated with 2,2-dipyridyl to limit iron (**Table S3**). Of the three remaining genes, two were downregulated and one was upregulated only by iron limitation. Thus, Fur seems not to exert a direct or indirect transcriptional effect on genes related to lipid synthesis. However, post-transcriptional effects in  $\Delta fur$  strains could cause an increase in the production of lipids other than lipid A.

Fur-regulated processes, rather than available iron levels, control the conditional essentiality of lipid A

LPS defects are usually associated with increased chemical sensitivity (Nikaido, 2003). Mutations in *fur* or O-antigen synthesis genes did not appreciably increase chemical sensitivity compared to NA1000, while strains lacking *ctpA* or *lpxC* had greater sensitivity to a subset of antibiotics and to all tested detergents (**Fig. 4A**). In sharp contrast, the  $\Delta lpxC$   $\Delta sspB$  and  $\Delta ctpA$   $\Delta sspB$  strains with suppressor mutations were much less susceptible to CHIR-090, an inhibitor of LpxC (McClerren et al., 2005) (**Fig. 4B**). We infer that suppressed  $\Delta lpxC$  and  $\Delta ctpA$  mutants are relatively insensitive to CHIR-090 because they already produce little lipid A or lack the target enzyme.

In agreement with its ability to suppress the lethality of  $\Delta lpxC$  and  $\Delta ctpA$  mutations, the  $\Delta fur$  allele by itself greatly reduced the sensitivity of *Caulobacter* to CHIR-090 (**Fig. 4B**). Fur is a widespread bacterial regulator of iron homeostasis that senses available Fe<sup>2+</sup>, likely by reversibly binding a [2Fe-2S] cluster (Andrews et al., 2013; Fontenot et al., 2020). When bound to iron, Fur represses the transcription of genes for iron uptake and activates (directly or indirectly) the transcription of genes for iron-utilizing enzymes. Since iron is required for Fur-

directed transcriptional regulation, we asked whether iron limitation could mimic the phenotypes of a  $\Delta fur$  mutant. Culturing NA1000 with the iron chelator 2,2'-dipyridyl reduced its susceptibility to CHIR-090 to match that of the  $\Delta fur$  mutant (**Fig. 4B**). Neither depleting LpxC in  $fur^+$  cells nor inducing fur in  $\Delta lpxC$   $\Delta fur$   $\Delta sspB$  cells caused a reduction in viability in the presence of 2,2'-dipyridyl (**Fig. 4C, D**). The NA1000,  $\Delta sspB$ , and  $\Delta fur$   $\Delta sspB$  strains cultured in 2,2'-dipyridyl retained LPS and lipid A +/- core species (**Fig. 4E**). Therefore, low iron availability does not induce the loss of lipid A, but is sufficient to maintain *Caulobacter* viability when lipid A is eliminated by chemical or genetic means.

Because they are impaired in iron sensing, *fur* mutants of other bacteria accumulate more available iron than the corresponding wild-type strains (Liu et al., 2020; Wofford et al., 2019). We measured available iron levels using a streptonigrin (SNG) sensitivity assay (Justino et al., 2007; Nachin et al., 2001), because SNG killing is linked to the intracellular formation of oxygen radicals in the presence of iron (Hassett et al., 1987; Yeowell and White, 1982). Growth of the  $\Delta fur$  and  $\Delta fur$   $\Delta sspB$  strains was almost completely inhibited by 0.25  $\mu$ g/ml SNG, while NA1000 was only mildly inhibited (**Fig. 4F**), consistent with higher levels of available iron in  $\Delta fur$  mutants. These findings indicate that both excess available iron (in *fur* mutants) and iron depletion (by 2,2-dipyridyl) can support viability when lipid A synthesis is blocked chemically or genetically. Since *fur* deletion and iron chelation have the same effect on Fur-regulated gene expression, but are predicted to have opposite long-term effects on Fur-independent iron signaling (**Fig. 4G**), this implies that processes regulated by Fur in concert with iron are specifically responsible for the survival of lipid A-deficient *Caulobacter* (Leaden et al., 2018; da Silva Neto et al., 2013).

RB-Tnseq identifies sphingolipid synthesis genes needed for fitness when lipid A synthesis is chemically inhibited

To uncover additional factors that promote the survival of lipid A-deficient *Caulobacter*, we challenged an RB-Tnseq library constructed in NA1000 (Price et al., 2018) with CHIR-090. Individual barcode frequencies were measured by high-throughput sequencing before each trial and after growth in either PYE or PYE + 2 µg/ml CHIR-090. To identify genes that are particularly important when LpxC is inhibited, we averaged and compared the gene fitness scores (Wetmore et al., 2015) from three trials in each condition (**Fig. 5A**). We anticipated that mutations in *fur* would increase fitness in CHIR-090, but the NA1000 RB-Tnseq library contained no insertions in *fur*. Surprisingly, nearly all genes known to be regulated by Fur

(Leaden et al., 2018; da Silva Neto et al., 2013) had similar fitness scores in unstressed and CHIR-090-exposed cultures (**Fig. 5A**).

Focusing on genes whose average fitness scores were  $\geq$  1 point lower in CHIR-090-treated cultures than in control cultures (**Table S4**), we identified five genes involved in sphingolipid synthesis: serine palmitoyltransferase (spt,  $CCNA_01220$ ), acyl-carrier protein (acp,  $CCNA_01221$ ), ceramide reductase (cerR,  $CCNA_01222$ ), ACP-synthetase (acps,  $CCNA_01223$ ), and bacterial ceramide synthase (bcerS,  $CCNA_01212$ ) (Olea-Ozuna et al., 2021; Stankeviciute et al., 2021). Fitness scores were also significantly lower for transposon insertions in a neighboring operon of three uncharacterized genes predicted to modify lipids ( $CCNA_01217-01219$ , Marks et al., 2010) (**Fig. 5A**). None of the genes listed above is known to be regulated by Fur or iron (Leaden et al., 2018; da Silva Neto et al., 2013). Using qPCR, we demonstrated that transcription of  $CCNA_01217-01219$  is unchanged in  $\Delta fur \Delta sspB$  cells and in the  $\Delta lpxC \Delta fur \Delta sspB$  mutant (**Fig. 5B**). As controls, lpxC transcripts were not detected in  $\Delta lpxC \Delta fur \Delta sspB$  cells, and bfd ( $CCNA_03372$  bacterioferritin-associated ferredoxin) transcripts were significantly increased in both mutants, as previously observed (**Fig. 5B**), (Leaden et al., 2018).

To examine the roles of genes in the uncharacterized operon, we constructed unmarked deletions in the NA1000 and  $\Delta fur \Delta sspB$  backgrounds and complemented them with the corresponding genes expressed from the inducible vanA promoter (Thanbichler et al., 2007). Loss of spt,  $CCNA_01217$ ,  $CCNA_01218$ , or  $CCNA_01219$  greatly increased the susceptibility to CHIR-090, either in NA1000 or in  $\Delta fur \Delta sspB$  cells (**Fig. 5C**), and expression of the complementing gene from the vanA locus restored the wild-type level of susceptibility, validating the RB-Tnseq results.

Mutations in *CCNA\_01217-01219* or *spt* could increase CHIR-090 sensitivity via distinct mechanisms: by damaging the cell's permeability barrier and giving easier access to CHIR-090, by making it more difficult for cells to grow after lipid A synthesis is inhibited, or both. To eliminate changes in drug access as a factor in the experiment, we measured the effects of *CCNA\_01217*, *CCNA\_01218*, and *spt* upon cell viability when LpxC was depleted. We deleted individual genes in the strain Δ*lpxC* Δ*fur* Δ*sspB* + P*xyl-lpxC::3xFLAG-ssrA* (KR4091) and complemented them with *vanA*-driven copies as described above. The parent strain lacks *fur* and grows in PYED medium (with or without vanillate) when LpxC is depleted. In contrast, KR4091 lacking *CCNA\_01217*, *CCNA\_01218*, or *spt* grew poorly in PYED medium, and growth in PYED was fully or partially restored by expressing the complementing gene from the vanillate promoter (**Fig. 5D**). Since this assay does not rely on an exogenous inhibitor of LpxC, we

conclude that *CCNA\_01217-8* and *spt* are critical for the fitness of lipid A-deficient *Caulobacter*, not simply for the exclusion of CHIR-090.

KR4091 lacking  $CCNA\_01218$  grew poorly in PYEX medium without vanillate, where IpxC is transcribed (**Fig. 5D**), and we were unable to isolate a stable derivative of KR4091 harboring  $\Delta CCNA\_01219$  and vanA::01219. These findings could indicate that  $\Delta CCNA\_01218$  and  $\Delta CCNA\_01219$  have a negative genetic interaction with  $\Delta fur$  and/or  $\Delta sspB$ . However, we detected no significant additive growth phenotypes when  $\Delta CCNA\_01218$  or  $\Delta CCNA\_01219$  was combined with  $\Delta fur$   $\Delta sspB$  in strains where LpxC was expressed from the native locus (**Fig. 5E**). We therefore favor the hypothesis that  $\Delta CCNA\_01218$  or  $\Delta CCNA\_01219$  is particularly detrimental in the highly modified KR4091 background, where fur and sspB are absent, and an epitope-tagged version of LpxC is expressed from a nonnative promoter.

CCNA\_01217-01219 convert neutral ceramide to an anionic sphingolipid, ceramide phosphoglycerate

The importance of Spt for viability in the absence of lipid A indicated a role for sphingolipids in this phenotype. Since *Sphingomonads* produce anionic glycosphingolipids (GSLs) on the outer membrane (Kawasaki et al., 1994), we initially hypothesized that *Caulobacter* responds to *lpxC* deletion by upregulating GSL production. The *Caulobacter* sphingolipid glycosyltransferases Sgt1 and Sgt2 are expressed specifically in phosphate-limiting conditions (Stankeviciute et al., 2019), and their transcripts were not upregulated in  $\Delta fur \Delta sspB$  or  $\Delta lpxC \Delta fur \Delta sspB$  cells grown in PYE (**Fig. 5B**). Further, transposon insertions in *sgt1* or *sgt2* did not reduce the fitness of CHIR-090-treated cells in RB-Tnseq experiments. Thus, while Sgt1 and Sgt2 are not critical in these experiments, they may be important for the fitness of lipid A-deficient *Caulobacter* under other conditions.

A careful analysis of the *Caulobacter* lipidome revealed a previously unidentified sphingolipid species, ceramide phosphoglycerate (**Fig. 6A**). In fact, we identified two forms of this lipid containing either one or two phosphoglycerate moieties (**Fig. 6A**) that we have designated CPG and CPG2. LC/MS/MS analysis confirmed the proposed structures of these lipids (**Fig. 6B**). To determine whether *CCNA\_01217-01219* are involved in CPG/CPG2 synthesis, we analyzed lipid extracts from mutant and complemented mutant strains. Deletion of *CCNA\_01218* led to the loss of CPG, CPG2 and ceramide phosphate, but preserved neutral ceramide (**Fig. 6C**). CCNA\_01218 is annotated as a sphingosine kinase-related protein and has a conserved LCB5 domain (Nagiec et al., 1998). Therefore, we propose that CCNA\_01218 adds the initial phosphate on the ceramide (**Fig. 6D**). The Δ*CCNA\_01219* mutant lost CPG and

CPG2 but retained ceramide-phosphate (**Fig. 6C**). This is consistent with CCNA\_01219 adding a glycerate molecule to ceramide phosphate to form CPG (**Fig. 6D**). CCNA\_01219 has no conserved domains, and a BLAST analysis identified homologs only in Caulobacterales and Sphingomonadales. Deletion of *CCNA\_01217* resulted in the loss of CPG2 but had no effect on CPG, ceramide phosphate, or neutral ceramide (**Fig. 6C**). CCNA\_01217 has a conserved phosphatidylglycerophosphate synthase (PgsA) domain which is normally involved in phosphatidylglycerol (PG) synthesis. PG is the dominant phospholipid in *Caulobacter* (Stankeviciute et al., 2019), but the essential PgsA ortholog *CCNA\_03002* is likely responsible for PG synthesis (Christen et al., 2011; Marks et al., 2010). Thus, we conclude that CCNA\_01217 adds a second phosphoglycerate to CPG to form CPG2 (**Fig. 6D**). Each deletion could be complemented by expressing the respective gene from a vanillate-inducible promoter (**Fig. 6C**).

We note that the amount of CPG/CPG2 detected appears to be a relatively small percentage of the total lipidome (**Fig. S4**), raising the question of how these lipids can enable survival in the absence of lipid A. The CPG2 molecule is very polar, as evidenced by its very long LC retention time, and we expect that this lipid is not efficiently extracted by standard methods. Though we tried several modifications to increase the extraction yield, we made only marginal improvements. Additionally, our genetic data show that CpgA adds the second phosphoglycerate molecule to generate CPG2, but we cannot rule out the possibility of higher-order polymers containing additional phosphoglycerates, which would be even more polar and difficult to extract.

### Ceramide phosphoglycerate mediates susceptibility to colistin

Cationic antimicrobial peptides (CAMPs) have been demonstrated to kill Gram-negative bacteria by first interacting with negatively charged groups on surface-exposed LPS . Phosphates at the 1 and 4' positions of lipid A are particularly important for this interaction, and several bacteria possess mechanisms to modify them, reducing their negative surface charge and sensitivity to CAMPs (Moffatt et al., 2019; Velkov et al., 2010). Despite lacking phosphate groups on its lipid A, *Caulobacter* is highly sensitive to colistin (**Fig. 7A**), and the antimicrobial effect is retained in the lipid A-deficient strain  $\Delta lpxC$   $\Delta fur$   $\Delta sspB$  (**Fig. 7A**). Since the CPG/CPG2 lipids are anionic, we considered whether they may be the colistin target in *Caulobacter*. Indeed, the growth of mutants lacking cpgA, cpgB, or cpgC was unaffected by colistin (**Fig. 7A**). Since the deletion of cpgA, catalyzing the conversion of CPG to CPG2, can alone greatly reduce

colistin sensitivity, and since the elimination of lipid A had no effect, we infer that a primary target of colistin on the *Caulobacter* surface is CPG2. Furthermore, these findings are consistent with our hypothesis that CPG lipids are a significant component of the outer leaflet of the OM whose detection is limited by inefficient extraction.

## **Discussion**

# CtpA is required for wild-type lipid A structure and abundance

We performed a suppressor screen to discover the essential function of CtpA, which contains active site residues characteristic of tyrosine phosphatases. Inactivation of *fur* or genes involved in O-antigen synthesis permitted the deletion of *ctpA* and yielded cells with drastically reduced amounts of lipid A. MS/MS analysis of the remaining lipid A extracted from  $\Delta ctpA$   $\Delta fur$   $\Delta sspB$  were consistent with species that retain phosphoryl groups at the 1 and 4' positions of the central disaccharide, suggesting that CtpA is responsible for dephosphorylating at least one of these positions, in preparation for the addition of GalpA residues.

Some alphaproteobacteria produce lipid A species with a tri- or tetrasaccharide backbone (De Castro et al., 2008). In *Rhizobia*, the phosphatases LpxE and LpxF dephosphorylate the 1 and 4' positions, respectively, of lipid A at the periplasmic surface of the IM (Karbarz et al., 2003; Wang et al., 2006). Sugars are then added to the 1 and 4' positions by the glycosyltransferases RgtF and RgtD, respectively, before the transport of mature LPS molecules to the OM (Brown et al., 2012, 2013). NA1000 harbors a gene (*CCNA\_03113*) with similarity to *lpxE*, but none with similarity to *lpxF*, raising the possibility that CtpA substitutes for LpxF. Additional work is needed to test this hypothesis and to understand how mutations in *ctpA* affect the structure and abundance of lipid A.

### Caulobacter requires a novel anionic sphingolipid to survive without lipid A

Here we demonstrate that the enzyme LpxC and lipid A itself are dispensable for viability in *Caulobacter crescentus*, conditional upon the absence of Fur and the presence of a previously uncharacterized anionic sphingolipid, ceramide phosphoglycerate (**Fig. 7B**). LPS molecules form a robust permeability barrier based on 1) tight packing of the six saturated acyl chains of lipid A, and 2) a lateral network formed by the bridging of phosphate groups on lipid A or the core polysaccharide by divalent cations such as Mg<sup>2+</sup> and Ca<sup>2+</sup> (Nikaido, 2003). *Caulobacter* lipid A and core polysaccharide lack the phosphates that would participate in a lateral network with divalent cations (Smit et al., 2008). We propose that negative charges on

CPG/CPG2 can provide this function in the *Caulobacter* OM, accounting for the observation that *cpgABC* and other sphingolipid synthesis genes are important for fitness even in non-stress conditions (**Fig. 5A** and Christen et al., 2011). Evidence that CPG/CPG2 contribute negative charge to the *Caulobacter* OM comes from studies of CAMP sensitivity. We previously observed that Spt is necessary for susceptibility to polymyxin B, but Sgt1 and Sgt2, which convert neutral ceramide to the anionic glycosphingolipid GSL-2, are not required (Stankeviciute et al., 2019). This result was puzzling, because neutral ceramide was not expected to be a target for CAMP activity. Here we provide an explanation by showing that neutral ceramide is converted by CpgABC to a different anionic species, CPG2, and that this lipid, rather than LPS, is critical for colistin susceptibility.

Inhibition of Fur-mediated gene expression is necessary to survive in the absence of lipid A

In contrast to Sphingomonads, the presence of cell surface sphingolipids is not sufficient for *Caulobacter* to survive in the absence of lipid A. Instead, the iron-responsive transcription factor Fur must also be deactivated. Both iron limitation (via growth in 2,2-dipyridyl) and excess available iron (due to a disruption in iron homeostasis in  $\Delta fur$ ) supported the viability of lipid A-deficient *Caulobacter*. These results imply that genes or processes regulated by Fur in complex with iron, rather than those regulated by iron independently of Fur, are the critical factors.

Fur controls iron homeostasis in *Caulobacter* by directly or indirectly regulating ~120 genes in combination with iron (Leaden et al., 2018; da Silva Neto et al., 2009, 2013). A significant fraction of the Fur regulon, comprising 45 genes, is predicted to encode membrane proteins functioning in transport reactions or energy metabolism. *Caulobacter* Fur represses the transcription of genes predicted to mediate iron uptake, and it activates the expression of genes encoding iron-containing enzymes, including respiratory complexes harboring Fe/S clusters or heme groups. Fur is linked to oxygen signaling in *Caulobacter* by activating the transcription of *fixK*, which mediates the response to hypoxia (Crosson et al., 2005). In addition, the  $\Delta fur$  mutant has a constitutively elevated level of intracellular oxidation and displays impaired growth under oxidative stress, implicating Fur in the prevention of oxidative stress (da Silva Neto et al., 2009; Leaden et al., 2018).

Our *ctpA* suppressor screen retrieved mutations in *fur*, but not in genes whose transcription is activated by Fur. Thus, there is unlikely to be a singular Fur-activated gene whose expression is lethal when lipid A is depleted. Consistently, RB-Tnseq revealed that no transposon insertions in Fur-activated genes led to significantly increased fitness during challenge with CHIR-090. Since mutations would be more likely to cause loss than gain of

function, we might not retrieve suppressors that work by increasing gene expression or activity. However, if there were a singular Fur-repressed gene whose upregulation was required to render lipid A dispensable, then transposon insertions in this gene would be expected to reduce the fitness of CHIR-090-treated cells. Again, no individual gene fits this profile, but one caveat is that essential genes are excluded from RB-Tnseq analysis.

Based on our genetic data, mutations in *fur* could support the viability of lipid A-deficient *Caulobacter* via 1) downregulation of multiple Fur-activated genes, 2) upregulation of multiple Fur-repressed genes, and/or 3) activation of compensatory cellular stress responses. Since Fur regulates the expression of many OM and IM proteins (da Silva Neto et al., 2009; Leaden et al., 2018), deletion of *fur* could alter envelope composition in a manner that renders lipid A nonessential. Alternatively, the transcriptional changes and oxidative stress which follow from *fur* deletion could activate a network of stress responses which together make it possible to survive in the absence of lipid A.

## The search for principles governing lipid A essentiality

Hypotheses to explain the essential nature of lipid A include its chemical barrier function, the detrimental activation of stress responses when it is depleted, its role in OM protein biogenesis or function, and its mechanical role in resisting turgor pressure (Rojas et al., 2018; Zhang et al., 2013). Caulobacter is only the fourth LPS-bearing Gram-negative bacterium demonstrated to survive in the absence of lipid A, following N. meningitidis, M. catarrhalis, and A. baumannii. So far, however, no single theme has emerged to explain why this select and phylogenetically diverse group of Gram-negative species is capable of surviving without lipid A. In A. baumannii, proteins which synthesize PG in lateral cell walls (the elongasome) are critical for the fitness of lipid A-deficient strains, suggesting that alterations in PG structure are needed to compensate for the OM's loss of mechanical strength (Simpson et al., 2021). However, since elongasome components are essential for viability in wild-type Caulobacter (Christen et al., 2011), RB-Tnseq could not reveal their fitness effects in CHIR-090-treated cultures. Lipid Adeficient strains of A. baumannii consistently display increases in the expression of lipoproteins and the Lol pathway for lipoprotein transport to the OM (Boll et al., 2016; Henry et al., 2015). Two lipoprotein synthesis genes, Igt (CCNA 00525) and Int (CCNA 00050), had markedly reduced fitness scores in CHIR-090-treated Caulobacter cultures compared to unstressed cultures, so OM lipoproteins may help to compensate for the absence of lipid A in diverse species.

A. baumannii  $\Delta lpxC$  mutants have growth and morphological defects that are corrected when the growth rate is limited by environmental factors such as low temperature or nutrient limitation (Nagy et al., 2019), suggesting that one barrier to the elimination of lipid A is the rate of synthesis of alternative molecules to constitute the OM. Although  $\Delta fur$  slows the growth of Caulobacter (Fig. S1, Table S5, and da Silva Neto et al., 2009), we found that slow growth in PYE medium at a reduced temperature was not sufficient to support the viability of  $fur^+$  Caulobacter depleted of LpxC (Fig. S5A), or of  $\Delta lpxC$   $\Delta fur$   $\Delta sspB$  cells with fur expression restored (Fig. S5B). Furthermore, if slow growth were sufficient to render lipid A nonessential, then our screen for ctpA suppressors should have retrieved a wider variety of mutations that slow Caulobacter growth, rather than repeated mutations in fur and genes for O-antigen synthesis. Although reduced growth rate may play a role, we propose that the  $\Delta fur$  mutation provides specific, unknown benefits which support viability in the absence of lipid A.

Our work suggests that possession of genes to produce anionic sphingolipids may provide certain Gram-negative bacteria with an unusual capacity to survive without lipid A. Anionic sphingolipids can also underlie clinically important phenotypes in wild-type membranes that retain LPS, such as the susceptibility to CAMPs, which are used as a last line of defense against multidrug-resistant bacterial infections. Thus, functions traditionally attributed to lipid A may be performed wholly or in part by alternative lipids, underscoring the need to study lipid A functions in diverse species and to identify and functionally characterize novel lipids.

## Limitations of the study

Although the absence of Fur is clearly important for survival without lipid A, we do not yet understand how  $\Delta fur$  renders lipid A inessential in *Caulobacter*. Deletion of *fur* may upregulate the synthesis of lipids other than lipid A posttranscriptionally, which was not assessed in this study. Although CtpA is needed for the correct structure and abundance of *Caulobacter* lipid A, this work did not uncover its precise biochemical function. Finally, due to technical difficulties with extracting polar lipids, we do not yet know how much CPG or CPG2 is present in the outer membrane, or if CPG polymers exist with more than two glycerates per molecule.

### **Acknowledgments**

The authors thank Charlie Huang, Morgan Price, Laura Herron and Henry Seaborne for experimental assistance. Cryoelectron microscopy data acquisition was performed using instrumentation of Lawrence Berkeley National Laboratory and the Bay Area CryoEM resource, maintained by Jonathan Remis and Daniel Toso. Linux computer maintenance was provided by

579 Paul Tobias. D.R.G. thanks the International Centre for Cancer Vaccine Science project of the 580 International Research Agendas program of the Foundation for Polish Science co-financed by 581 the European Union under the European Regional Development Fund MAB/2017/03 at the 582 University of Gdansk. Funding for this work was provided by National Science Foundation 583 awards 1553004 and 2031948 to E.A.K. and 1615287 to K.R.R., and National Institutes of 584 Health awards GM111066-01 and 1R01Al123820-01 to D.R.G. Cryoelectron tomography work 585 was supported by the Laboratory Directed Research and Development Program of Lawrence 586 Berkeley National Laboratory under U.S. Department of Energy Contract No. DE-AC02-587 05CH11231.

588

589

590

591

592

593

594

#### **Author contributions**

J.J.Z., E.A.K., and K.R.R. conceived the project. Mass spectrometry experiments were performed and analyzed by S.H.Y., D.R.G., and Z.G. Electron cryotomography experiments were performed and analyzed by R.G. and K.M.D. RB-Tnseq experiments, sequencing, and data analysis were performed by J.J.Z and A.M.D., and K.R.R. All other experiments were performed and analyzed by J.J.Z., G.S, E.A.K., and K.R.R. The manuscript was written by J.J.Z., E.A.K, and K.R.R. with input from all authors.

595596597

#### **Declaration of interests**

598 The authors declare no competing interests.

599

600

### Figure Legends

- **Figure 1**. Suppressor mutations affecting *fur* or O-antigen biosynthesis permit the loss of *ctpA*.
- 602 (A) Strategy for isolation of  $\Delta ctpA$  suppressor mutants. (B) Viability of suppressor strains during
- 603 CtpA depletion on PYED. (C) Differential interference contrast (DIC) images of the indicated
- strains grown in CtpA-expressing (PYEX) or non-expressing (PYED) conditions. D) DIC images
- of the indicated strains grown to exponential phase in PYE. Scale bar, 3 µm.

- Figure 2.  $\triangle ctpA$  and  $\triangle lpxC$  strains with suppressor mutations contain little or no lipid A. (A)
- 608 Endotoxin units (EU) per mL of whole cells of the strains indicated in panel B (mean ± S.D.).
- Dots represent individual data points, and mean values are displayed above bars. (B) Hot
- aqueous-phenol LPS extracts of the indicated strains. \*\*\* = S-LPS, \*\* = putative full-length lipid
- A-core, \* = putative lipid A. (C) Lipid A (left) or rough LPS (right) extracted from the indicated
- strains. \* = lipid A. \*\* = rough LPS. (D) Proteinase K-treated lysates of the indicated strains.

Cells were maintained in PYED or shifted into PYEX for 6 hours before harvesting. Samples were normalized by OD<sub>660</sub>. NA1000 was grown in PYE. Leaky expression of LpxC can generate S-LPS (\*\*\*) and lipid A + core (\*\*) in PYED. Full-length S-LPS is not restored to *ctpA* and the lipid A-core species is reduced in size (\*) because *CCNA\_03733* is needed for mannose incorporation. (E) Electron cryotomography images of the indicated strains noting the inner membrane (IM), peptidoglycan (PG), outer membrane (OM), and S-layer. All strains were grown to exponential phase in PYE medium, except that CtpA was depleted from KR3906 during 12 hours of growth in PYED prior to analysis. Scale bars, 100 nm.

**Figure 3.** Deletion of *fur* supports the viability of  $\Delta lpxC$  cells. (A) DIC images of the LpxC depletion strain alone or harboring the indicated mutations, grown in PYEX or PYED for 10 hours. Scale bar, 3 µm. (B) Viability of the LpxC depletion strain, alone or harboring the indicated mutations, plated on PYEX or PYED. (C) Viability of  $\Delta lpxC$   $\Delta fur$   $\Delta sspB$  cells harboring a Pxyl-*fur* or a Pxyl-*cerulean* expression vector. Plates included kanamycin to retain expression vectors.

Figure 4. Fur-regulated processes control the conditional essentiality of lipid A. (A) Sensitivity to the indicated chemicals measured by disc diffusion assay. Dots indicate individual data points. Suppressor mutations present in strains represented by blue or green bars are, from left to right. ΔCCNA 00497, ΔCCNA 01553, ΔCCNA 03733, and Δfur. (B) CHIR-090 sensitivity measured by disc diffusion assay. Partial clearing indicates the diameter of a ring of intermediate growth. Dots indicate individual measurements of cleared and partially cleared zones (mean ± S.D.). \*\*\*\*, p < 0.0001; n.s., p > 0.05; one-way ANOVA followed by Dunnett's posttest comparison to NA1000. Strains exhibiting rings of partial growth were excluded from the analysis. (C) Viability of the LpxC depletion strain in inducing (PYEX) or depleting (PYED) conditions, in the presence or absence of 100  $\mu$ M 2,2'-dipyridyl. (D) Viability of the  $\Delta lpxC$   $\Delta fur$   $\Delta sspB$  strain harboring a Pxyl-fur plasmid, grown in noninducing (PYED) or inducing (PYEX) conditions, in the presence or absence of 100 µM 2,2'-dipyridyl. Plates included kanamycin to retain the expression vector. Brightness was reduced and contrast increased to improve the clarity of colonies grown on 2,2'dipyridyl. (E) Proteinase K-treated lysates of the indicated strains grown overnight in the presence or absence of 100 µM 2,2'-dipyridyl. Samples were normalized by OD<sub>660</sub>. (F) Growth inhibition by SNG in liquid PYE cultures of the indicated strains. Dots represent individual OD660 ratios (mean  $\pm$  S.D.). \*\*\*\*, p < 0.0001; n.s., p > 0.05; one-way ANOVA followed by Šídák's multiple comparisons test, where each strain was compared to NA1000 grown in the same

condition. (G) Changes in Fur-regulated gene expression correlate with the ability to survive in the absence of lipid A. Genes regulated by Fur in concert with iron (sets A and B) are modulated similarly by deletion of *fur* or by iron limitation, while genes regulated by iron alone (sets C and D) are modulated in opposite directions in these two conditions.

650651652

653

654

655

656

657

658

659

660

661

662

663

664

665

666

667

668

669

670

671

672

647

648

649

Figure 5. RB-Tnseg identifies sphingolipid synthesis genes needed for fitness when LpxC is inhibited. (A) Average gene fitness scores for three challenges of the NA1000 RB-Tnseq library with PYE or PYE+2 µg/ml CHIR-090. Fitness scores are color-coded based on regulation of the corresponding genes. Fitness scores of selected genes are indicated by colors matching the open reading frame diagram below. (B) Wild-type,  $\Delta fur \Delta sspB$ , and  $\Delta fur \Delta lpxC \Delta sspB$  cells were grown to mid-log phase in PYE, and expression of the indicated genes was measured by qRT-PCR (n = 3 biological replicates, mean ± S.D). Gene expression is normalized to the wild-type sample for each gene tested. n.s., p > 0.05; \*, p < 0.05; one-way ANOVA followed by Šídák's multiple comparisons test, where each strain was compared to wild-type. (C) CHIR-090 sensitivity of the indicated strains measured by disc diffusion assay. Where indicated, 0.5 mM vanillate was included in the medium. Dots represent individual measurements (mean ± S.D.). n.s., p > 0.05; \*, 0.01 < p < 0.05; \*\*, 0.001 < p < 0.01; \*\*\*\*, p < 0.0001; one-way ANOVA followed by Šídák's multiple comparisons test, where each condition was compared to NA1000 without vanillate or, for strains harboring  $\Delta fur \Delta sspB$ , to  $\Delta fur \Delta sspB$  without vanillate. The shaded bar indicates a ring of partial growth, rather than complete clearing, and this sample was excluded from the analysis. (D) Overnight growth of strains expressing (xylose) or depleting (dextrose) LpxC, and expressing (vanillate) or not expressing the indicated genes. Dots represent individual measurements (mean  $\pm$  S.D.). \*\*\*\*, p < 0.0001; n.s., p > 0.05; one-way ANOVA followed by Šídák's multiple comparisons test, where each condition was compared to growth of the same strain in PYED. (E) Growth curves of the indicated strains in PYE medium (mean ± S.D.).

673674

675

676

677

678

679

680

**Figure 6.** *CCNA\_01217-01219* convert neutral ceramide to an anionic sphingolipid, ceramide phosphoglycerate. (A) Extracted ion-chromatograms identified the indicated sphingolipid species in NA1000 lipid extracts. (B) Structural determination of anionic sphingolipids was performed by MS/MS analysis. (C) The presence of the indicated sphingolipids was assessed in each deletion mutant and its respective complemented strain. x, no lipid of that type was detected in the indicated strain. The presence of neutral ceramide served as an extraction control for each strain. (D) Proposed mechanism for CPG2 synthesis.

**Figure 7.** Ceramide phosphoglycerate mediates susceptibility to colistin. (A) Overnight growth of the indicated strains in the presence or absence of 10 μg/ml colistin. Dots represent individual OD<sub>660</sub> measurements (mean  $\pm$  S.D.) \*\*\*\*, p < 0.0001; n.s., p > 0.05; one-way ANOVA followed by Šídák's multiple comparisons test, where each strain treated with colistin was compared to the same strain without colistin. (B) Model of the *Caulobacter* cell envelope containing LPS and CPG2. Consequences for OM composition and colistin sensitivity when either lipid A (Δ*lpxC* Δ*fur*) or sphingolipids (Δ*spt*) are eliminated. The presence of CPG2 and the absence of *fur* are together required for the viability of lipid A-deficient *Caulobacter*.

## **STAR Methods**

#### RESOURCE AVAILABILITY

#### Lead contact

• Further information and requests for resources and reagents should be directed to and will be fulfilled by the lead contact, Kathleen R. Ryan (<a href="mailto:krr@berkeley.edu">krr@berkeley.edu</a>).

## Materials availability

 Plasmids and bacterial strains generated in this study are available upon request from the lead contact.

#### Data and code availability

- Sequence data that support the findings of this study are openly available in the Sequence Read Archive at <a href="https://www.ncbi.nlm.nih.gov/sra">https://www.ncbi.nlm.nih.gov/sra</a>, under BioProject ID PRJNA526705, with specific NCBI BioSample accession numbers listed in the key resources table and Table S6. RB-Tnseq data are publicly available at <a href="https://fit.genomics.lbl.gov/">https://fit.genomics.lbl.gov/</a>, with set and index numbers listed the key resources table and under RB-Tnseq analysis. Microscopy and gel electrophoresis images and mass spectrometry data reported here will be shared by the lead contact upon request. This paper analyzes existing, publicly available data, whose sources are listed in the key resources table.
- This paper does not report original code.
- Any additional information required to reanalyze the data reported in this paper is available from the lead contact upon request.

# **EXPERIMENTAL MODEL AND SUBJECT DETAILS**

All Caulobacter crescentus strains were derived from NA1000 (Evinger and Agabian, 1977) and are listed in **Table S6**. Caulobacter was grown in peptone-yeast extract medium (PYE, Ely, 1991) at 30°C. PYE was supplemented with 0.3% xylose (PYEX) or 0.2% dextrose (PYED) where indicated. When changing between inducing and non-inducing conditions, cells were washed twice with PYE medium lacking supplemental sugars or vanillate before being released into or plated on medium with a different supplement. Counter-selection using sacB was performed using 3% sucrose. 100 µM 2,2'-dipyridyl was added to culture media to achieve low-iron conditions. Vanillic acid was added to PYE media at final concentrations of 0.5 mM (plate assays) or 0.1 mM (liquid assays) to drive gene expression from the *vanA* promoter. Antibiotics added to PYE were used at the following concentrations (µg/mL) for liquid (L) or solid (S) medium: kanamycin, 5 (L), 25 (S); chloramphenicol, 1 (L/S); nalidixic acid, 20 (S); gentamycin, 25 (L), 5 (S); oxytetracycline, 1 (L), 2 (S); spectinomycin, 25 (L), 100 (S); hygromycin, 100 (L/S); streptonigrin 0.025 or 0.25 (L). E. coli strains were grown in lysogeny broth (10 g/L tryptone, 5 g/L yeast extract, 5 g/L NaCl) at 37°C, supplemented with antibiotics at the following concentrations (µg/mL) for liquid (L) or solid (S) medium: kanamycin, 30 (L), 50 (S); chloramphenicol, 20 (L), 30 (S); gentamicin, 15 (L), 20 (S); tetracycline, 12 (L/S); spectinomycin, 50 (L/S); hygromycin, 100 (L/S). Diaminopimelic acid (0.3 mM) was added to solid or media to support the growth of *E. coli* strain WM3064 (Dehio and Meyer, 1997).

#### METHOD DETAILS

715716

717

718

719

720

721

722

723

724

725

726

727

728

729

730

731

732

733

734

735736

737

738

739

740

741742

743

744

745

746

- **Plasmid construction.** Plasmid descriptions are listed in **Table S7**. Primer sequences used for plasmid construction are listed in **Table S8**. Gibson assembly was performed using vectors linearized with restriction enzymes, DNA fragments amplified with Q5 High-Fidelity DNA Polymerase, and NEBuilder HiFi DNA Assembly Master Mix.
- pZIK133. The LpxC depletion vector was constructed by placing the *lpxC* coding region, C-terminally fused to a 3xFLAG tag (amino acid sequence: DYKDHDGDYKDHDIDYKDDDDK) followed by the *Caulobacter* ssrA tag (amino acid sequence: AANDNFAEEFAVAA), under control of the *xyIX* promoter. The *xyIX* promoter was amplified using the pJS14-PxyIX and PxyIX-lpxC R primers. The PxyIX-lpxC F and lpxC-3xFLAG R primers were used to amplify *lpxC*. The C-terminal fusion was amplified from pAB6 using the lpxC-3xFLAG F and ssrA-pJS14

748 primers. The final plasmid was assembled via Gibson cloning into a BamHI/EcoRI-digested 749 pJS14 backbone. 750 751 pZIK134. For the IpxC knockout construct, flanking homology regions were amplified using the 752 primers lpxC UpF and lpxC UpR for the 5'- region, and lpxC DownF and lpxC DownR for the 3'-753 region. The 5'- arm included a 5'- Spel site and a 3'- EcoRI site, and the 3'- arm included a 5'-754 EcoRI site and a 3'- SphI site. These fragments were digested with the indicated enzymes and 755 ligated into Spel/Sphl-digested pNPTS138. This intermediate plasmid was linearized with 756 EcoRI, and the EcoRI-digested tetAR cassette from pKOC3 was inserted to make the final 757 construct. 758 759 pZIK73 and pZIK78. For knockouts of CCNA 01553 or CCNA 00497, flanking homology 760 regions were amplified using the following primer pairs: pZIK73 5'- region (01553 UpF; 01553 761 UpR), pZIK73 3'- region (01553 DownF; 01553 DownR), pZIK78 5'- region (00497::hyg UpF; 762 00497::hyg UpR), pZIK78 3'- region (00497::hyg DownF; 00497::hyg DownR). For each 763 construct, the 5'- arm included a 5'- Spel site and a 3'- Smal site, and the 3'- arm included a 5'-764 Small site and a 3'- EcoRI site. These fragments were digested with the indicated enzymes and 765 ligated into Spel/EcoRI-digested pNPTS138. The intermediate plasmids were linearized with 766 Smal, and the Smal-digested hyg cassette from pHP45 $\Omega$ -hyg was inserted to make the final 767 constructs. 768 769 pZIK80, pZIK81, pZIK82, and pZIK161. For the knockouts of CCNA 03733, CCNA 01068, 770 CCNA 01055, or CCNA 00055, flanking homology regions were amplified using the following 771 primer pairs: pZIK80 5'- region (03733::hyg UpF; 03733::hyg UpR), pZIK80 3'- region 772 (03733::hyg DownF; 03733::hyg DownR), pZIK81 5'- region (01068::hyg UpF; 01068::hyg UpR), pZIK81 3'- region (01068::hyg DownF; 01068::hyg DownR), pZIK82 5'- region (01055::hyg UpF; 773 774 01055::hyg UpR), pZIK82 3'- region (01055::hyg DownF; 01055::hyg DownR), pZIK161 5'-775 region (fur UpF; fur UpR), pZIK161 3'- region (fur DownF; fur DownR). Each 5'- arm included a 776 5'- Spel site and a 3'- BamHl site, and each 3'- arm included a 5'- BamHl site and a 3'- EcoRl 777 site. These fragments were digested with the indicated enzymes and ligated into Spel/EcoRI-778 digested pNPTS138. The intermediate plasmids were linearized with BamHI, and the BamHI-

digested hyg cassette from pHP45 $\Omega$ -hyg was inserted to make the final constructs.

779

- 781 *pZIK172-174. CCNA\_00497, CCNA\_01553, or CCNA\_03733* were placed under control of the
- 782 xylX promoter on pXCERN-2, which integrates at the xylX promoter. The corresponding genes
- 783 were initially cloned into pVCERN-2 before being moved into pXCERN-2. Genes were amplified
- with the following primer pairs: CCNA\_00497 (pVCERN-2 00497 F; pVCERN-2 00497 R),
- 785 CCNA 01553 (pVCERN-2 01553 F; pVCERN-2 01553 R), CCNA 03733 (pVCERN-2 03733 F;
- 786 pVCERN-2 03733 R). Primer sets replace the start codon with an Ndel site and add a Sacl site
- 787 after the stop codon. The corresponding gene fragment and pVCERN-2 were digested with
- 788 Ndel and Sacl and ligated together. An Ndel/Mlul fragment was subsequently excised from
- 789 each vector and moved to pXCERN-2 cut with the same enzymes.

790

- 791 pZIK175. CCNA 00055 (fur) was placed under control of the xylX promoter on pXCERN-2,
- 792 which integrates at the *xyIX* promoter. *CCNA 00055* was initially cloned into pVCERN-2 before
- 793 being moved into pXCERN-2. CCNA\_00055 was amplified using the Pvan-fur and fur-pVCERN
- 794 primers, and this fragment was inserted into Ndel/Sacl-digested pVCERN-2 via Gibson
- 795 assembly. The Ndel/Mlul fragment was subsequently excised and ligated into Ndel/Mlul-
- 796 digested pXCERN-2.

797

- 798 pGS74 and pGS76. For markerless deletions of CCNA 01217 or CCNA 01219, 5'- and 3'-
- flanking homology regions, respectively, were amplified using the primer pairs EK1047/1048
- and EK1049/1050 (CCNA 01217) and EK1055/1056 and EK1057/1058 (CCNA 01219).
- 801 pNPTS138 was amplified with primers EK897/898, and vectors were constructed by Gibson
- 802 assembly.

803

- 804 pKR429. For markerless deletion of CCNA 01218, 5'- and 3'- flanking homology regions,
- respectively, were amplified using the primer pairs 01218 up fwd/01218 up rev and 01218
- down fwd/01218 down rev. pNPTS138 was digested with EcoRI and HindIII, and the vector was
- constructed by Gibson assembly.

808

- 809 *pEK406.* For complementing the deletion of *CCNA\_01217* in LC-MS/MS experiments,
- 810 CCNA\_01217-FLAG was amplified using primers EK1357/1358. The PCR product was ligated
- into the Ndel/Nhel sites of pVCHYC-5.

- 813 *pKR432-4*. For appending a C-terminal FLAG tag to the *CCNA 01218-20* open reading frames.
- The indicated genes were amplified from NA1000 genomic DNA using primer pairs Nde-

815 01218/01218-Mlu, Nde-01219/01219-Mlu, Nde-01220/01220-Mlu. Fragments were digested 816 using Ndel/Mlul and ligated into pFLGC-1 digested with the same enzymes. 817 818 pKR435. For expressing CCNA 01218-FLAG from the chromosomal vanA promoter. 819 CCNA 01218-FLAG was amplified from pKR432 using primers 01218-FLAG F/01218-FLAG R 820 and inserted in Ndel-digested pVGFPC-2 by Gibson assembly. 821 822 pKR436. For expressing CCNA 01219-FLAG from the chromosomal vanA promoter. 823 CCNA\_01219-FLAG was amplified from pKR433 using primers 01219-FLAG F/01219-FLAG R 824 and inserted in Ndel-digested pVGFPC-2 by Gibson assembly. 825 826 pKR437. For expressing CCNA 01220-FLAG from the chromosomal vanA promoter. 827 CCNA 01220-FLAG was amplified from pKR434 using primers 01220-FLAG F/01220-FLAG R 828 and inserted in Ndel-digested pVGFPC-2 by Gibson assembly. 829 830 pKR438. For expressing CCNA\_01217-FLAG from the chromosomal vanA promoter. 831 CCNA 01217-FLAG was amplified from pEK406 using primers 01217-FLAG F/01217-FLAG R 832 and inserted in Ndel-digested pVGFPC-4 by Gibson assembly. 833 834 Strain construction. Unless otherwise stated, plasmids were mobilized from *E. coli* into *C.* 835 crescentus by conjugation. E. coli donors were counterselected by the addition of nalidixic acid, 836 or when WM3064 was used as the donor, by omitting diaminopimelic acid from selection plates. 837 Gene deletion or disruption was achieved by two-step homologous recombination using sacB 838 counterselection (Ely, 1991). 839 840 LpxC depletion strain. The LpxC depletion strain KR4007 was constructed in a parallel manner 841 to the CtpA depletion strain KR3906. pZIK133 was introduced to KR1499 (ΔsspB) by 842 conjugation and selection on PYE/chloramphenicol. pZIK134 was conjugated into this 843 intermediate strain, and colonies were selected on PYEX/chloramphenicol/oxytetracycline. After 844 sacB counterselection on PYEX/sucrose/oxytetracycline, colonies were screened for 845 chloramphenicol<sup>R</sup> kanamycin<sup>S</sup> on PYEX. 846 847 Stable  $\Delta ctpA$  or  $\Delta lpxC$  strains. To generate stable  $\Delta ctpA$  or  $\Delta lpxC$  strains without covering 848 plasmids, candidate suppressor genes identified by screening were disrupted in KR3906 or

KR4007, respectively, using two-step homologous recombination while cultivating the cells on PYEX. Intermediate strains (sucrose<sup>R</sup> hygromycin<sup>R</sup> kanamycin<sup>S</sup>) were grown in liquid PYED without chloramphenicol to permit loss of the *ctpA* or *lpxC* covering plasmid, plated on PYED, and tested for chloramphenicol<sup>S</sup>. Absence of *ctpA* was confirmed using primers ctpA KO F and ctpA KO R, and absence of *lpxC* was confirmed using primers lpxC KO F and lpxC KO R. The genomes of  $\Delta ctpA$   $\Delta fur$   $\Delta sspB$  (KR4102) and  $\Delta lpxC$   $\Delta fur$   $\Delta sspB$  (KR4103) were resequenced and contained no additional mutations. Stable  $\Delta ctpA$  or  $\Delta lpxC$  strains were further modified by electroporation with purified plasmids (Gilchrist and Smit, 1991) to restore xylose-driven suppressor gene expression.

Deletions of sphingolipid synthesis genes. Deletions in CCNA 01217, CCNA 01218, CCNA 01219, and CCNA 01220 in NA1000 or KR4077 were made by conjugation of the appropriate pNPTS138-based plasmid, followed by selection on PYE/kanamycin/nalidixic acid. After overnight growth in PYE, cells were plated on PYEX/sucrose, and sucrose<sup>R</sup> colonies were screened for kanamycin<sup>s</sup>. Colony PCR with the following primers was used to detect the deletion of the indicated chromosomal genes: CCNA\_01217, EK S238/S239; CCNA\_01218, EK S240/S241; CCNA 01219, EK S242/S243; CCNA 01220, EK S216/S217. Loci were sequenced with the indicated primers to ensure the accuracy of in-frame deletions. Unmarked deletions of CCNA 01217, CCNA 01218, CCNA 01219, and CCNA 01220 were made in KR4091 by conjugation of KR4091 with WM3064 harboring the appropriate pNPTS138-based plasmids, followed by selection on PYEX/kanamycin medium omitting diaminopimelic acid. After growth overnight in PYEX, cells were plated on PYEX/sucrose, and sucrose<sup>R</sup> colonies were screened for kanamycin<sup>s</sup>. Colony PCR with the following primers was used to detect the deletion of the indicated chromosomal genes: CCNA 01217, EK S238/S239; CCNA 01218, EK S240/S241; CCNA 01219, EK S242/S243; CCNA 01220, EK S216/S217. Loci were sequenced with the indicated primers to ensure the accuracy of in-frame deletions. Strains were screened for oxytetracycline<sup>R</sup> and hygromycin<sup>R</sup> to ensure that they maintained deletions of *lpxC* and fur, respectively.

Complementation of spt and cpg genes. To complement deletions of CCNA\_01217-01220, the following plasmids were introduced by conjugation to place the complementing gene under control of the chromosomal *vanA* promoter: ΔCCNA\_01217, pEK406 (for LC-MS studies) or pKR438 (for growth and chemical sensitivity assays); ΔCCNA\_01218, pKR435; ΔCCNA\_01219, pKR436; or ΔCCNA\_01220, pKR437. When introducing plasmids into strains capable of *lpxC* 

depletion (based on KR4091), plasmids were delivered from WM3064 to avoid the use of multiple antibiotics for selection/counterselection. Correct integration of plasmids at the *vanA* locus was confirmed by colony PCR using primers RecUni-1 and RecVan-2 (Thanbichler et al., 2007).

**Suppressor selection.** KR3906 was grown to full density in PYEX. 300 μL of culture was transferred onto an open, sterile Petri dish and mutagenized in a UV Stratalinker 1800 (Stratagene) with 30,000 μJ of energy. Mutagenized cells were plated on PYED. Recovered colonies were grown in liquid PYED overnight to allow loss of the covering plasmid, and samples were streaked onto PYED. Isolated colonies were screened for chloramphenicol sensitivity. Chlor<sup>S</sup> isolates were grown in PYE and saved at -80°C in 10% dimethylsulfoxide. Loss of *ctpA* was confirmed via PCR using the primers ctpA KO F and ctpA KO R, which anneal to the interior of the open reading frame.

**Genome resequencing.** Strains were grown to full density in PYE, and genomic DNA was extracted using the DNeasy Blood & Tissue Kit (Qiagen). Genomic DNA was submitted to the UC Berkeley Functional Genomics Laboratory, where libraries were prepared using a PCR-free protocol with multiplexing (http://qb3.berkeley.edu/gsl/). Samples were sequenced at the UC Berkeley Vincent J. Coates Genomics Sequencing Laboratory using a 300PE or 150PE MiSeq v3 run. Genomic sequencing data were analyzed for variants using the Galaxy platform at usegalaxy.org (Afgan et al., 2016). Adapter sequences were removed using Cutadapt (Martin, 2011(Martin, 2011)), and sequences were aligned to the NA1000 genome (Marks et al., 2010) using Bowtie2 (Langmead and Salzberg, 2012). FreeBayes (Garrison and Marth, 2012) was used to analyze the BAM files for variants. Variants with quality scores below 300 were discarded as noise.

**qRT-PCR assays.** RNA from mid-log phase cells was extracted with the RNeasy kit (Qiagen). Purified RNA was treated with DNase (Thermo Scientific) to remove any contaminating DNA, and the RNA was re-purified using the RNeasy kit to remove the DNase. RNA concentrations were measured on a Nanodrop and normalized to 10 ng/μl. The RNA was reverse-transcribed with the High Capacity cDNA Reverse-Transcription Kit (Thermo Scientific). qRT-PCR was performed with technical duplicate and biological triplicate samples on a QuantStudio 6 instrument (Thermo Scientific) using the PowerUP SYBR Green master mix (Thermo Scientific)

and 300 nM primers (**Table S8**). Relative expression was determined by the relative  $\Delta\Delta$ Ct method (Livak and Schmittgen, 2001) and normalized to *rpoD* expression.

Growth and viability assays. For plate assays, strains were grown to  $OD_{660} = 0.2$ -0.5 in permissive media, washed twice in PYE medium with no additions, and diluted to  $OD_{660} = 0.1$ . 10 µl drops of ten-fold serial dilutions were pipetted onto permissive and nonpermissive media. Plates were incubated for 3 days at 30°C, and images are representative of at least three independent trials. For end-point growth assays in liquid media, strains were grown in permissive media to  $OD_{660} = 0.2$ -0.5. After washing in PYE medium without additions, cells were resuspended at  $OD_{660} = 0.01$  in permissive and nonpermissive media.  $OD_{660}$  values were measured after 24 h growth at 30°C. Growth curves where  $OD_{660}$  and colony forming units (cfu)/ml were measured at 3h intervals were performed using 3-4 ml cultures shaken at 250 rpm in a 30°C incubator. Growth curves where  $OD_{660}$  was measured every 15 min were performed in a BioTek Epoch2 microplate reader held at 30°C with constant shaking at 567 cpm between reads.

**Disc diffusion assays.** Cultures were grown to mid-exponential phase (OD<sub>660</sub> 0.2-0.5), and an amount of cells equivalent to 250 µl of culture at OD<sub>660</sub> = 0.2 was added to 4 ml of PYE swarm agar (0.3% w/v agar) pre-warmed to 42°C. Swarm agar containing bacteria was spread onto solid PYE and allowed to set. Antibiotics or detergents (10 µl each) were added to sterile Whatman filter disks and allowed to dry in a fume hood before discs were placed onto swarm agar surfaces. Plates were incubated upright at 30°C for 24 hours. The diameters of the zones of clearing or haze were measured, and the diameter of the disk (6 mm) was subtracted from all measurements to yield the reported values. The total amount of antibiotic or detergent added to each disk is as follows: kanamycin (100 μg), rifampicin (100 μg), vancomycin (1 mg), CHIR-090 (100  $\mu g$ , APExBIO), bacitracin (50  $\mu g$ ), TWEEN 20 (10  $\mu L$  of 10% solution), Triton X-100 (10  $\mu L$ of 10% solution), sodium dodecyl sulfate (10 µL of 10% solution). Tests using CHIR-090 used one quarter of the standard amount of cells to reduce growth haze. For strains overexpressing genes integrated at the vanA locus, uninduced cells were grown in PYE/kanamycin or PYE/gentamicin, and aliquots were plated in PYE swarm agar on PYE medium. Induced cells were grown in PYE/kanamycin or PYE/gentamicin containing 0.5 mM vanillate before plating in/on PYE medium containing 0.5 mM vanillate. 100 µM 2,2'-dipyridyl was included in media for testing chemical sensitivity in iron-restricted conditions.

**Streptonigrin sensitivity.** Isolated colonies of the indicated strains were grown in PYE medium to  $OD_{660} = 0.2$ -0.5 and diluted to  $OD_{660} = 0.01$ . The diluted culture was aliquoted into separate tubes, which received 0.025 µg/ml, 0.25 µg/ml, or no streptonigrin (SNG). After 24 h of growth at 30°C,  $OD_{660}$  values were measured, and optical density ratios (0.25 µg/ml SNG/no addition and 0.025 µg/ml SNG/no addition) were calculated as a measure of growth inhibition.

**Limulus amebocyte lysate assay.** The ToxinSensor Chromogenic LAL Endotoxin Assay kit (GenScript) was used to determine endotoxin units/mL of culture. Cells were grown to midexponential phase (OD<sub>660</sub> 0.2-0.5), washed twice with non-pyrogenic LAL reagent water, and normalized in this water to OD<sub>660</sub> = 0.1. Cell suspensions were serially diluted in non-pyrogenic water and analyzed according to manufacturer's instructions.

 Gel electrophoresis of lipid A species. For visualizing LPS species from whole-cell lysates, cells were harvested after overnight growth in the indicated medium. All cultures were normalized by OD<sub>660</sub>, pelleted, and resuspended to 100 μL in 1x tricine loading buffer (100 mM Tris-HCl pH 6.8, 1% sodium dodecyl sulfate (SDS), 20% glycerol, 0.02% Coomassie G-250, 1% 2-mercaptoethanol). Proteinase K (125 ng/μL final concentration) was added, and samples were incubated overnight at 55°C. Lysates were boiled 5 min, and equal volumes (10% of each sample) were analyzed by gel electrophoresis.

Hot aqueous-phenol LPS extractions were adapted from Westpahl and Jann (Davis and Goldberg, 2012; Westphal and Jann, 1965). 1 mL of culture at  $OD_{660}$  = 0.75 was pelleted and resuspended in 200 µL 1x tricine loading buffer. Suspensions were boiled for 15 min and cooled to room temperature. 5 µL of 20 mg/mL Proteinase K was added to each sample before incubation at 55°C for three hours. Suspensions were mixed with 200 µL ice-cold Tris-saturated phenol, vortexed, and incubated at 65°C for 15 minutes before being cooled to room temperature. 1 mL diethyl ether was added to each sample before vortexing and spinning for 10 minutes in a table-top centrifuge at 16,000 x g. The bottom blue layer was removed to a fresh tube, and the extraction was repeated on the blue layer starting from the phenol step. 200 µL 2x tricine loading buffer was added to each sample before gel electrophoresis.

Rough LPS was extracted by the method of Darveau and Hancock (Darveau and Hancock, 1983), modified as described (Hershey et al., 2019), beginning with 50 ml PYE cultures grown to  $OD_{660} = 0.85$ . Cultures were centrifuged, and cell pellets were resuspended in 2 ml 10 mM Tris-HCl (pH 8.0) containing 2 mM MgCl<sub>2</sub>. Samples were sonicated (Qsonica Q500) on ice for 5 min at 20% amplitude, in cycles of 10 sec on/20 sec off so that fewer than 5% of

cells remained intact. DNase I and RNase A were added to final concentrations of 100  $\mu$ g/ml and 25  $\mu$ g/ml, respectively, and lysates were incubated at 37°C for 1 hour. Additional DNase I and RNase A were added to reach final concentrations of 200  $\mu$ g/ml and 50  $\mu$ g/ml, respectively, and lysates were incubated for 1 hour at 37°C. SDS and EDTA were added to achieve final concentrations of 2% and 100 mM, respectively, and lysates were incubated for 2 h at 37°C before centrifugation (30 min at 50,000 x g, 30 min, 4°C). Proteinase K (50  $\mu$ g/ml) was added to each supernatant, followed by incubation for 2 h at 60°C. LPS was precipitated by the addition of 2 volumes of ice-cold 0.375 M MgCl<sub>2</sub>/95% ethanol and collected by centrifugation (12,000 x g, 15 min, 4°C). Precipitates were resuspended in 3.3 ml 10 mM Tris-HCl (pH8.0)/2% SDS/100 mM EDTA and incubated with shaking overnight at 37°C. Rough LPS was reprecipitated using 2 volumes ice-cold 0.375 M MgCl<sub>2</sub>/95% ethanol and collected by centrifugation (12,000 x g, 15 min, 4°C). Precipitates were suspended in 10 mM Tris-HCl (pH 8.0) and centrifuged (200,000 x g, 2 h, 4°C). After removal of the supernatant by pipetting, LPS pellets were resuspended in 1 mll 1x tricine loading buffer, and 5  $\mu$ l were analyzed by gel electrophoresis.

Free lipid A was extracted by the Caroff method (El Hamidi et al., 2005), modified as described (Leung et al., 2017), starting with 10 ml of PYE culture grown to  $OD_{600} = 0.6$ . Cultures were divided into multiple tubes and centrifuged at 14,000 x q for 2 min. In a fume hood, cell pellets from each culture were resuspended, combined, and transferred to a gasketed microcentrifuge tube using 250 µl 70% (v/v) isobutyric acid + 150 µl 1 M ammonium hydroxide. Samples were incubated in a boiling water bath in a fume hood for 1 h, with vortexing every 15 min. Samples were cooled on ice and centrifuged at 2000 x g for 15 min. In a fume hood, supernatants (~400 µl) were transferred to new gasketed tubes, each containing 400 µl endotoxin-free water. Small holes were punched in the gasketed caps using a syringe needle before the samples were frozen in liquid nitrogen and lyophilized overnight. Methanol (1 ml) was added, and samples were sonicated in a water bath for 5 min. Samples were centrifuged at 10,000 x g for 5 min, and methanol was aspirated. The methanol wash was repeated before lipids were solubilized in 190 µl 3:1.5:0.25 v/v/v chloroform:methanol:endotoxin-free water. After vortexing, samples were centrifuged at 8,000 x g for 5 min. Supernatants were transferred to fresh gasketed tubes, and extracts were dried under a stream of nitrogen before analysis by mass spectrometry (see below) or gel electrophoresis. Samples for gel electrophoresis were resuspended using 100 μl 1x tricine loading buffer, and 10 μl of each sample was analyzed.

All lipid samples were analyzed on 16.5% Mini-PROTEAN Tris-Tricine gels (Bio-Rad). Carbohydrates were stained using Pro-Q Emerald 300 Lipopolysaccharide Gel Stain Kit (Molecular Probes; P20495) per manufacturer's instructions. For Western blot analysis of S-

LPS, equal numbers of cells grown in PYE with appropriate additions were pelleted, resuspended in 1x SDS loading buffer, and boiled before analysis on 12% polyacrylamide gels and transfer to Immobilon-P PVDF membranes. Blots were probed with α-S-LPS (1:20,000) (Walker et al., 1994) and horseradish peroxidase-conjugated anti-rabbit antibodies (1:5000) and analyzed using Western Lightning (Perkin Elmer). Stained lipid species were visualized using a Bio-Rad Gel Doc XR.

102310241025

1026

1027

1028

1029

1030

1031

1032

1033

1034

1035

1036

1037

1038

1039

1040

1041 1042

1043

1044

1018

1019

1020

1021

1022

High performance liquid chromatography-tandem mass spectrometry (HPLC-MSMS) of lipid A extracts. All samples for HPLC-electrospray ionization tandem mass spectrometry were generated by the modified Caroff extraction protocol described above. Each extract was initially dissolved in 100 µL 1:2 chloroform: methanol before dilution 1:10 with methanol for analysis. A 2-5 µL aliquot of each solution was injected onto a Phenomenex Jupiter C4 column (2 x 50 mm, 5 μm, 300 Å) for HPLC-MSMS analysis with a Waters Acquity UPLC system coupled to a Thermo LTQ-Orbitrap Velos Pro mass spectrometer, which was equipped with an atmospheric pressure electrospray ionization source. For lipid detection, the HPLC-MSMS analyses were carried out with full-mass detection over a mass range of *m/z* 250 to 2000 in the Fourier transform MS mode, with negative-ion detection. The mass resolution was 60,000 FWHM @ m/z 400. Fragmentation product ion masses of the three most intense precursor ions were measured in the ion trap or orbitrap (7500 resolution) mass analyzer using stepped collisioninduced dissociation (35% of the normalized collision energy) or Higher energy collision-induced dissociation (35% of the normalized collision energy) activation energies. During data acquisitions, real-time mass calibration was applied with m/z 283.26454 as the lock mass for negative-ion detection. The mobile phase for separation was (A) 1 mM ammonium acetate solution and (B) 90% (1:1 acetonitrile/propanol)/10% water/1 mM ammonium acetate as the binary solvents for the 16-minute gradient elution: 0 to 10 min, 30% to 100%B; 10 to 12 min, 100% B and 12 to 12.1 min at 30% B, followed by column equilibration at 30% B from 12.1 to 16 min. The column flow rate was 0.35 mL/min and the column temperature was maintained at 40°C.

104510461047

1048

1049

10501051

**Lipid A structure analysis.** MALDI-TOF MS was used to screen lipid extracts. To check structures, tandem MS and ancillary separation techniques were required. These are described below. HPLC-MSMS (above) describes the generation of data for structure determinations in Fig. S3. Notably, the triple deletion strain  $\Delta ctpA$   $\Delta fur$   $\Delta sspB$  contained no lipid A with sugars at the terminal (1 and 4') positions but rather contained phosphates, as found in canonical lipid A

structures. The  $\Delta lpxC$   $\Delta fur$   $\Delta sspB$  strain contained an ion at 1412 m/z, the structure of which remains unclear. The HPLC-MSMS data of this ion showed no loss of phosphate, as seen in  $\Delta ctpA$   $\Delta fur$   $\Delta sspB$ , nor loss of sugars, as seen for the NA1000,  $\Delta sspB$ , or  $\Delta fur$   $\Delta sspB$  strains. The fragmentation pattern strongly suggested that something other than lipid A was responsible for the ion at 1412 m/z. Given that cardiolipin is a common microbial membrane lipid, we carried out HILIC-MS (described below) with cardiolipin and lipid A standards. Both standards were retained by HILIC, as expected for hydrophobic molecules, but extracts from the  $\Delta lpxC$   $\Delta fur$   $\Delta sspB$  mutant showed no ions at all, suggesting that the species at 1412 m/z is not hydrophobic enough to be retained. Regrettably, there remains no structure identified for the ion at 1412 m/z. Generally, structure analysis was conducted manually according to our prior effort in this field (Yoon et al., 2016).

Hydrophobic interaction liquid chromatography-mass spectrometry (HILIC-MS). A 10-μL aliquot of each solution was injected into a Waters Atlantis HILIC column (4.6 mm x 150 mm, 5 μm) to run LC-MS on a Water Acquity UPLC system coupled to a Thermo LTQ-Orbitrap Velos Pro mass spectrometer, which was equipped with an atmospheric pressure electrospray ionization source. For lipid detection, the HILIC-MS runs were carried out with full-mass detection over a mass range of *m/z* 80 to 2000 in the Fourier transform MS mode, with positive-ion and negative-ion detection, respectively, in two rounds of LC injections. The mass resolution was 60,000 FWHM @ *m/z* 400. During data acquisitions, real-time mass calibration was applied with *m/z* 391.28426 as the lock mass for positive-ion detection and with *m/z* 112.98563 as the lock mass for negative-ion detection. The mobile phase of HILIC was (A) 20 mM ammonium acetate solution (pH adjusted to 4.0 with acetic acid) and (B) methanol as the binary solvents for gradient elution: 0-4 min, 99% B; 4 to 12.5 min, 99% to 20% B and 12.5 to 15 min at 20% B, followed by column equilibration at 99% B for 5 min between injections. The column flow rate was 0.4 mL/min and the column temperature was maintained at 40°C.

**Microscopy.** Cells were immobilized on agarose pads (1% w/v in reverse osmosis-purified water). Images were taken using a Zeiss EC Plan-Neofluar 100x/1.3 Oil M27 objective on a Zeiss AxioImager M1 microscope with a Hamamatsu Digital CCD Camera (C8484-03G01). Images were acquired using iVision-Mac software (BioVision Technologies) and processed using ImageJ (Rasband, W.S., ImageJ, U. S. National Institutes of Health, Bethesda, Maryland, USA, https://imagej.nih.gov/ij/, 1997-2018).

**CryoEM imaging.** Cultures (5 mL) of KR4000, KR4102, KR4103, and KR3906 grown to OD<sub>660</sub> 0.2-0.5 were centrifuged (4°C, 16,000 x g, 15 minutes), and cell pellets were resuspended in 50  $\mu$ L PYE. For KR3906, cells grown in PYEX were washed twice with PYE, released into PYED at OD<sub>660</sub> = 0.02, and incubated for 12 hours before harvest. 3  $\mu$ L of cell suspension, mixed 1:1 with Fiducial markers (10-nm gold particles conjugated to Protein A; Aurion) was applied to glow-discharged quantifoil grids (R2/2) and frozen in liquid ethane using an automatic plunge freezing device (Vitrobot, FEI. 12°C, 8-12s blot time, blot force 8, humidity 100%).

Grids of KR4000 and KR4103 were imaged on a Jeol3100 cryoTEM operating at 300kV with in column omega energy filter and K2 direct electron camera. Grids of KR4102 and KR3906 were imaged on a Krios Cryo TEM (FEI) operating at 300kV with post column energy filter (Quantum, GATAN) and K2 direct electron camera. All data were collected with the automatic data collection program serialEM (Mastonarde, 2005). Square overview images were acquired using a defocus of 80-100 microns at a nominal magnification of 3600-6500x (Krios) or 1200x (Jeol) using the polygon montage operation (specimen pixel size: 33-67Å). Beam intensity was set to 8e<sup>-</sup>/px/s over an empty hole and exposure times ranged from 2-5s depending on ice thickness. Bidirectional tomographic tilt series were collected from ±60° using a defocus of 6-8 µm and at a magnification which provided specimen pixel size of 4-7 Å. Total dose of the tilt series were kept between 60-90 e<sup>-</sup>/Å<sup>2</sup>. All tilt series images were collected in movie mode and the frames aligned using MotionCor2 (Zheng et al., 2017), Aligned frames were compiled into stacks and processed using IMOD (Kremer et al., 1996). Contrast of resulting tomograms was enhanced using a non-linear anisotropic diffusion filter (Frangakis and Hegerl, 2001) and manually segmented using the 3D visualization program AMIRA (ThermoFisher).

**RB-Tnseq analysis.** A 1 ml aliquot of the RB-Tnseq library in NA1000 (Price et al., 2018) was thawed and grown to  $OD_{660} = 0.65$  in 25 ml PYE medium with kanamycin. Aliquots of this culture were saved for sequencing of pre-challenge barcodes, or were diluted to  $OD_{660} = 0.02$  in PYE medium (set8IT011, set8IT023, and set8IT035) or PYE medium with 2 µg/ml CHIR-090 (set8IT012, set8IT024, and set8IT036). Cultures were grown for 9 hours at 30°C as described (Price et al., 2018) before cells were harvested and post-challenge barcodes were sequenced. Gene fitness (f) and significance (t) scores were calculated as described (Wetmore et al., 2015). Candidate genes examined in this study ( $CCNA_01217-01220$ ) had fitness scores between -1.5 and -3.7, with signficance scores between -3.0 and -8.4, for individual trials of library growth in PYE + CHIR-090.

1120 1121 Sphingolipid extraction and liquid chromatography-tandem mass spectrometry (LC-1122 MS/MS). Caulobacter strains were grown overnight with or without 0.5 mM vanillate (5 ml), and 1123 lipids were extracted by the method of Bligh and Dyer (Bligh and Dyer, 1959). Cells were 1124 harvested and resuspended in 1 ml of water, 3.75 ml of 1:2 (v/v) chloroform: methanol was 1125 added, and the samples were mixed by vortexing. Chloroform (1.25 ml) and water (1.25 ml) 1126 were added sequentially with vortexing to create a two-phase system and the samples were 1127 centrifuged at 200 x g for 5 minutes at room temperature. The bottom, organic phase was 1128 transferred to a clean glass tube with a Pasteur pipette and washed twice in "authentic" upper 1129 phase. Subsequently, the organic phase containing lipids was collected and dried under argon. 1130 Our methods for lipid analysis by normal phase LC/ESI-MS/MS have been described (Guan et 1131 al., 2014). Briefly, normal phase LC was performed on an Agilent 1200 Quaternary LC system 1132 equipped with an Ascentis Silica HPLC column, 5 µm, 25 cm × 2.1 mm (Sigma-Aldrich, St. 1133 Louis, MO) as described. The LC eluent (with a total flow rate of 300 µl/min) was introduced into 1134 the ESI source of a high resolution TripleTOF5600 mass spectrometer (Applied Biosystems, 1135 Foster City, CA). Instrumental settings for negative ion ESI and MS/MS analysis of lipid species were as follows: ion spray voltage (IS) = -4500 V; curtain gas (CUR) = 20 psi; ion source gas 1 1136 1137 (GSI) = 20 psi; declustering potential (DP) = -55 V; and focusing potential (FP) = -150 V. The

11401141

1142

1143

1139

1138

#### **QUANTIFICATION AND STATISTICAL ANALYSIS**

TF1.5 software (Applied Biosystems, Foster City, CA).

GraphPad Prism 9.3.1 was used for statistical analyses. Statistical details of experiments can be found in the figure legends. Statistical analysis of RB-Tnseq data is described in Wetmore *et al.* 2015, and at <a href="https://fit.genomics.lbl.gov">https://fit.genomics.lbl.gov</a>.

MS/MS analysis used nitrogen as the collision gas. Data analysis was performed using Analyst

11441145

1146

# **KEY RESOURCES TABLE**

REAGENT or RESOURCE	SOURCE	IDENTIFIER
Antibodies		
rabbit α-S-LPS (recognizes smooth	John Smit, University of British	Walker <i>et al.,</i> 1994
LPS of Caulobacter crescentus)	Columbia	
Bacterial and Virus Strains		
	Adam Deutschbauer, Lawrence	Price, <i>et al.</i> 2018
constructed in Caulobacter crescentus NA1000	Berkeley National Laboratory and Plant & Microbial Biology, UC Berkeley	
Please see Table S6 for a list of strains.		
Chemicals, Peptides, and Recombinant Proteins		
streptonigrin	Sigma-Aldrich	Cat#S1014 CAS 3930-19-6
Q5 High-Fidelity DNA Polymerase	New England Biolabs	Cat#M0491
NEBuilder HiFi DNA Assembly Master Mix	New England Biolabs	Cat#E2621
2,2-dipyridyl	Acros Organics (now Thermo Scientific)	Cat#AC117500100 CAS 366-18-7
CHIR-090	APExBIO	Cat#A3307 CAS 728865-23-4
Bacto Peptone	Becton Dickinson, acquired through our stockroom	Lot# 9239004 Ref#211677
Agar Granulated Bacteriological Grade	Apex BioResearch Products	Cat#20-248 Lot#AB-2010160
PowerUp SYBR Green Master Mix	Thermo Scientific	Cat#A25777
High Capacity cDNA Reverse- Transcription Kit	Thermo Scientific	Cat#4368813
DNeasy Blood & Tissue Kit	Qiagen	Cat#69504
16.5% Mini- PROTEAN Tris- Tricine gels	Bio-Rad	Cat#4563063
RNeasy Kit	Qiagen	Cat#74004
Critical Commercial Assays		
Pro-Q Emerald 300 Lipopolysaccharide Gel Stain Kit	Thermo Fisher	Cat#P20495

ToxinSensor	ConCorint	Cat#1 00350
Chromogenic LAL	GenScript	Cat#L00350
Endotoxin Assay		
Deposited Data		
RB-Tnseq data	Fitness Browser	Caulobacter crescentus NA1000
·	https://fit.genomics.lbl.gov	library grown in PYE medium: set8IT011, set8IT023, and set8IT035. Caulobacter crescentus NA1000 library grown in PYE medium with 2µg/ml CHIR- 090: set8IT012, set8IT024, and set8IT036.
Transcriptomic data		da Silva Neto <i>et al</i> ., 2013
for Caulobacter		
crescentus NA1000		
wild-type, $\Delta fur$ , and wild-type treated		
with 2,2-dipyridyl		
Transcriptomic data		Leaden <i>et al</i> ., 2018
for Caulobacter		,
crescentus NA1000		
wild-type, $\Delta fur$ , and		
wild-type treated with 2,2-dipyridyl		
For genome	Sequence Read Archive,	
resequencing	https://www.ncbi.nlm.nih.gov/sra, BioProject	
accession	ID PRJNA526705	
numbers, see Table		
numbers, see Table S6		
S6 Oligonucleotides For oligonucleotide		
S6 Oligonucleotides For oligonucleotide sequences see		
S6 Oligonucleotides For oligonucleotide sequences see Table S8		
Oligonucleotides For oligonucleotide sequences see Table S8 Recombinant DNA		
S6 Oligonucleotides For oligonucleotide sequences see Table S8 Recombinant DNA For plasmids used		
Oligonucleotides For oligonucleotide sequences see Table S8 Recombinant DNA For plasmids used in this study see		
Oligonucleotides For oligonucleotide sequences see Table S8 Recombinant DNA For plasmids used in this study see Table S7		
Oligonucleotides For oligonucleotide sequences see Table S8 Recombinant DNA For plasmids used in this study see	rithms	
Oligonucleotides For oligonucleotide sequences see Table S8 Recombinant DNA For plasmids used in this study see Table S7 Software and Algo		
Oligonucleotides For oligonucleotide sequences see Table S8 Recombinant DNA For plasmids used in this study see Table S7 Software and Algo Bowtie2	rithms Langmead and Salzberg, 2013	
Oligonucleotides For oligonucleotide sequences see Table S8 Recombinant DNA For plasmids used in this study see Table S7 Software and Algo Bowtie2 FreeBayes	rithms Langmead and Salzberg, 2013 Garrison and Marth, 2012	
Oligonucleotides For oligonucleotide sequences see Table S8 Recombinant DNA For plasmids used in this study see Table S7 Software and Algo Bowtie2 FreeBayes iVision-Mac	rithms  Langmead and Salzberg, 2013  Garrison and Marth, 2012  BioVision Technologies  Rasband, W.S., ImageJ, U. S. National Institutes of Health, Bethesda,	
Oligonucleotides For oligonucleotide sequences see Table S8 Recombinant DNA For plasmids used in this study see Table S7 Software and Algo Bowtie2 FreeBayes iVision-Mac	rithms  Langmead and Salzberg, 2013  Garrison and Marth, 2012  BioVision Technologies  Rasband, W.S., ImageJ, U. S. National Institutes of Health, Bethesda, Maryland, USA,	
Oligonucleotides For oligonucleotide sequences see Table S8 Recombinant DNA For plasmids used in this study see Table S7 Software and Algo Bowtie2 FreeBayes iVision-Mac ImageJ	rithms  Langmead and Salzberg, 2013  Garrison and Marth, 2012  BioVision Technologies  Rasband, W.S., ImageJ, U. S. National Institutes of Health, Bethesda, Maryland, USA, https://imagej.nih.gov/ij/, 1997-2018	
Oligonucleotides For oligonucleotide sequences see Table S8 Recombinant DNA For plasmids used in this study see Table S7 Software and Algo Bowtie2 FreeBayes iVision-Mac	rithms  Langmead and Salzberg, 2013  Garrison and Marth, 2012  BioVision Technologies  Rasband, W.S., ImageJ, U. S. National Institutes of Health, Bethesda, Maryland, USA,	

Analyst TF1.5	Applied Biosystems
Galaxy	Afgan <i>et al.</i> 2016
Cutadapt	Martin, 2011
GraphPad Prism 9.3.1 for statistical analyses	GraphPad Software, LLC
IMOD	Kremer, <i>et al,</i> . 1996
serialEM	Mastonarde <i>et al.</i> , 2005

## **Supplemental Information Titles and Legends**

1149

Movie S1, related to Figure 2. Tomogram of *Caulobacter crescentus* NA1000 grown to midexponential phase in PYE.

1152

1153 **Movie S2, related to Figure 2.** Tomogram of  $\triangle ctpA$   $\triangle sspB$   $\triangle fur$  grown to mid-exponential phase in PYE.

1155

1156 **Movie S3, related to Figure 2.** Tomogram of  $\triangle lpxC \triangle sspB \triangle fur$  grown to mid-exponential phase in PYE.

1158

1159 **Movie S4, related to Figure 2.** Tomogram of  $\triangle ctpA$   $\triangle sspB$  + pJS14-P<sub>xy/x</sub>-ctpA-3xFLAG-ssrA 1160 grown to mid-exponential phase in PYEX, washed twice with PYE, released into PYED at OD<sub>660</sub> 1161 = 0.02, and incubated for 10 hours before harvest.

1162 1163

## References

1164

- Afgan, E., Baker, D., Beek, M. van den, Blankenberg, D., Bouvier, D., Cech, M., Chilton, J.,
- 1166 Clements, D., Coraor, N., Eberhard, C., et al. (2016). The Galaxy platform for accessible,
- reproducible and collaborative biomedical analyses: 2016 update. Nucleic Acids Res. *44*, W3–1168 W10.

1169

- 1170 Altschul, S. (1997). Gapped BLAST and PSI-BLAST: a new generation of protein database search programs. Nucleic Acids Research *25*, 3389–3402.
- Altschul, S.F., Gish, W., Miller, W., Myers, E.W., and Lipman, D.J. (1990). Basic local alignment search tool. J. Mol. Biol. *215*, 403–410.
- 1174 Andrews, S., Norton, I., Salunkhe, A.S., Goodluck, H., Aly, W.S.M., Mourad-Agha, H., and
- 1175 Cornelis, P. (2013). Control of iron metabolism in bacteria. Met. Ions Life Sci. 12, 203–239.

- 1177 Awram, P., and Smit, J. (2001). Identification of lipopolysaccharide O antigen synthesis genes
- required for attachment of the S-layer of *Caulobacter crescentus*. Microbiology *147*, 1451–1460.

- Bligh, E.G., and Dyer, W.J. (1959). A rapid method of total lipid extraction and purification. Can
- 1181 J. Biochem. Physiol. 37, 911–917.

1182

- Blondelet-Rouault, M.H., Weiser, J., Lebrihi, A., Branny, P., and Pernodet, J.L. (1997). Antibiotic
- resistance gene cassettes derived from the omega interposon for use in *E. coli* and
- 1185 Streptomyces. Gene 190, 315–317.

1186

- 1187 Boll, J.M., Crofts, A.A., Peters, K., Cattior, V., Vollmer, W., Davies, B.W., and Trent, M.S.
- 1188 (2016). A penicillin-binding protein inhibits selection of colistin-resistant, lipooligosaccharide-
- deficient Acinetobacter baumannii. Proc. Natl. Acad. Sci. USA 113, E6228–E6237.

1190

- Brown, D.B., Forsberg, L.S., Kannenberg, E.L., and Carlson, R.W. (2012). Characterization of
- galacturonosyl transferase genes rgtA, rgtB, rgtC, rgtD, and rgtE responsible for
- 1193 lipopolysaccharide synthesis in nitrogen-fixing endosymbiont *Rhizobium leguminosarum*:
- lipopolysaccharide core and lipid galacturonosyl residues confer membrane stability. J. Biol.
- 1195 Chem. 287, 935–949.

1196

- Brown, D.B., Muszynski, A., and Carlson, R.W. (2013). Elucidation of a novel lipid A alpha-(1,1)-
- 1198 GalA transferase gene (*rgtF*) from *Mesorhizobium loti*: Heterologous expression of *rgtF* causes
- 1199 Rhizobium etli to synthesize lipid A with alpha-(1,1)-GalA. Glycobiology 23, 546–558.

1200

- 1201 Christen, B., Abeliuk, E., Collier, J.M., Kalogeraki, V.S., Passarelli, B., Coller, J.A., Fero, M.J.,
- 1202 McAdams, H.H., and Shapiro, L. (2011). The essential genome of a bacterium. Mol. Syst. Biol.
- 1203 7, 528.

1204

- 1205 Crosson, S., McGrath, P.T., Stephens, C., McAdams, H.H., and Shapiro, L. (2005). Conserved
- modular design of an oxygen sensory/signaling network with species-specific output. Proc. Natl.
- 1207 Acad. Sci. USA 102, 8018-8023.

1208

- 1209 Darveau, R.P., and Hancock, R.E. (1983). Procedure for isolation of bacterial
- 1210 lipopolysaccharides from both smooth and rough *Pseudomonas aeruginosa* and *Salmonella*
- 1211 *typhimurium* strains. J. Bacteriol. *155*, 831–838.

1212

- 1213 Davis, M.R.J., and Goldberg, J.B. (2012). Purification and visualization of lipopolysaccharide
- 1214 from Gram-negative bacteria by hot aqueous-phenol extraction. J. Vis. Exp. e3916.

1215

- 1216 De Castro, C., Molinaro, A., Lanzetta, R., Silipo, A., and Parrilli, M. (2008). Lipopolysaccharide
- 1217 structures from Agrobacterium and Rhizobiaceae species. Carbohydr. Res. 343, 1924–1933.

- 1219 Dehio, C., and Meyer, M. (1997). Maintenance of broad-host-range incompatibility group P and
- 1220 group Q plasmids and transposition of Tn5 in Bartonella henselae following conjugal plasmid
- transfer from *Escherichia coli*. J. Bacteriol. 179, 538–540.

- 1223 El Hamidi, A., Tirsoaga, A., Novikov, A., Hussein, A., and Caroff, M. (2005). Microextraction of
- 1224 bacterial lipid A: Easy and rapid method for mass spectrometric characterization. J. Lipid Res.
- 1225 *46*, 1773–1778.

1226

1227 Ely, B. (1991). Genetics of *Caulobacter crescentus*. Methods Enzymol. 204, 372–384.

1228

- 1229 Evinger, M., and Agabian, N. (1977). Envelope-associated nucleoid from *Caulobacter*
- 1230 crescentus stalked and swarmer cells. J.Bacteriol. 132, 294–301.
- 1231 Fontenot, C.R., Tasnim, H., Valdes, K.A., Popescu, C.V., and Ding, H. (2020). Ferric uptake
- regulator (Fur) reversibly binds a [2Fe-2S] cluster to sense intracellular iron homeostasis in
- 1233 Escherichia coli. J. Biol. Chem. 295, 15454–15463.

1234

- 1235 Frangakis, A.S., and Hegerl, R. (2001). Noise reduction in electron tomographic reconstructions
- using nonlinear anisotropic diffusion. J. Struct. Biol. 135, 239–250.

1237

- 1238 Garrison, E., and Marth, G. (2012). Haplotype-based variant detection from short-read
- 1239 sequencing.

1240 Gilchrist, A., and Smit, J. (1991). Transformation of freshwater and marine caulobacters by

1241 electroporation. J. Bacteriol. 173, 921–925.

1242

- 1243 Guan, Z., Katzianer, D., Zhu, J., and Goldfine, H. (2014). Clostridium difficile contains
- 1244 plasmalogen species of phospholipids and glycolipids. Biochim. Biophys. Acta 1842, 1353-
- 1245 1359.

1246

- Hassett, D.J., Britigan, B.E., Svendsen, T., Rosen, G.M., and Cohen, M.S. (1987). Bacteria form
- 1248 intracellular free radicals in response to paraguat and streptonigrin. Demonstration of the
- 1249 potency of hydroxyl radical. J. Biol. Chem. 262, 13404–13408.

1250

- Henry, R., Crane, B., Powell, D., Lucas, D.D., Li, Z., Aranda, J., Harrison, P., Nation, R.L.,
- 1252 Adler, B., Harper, M., et al. (2015). The transcriptomic response of Acinetobacter baumannii to
- 1253 colistin and diripenem alone and in combination in an in vitro
- 1254 pharmacokinetics/pharmacodynamics model. J. Antimicrob. Chermother. 70, 1303–1313.

1255

- Hershey, D.M., Fiebig, A., and Crosson, S. (2019). A genome-wide analysis of adhesion in
- 1257 Caulobacter crescentus identifies new regulatory and biosynthetic components for holdfast
- 1258 assembly. mBio 10, 2273.

- 1260 Jones, M.D., Vinogradov, E., Nomellini, J.F., and Smit, J. (2015). The core and O-
- polysaccharide structure of the *Caulobacter crescentus* lipopolysaccharide. Carbohydr. Res.
- 1262 *402*, 111–117.

- Justino, M.C., Almeida, C.C., Teixeira, M., and Saraiva, L.M. (2007). *Escherichia coli* di-iron
- 1265 YtfE protein is necessary for the repair of stress-damaged iron-sulfur clusters. J. Biol. Chem.
- 1266 282, 10352-10359.

1267

- 1268 Karbarz, M.J., Kalb, S.R., Cotter, R.J., and Raetz, C.R.H. (2003). Expression cloning and
- biochemical characterization of a *Rhizobium leguminosarum* lipid A 1-phosphatase. J. Biol.
- 1270 Chem 278, 39269–39279.

1271

- 1272 Kawahara, K., Seydel, U., Matsuura, M., Danbara, H., Rietschel, E.T., and Zahringer, U. (1991).
- 1273 Chemical structure of glycosphingolipids isolated from *Sphingomonas paucimobilis*. FEBS Lett.
- 1274 292, 107–110.

1275

- 1276 Kawasaki, S., Moriguchi, R., Sekiya, K., Nakai, T., Ono, E., Kume, K., and Kawahara, K. (1994).
- 1277 The cell envelope structure of the lipopolysaccharide-lacking Gram-negative bacterium
- 1278 Sphingomonas paucimobilis. J. Bacteriol. 176, 284–290.

1279

- 1280 Kremer, J.R., Mastonarde, D.N., and McIntosh, J.R. (1996). Computer visualization of three-
- dimensional image data using IMOD. J. Struct. Biol. 116, 71–76.

1282

- Langmead, B., and Salzberg, S.L. (2012). Fast gapped-read alignment with Bowtie 2. Nat
- 1284 Methods 9, 357–359.
- Leaden, L., Silva, L.G., Ribiero, R.A., Santos, N.M.D., Lorenzetti, A.P.R., Alegria, T.G.P.,
- 1286 Schultz, M.L., Medeiros, M.H.G., Koide, T., and Margues, M.V. (2018). Iron deficiency
- 1287 generates oxidative stress and activation of the SOS response in Caulobacter crescentus.
- 1288 Front. Microbiol. 9, 2014.

1289

- Leung, L.M., Fondrie, W.E., Doi, Y., Johnson, J.K., Strickland, D.K., Ernst, R.K., and Goodlett,
- 1291 D.R. (2017). Identification of the ESKAPE pathogens by mass spectrometric analysis of
- microbial membrane glycolypids. Sci. Rep. 7, 6403.

1293

- Levchenko, I., Seidel, M., Sauer, R.T., and Baker, T.A. (2000). A specificity-enhancing factor for
- the ClpXP degradation machine. Science 289, 2354–2356.

1296

- Liu, L., Feng, X., Wang, W., Chen, Y., Chen, Z., and Gao, H. (2020). Free rather than total iron
- 1298 content is critically linked to the Fur physiology in *Shewanella oneidensis*. Front. Microbiol. 11,
- 1299 593246.

- 1301 Livak, K.J., and Schmittgen, T.D. (2001). Analysis of Relative Gene Expression Data Using
- 1302 Real-Time Quantitative PCR and the 2-ΔΔCT Method. Methods 25, 402–408.

- 1303 Mamat, U., Meredith, T.C., Aggarwal, P., Kuhl, A., Kirchoff, P., Lindner, B., Hanuszkiewicz, A.,
- Sun, J., Holst, O., and Woodard, R.W. (2008). Single amino acid substitutions in either YhjD or
- 1305 MsbA confer viability to 3-deoxy-D-manno-oct-2-ulosonic acid-depleted *Escherichia coli*. Mol.
- 1306 Microbiol. 67, 633–648.

- Marks, M.E., Castro-Rojas, C., Teiling, C., Du, L., Kapatral, V., Walunas, T.L., and Crosson, S.
- 1309 (2010). The genetic basis of laboratory adaptation in Caulobacter crescentus. J. Bacteriol. 192,
- 1310 3678–3688.

1311

- Martin, M. (2011). Cutadapt removes adapter sequences from high-throughput sequencing
- 1313 reads. EMBnet j. 17, 10.
- 1314 Mastonarde, D.N. (2005). Automated electron microscope tomography using robust prediction
- 1315 of specimen movements. J. Struct. Biol. 152, 36–51.

1316

- 1317 McClerren, A.L., Endsley, S., Bowman, J.L., Andersen, N.H., Guan, Z., Rudolph, J., and Raetz,
- 1318 C.R. (2005). A slow, tight-binding inhibitor of the zinc-dependent deacetylase LpxC of lipid A
- biosynthesis with antibiotic activity comparable to ciprofloxacin. Biochemistry 44, 16574–16583.

1320

- Meisenzahl, A.C., Shapiro, L., and Jenal, U. (1997). Isolation and characterization of a xylose-
- dependent promoter from *Caulobacter crescentus*. J. Bacteriol. 179, 592–600.

1323

- Meredith, T.C., Aggarwal, P., Mamat, U., Lindner, B., and Woodard, R.W. (2006). Redefining
- the requisite lipopolysaccharide structure in *Escherichia coli*. ACS Chem. Biol. 1, 33–42.

1326

- Moffatt, J.H., Harper, M., Harrison, P., Hale, J.D., Vinogradov, E., Seemann, T., Henry, R.,
- 1328 Crane, B., Michael, F.S., Cox, A.D., et al. (2010). Colistin resistance in *Acinetobacter baumannii*
- is mediated by complete loss of lipopolysaccharide production. Antimicrob. Agents Chemother.
- 1330 *54*, 4971–4977.

1331

- 1332 Moffatt, J.H., Harper, M., and Boyce, J.D. (2019). Mechanisms of polymyxin resistance. Adv.
- 1333 Exp. Med. Biol. 55-71.

1334

- Nachin, L., El Hassouni, M., Loiseau, L., Expert, D., and Barras, F. (2001). SoxR-dependent
- response to oxidative stress and virulence of *Erwinia chrysanthemi*: the key role of SufC, an
- orphan ABC ATPase. Mol. Microbiol. 39, 960–972.

1338

- Nagiec, M.M., Skrzypek, M., Nagiec, E.E., Lester, R.L., and Dickson, R.C. (1998). The LCB4
- 1340 (YOR171c) and LCB5 (YLR260w) genes of *Saccharomyces* encode sphingoid long chain base
- 1341 kinases. J. Biol. Chem. 273, 19437–19442.

1342

- 1343 Nagy, E., Losick, R., and Kahne, D. (2019). Robust suppression of lipopolysaccharide
- deficiency in *Acinetobacter baumannii* by growth in minimal medium. J. Bacteriol. 201, 420.

- 1346 Nikaido, H. (2003). Molecular basis of bacterial outer membrane permeability revisited.
- 1347 Microbiol. Mol. Biol. Rev. 67, 593-656.

- 1349 Olea-Ozuna, R.J., Poggio, S., Bergström, E., Quiroz-Rocha, E., García-Soriano, D.A.,
- 1350 Sahonero-Canavesi, D.X., Padilla-Gómez, J., Martínez-Aguilar, L., López-Lara, I.M., Thomas-
- Oates, J., et al. (2021). Five structural genes required for ceramide synthesis in *Caulobacter*
- and for bacterial survival. Environ. Microbiol. 23, 143–159.

1353

- Peng, D., Hong, W., Choudhury, B.P., Carlson, R.W., and Gu, X.-X. (2005). *Moraxella*
- 1355 cararrhalis bacterium without endotoxin, a potential vaccine candidate. Infect. Immun. 73, 7569–
- 1356 7577.

1357

- 1358 Plötz, B.M., Lindner, B., Stetter, K.O., and Holst, O. (2000). Characterization of a novel lipid A
- 1359 containing D-galacturonic acid that replaces phosphate residues. The structure of the lipid a of
- the lipopolysaccharide from the hyperthermophilic bacterium *Aquifex pyrophilus*. J. Biol. Chem.
- 1361 275, 11222–11228.

1362

- 1363 Price, M.N., Wetmore, K.M., Waters, R.J., Callaghan, M., Ray, J., Liu, H., Kuehl, J.V., Melnyk,
- 1364 R.A., Lamson, J.S., Suh, Y., et al. (2018). Mutant phenotypes for thousands of bacterial genes
- 1365 of unknown function. Nature *557*, 503–509.

1366

- 1367 Qureshi, N., Takayama, K., Mascagni, P., Honovich, J., Wong, R., and Cotter, R.J. (1988).
- 1368 Complete structural determination of lipopolysaccharide obtained from deep rough mutant of
- 1369 Escherichia coli. Purification by high performance liquid chromatography and direct analysis by
- 1370 plasma desorption mass spectrometry. J. Biol. Chem. 263, 11971–11976.

1371

- 1372 Radolf, J.D., and Kumar, S. (2018). The *Treponema pallidum* outer membrane. Curr. Top.
- 1373 Microbiol. Immuno. *415*, 1–38.

1374

- Rojas, E.R., Billings, G., Odermatt, P.D., Auer, g K., Zhu, L., Miguel, A., Chang, F., Weibel,
- D.B., Theriot, J.A., and Huang, K.C. (2018). The outer membrane is an essential load-bearing
- 1377 element in Gram-negative bacteria. Nature 559, 617–621.

1378

- 1379 Samuel, G., and Reeves, P. (2003). Biosynthesis of O-antigens: Genes and pathways involved
- in nucleotide sugar precursor synthesis and O-antigen assembly. Carboyhdr. Res. 338, 2503–
- 1381 2519.

1382

- 1383 Shapland, E.B., Reisinger, S.J., Bajwa, A.K., and Ryan, K. (2011). An essential tyrosine
- phosphatase homolog regulates cell separation, outer membrane integrity, and morphology in
- 1385 Caulobacter crescentus. J. Bacteriol. 193, 4361–4370.

- da Silva Neto, J.F., Braz, V.S., Italiani, V.C.S., and Marques, M.V. (2009). Fur controls iron
- 1388 homeostasis and oxidative stress defense in the oligotrophic alpha-proteobacterium
- 1389 Caulobacter crescentus. Nucleic Acids Res. 37, 4812–4825.

- da Silva Neto, J.F., Lourenco, R.F., and Marques, M.V. (2013). Global transcriptional response
- of Caulobacter crescentus to iron availability. BMC Genomics 14, 549.

1393

- 1394 Simpson, B.W., Nieckarz, M., Pinedo, V., McLean, A.B., Cava, F., and Trent, M.S. (2021).
- 1395 Acinetobacter baumannii can survive with an outer membrane lacking lipooligosaccharide due
- to structural support from elongasome peptidoglycan synthesis. mBio 12, e0309921.

1397

- 1398 Skerker, J.M., Prasol, M.S., Perchuk, B.S., Biondi, E.G., and Laub, M.T. (2005). Two-
- 1399 component signal transduction pathways regulating growth and cell cycle progresion in a
- 1400 bacterium: A systems-level analysis. PLoS Biol. 3, e334.

1401

- 1402 Smit, J., Kaltashov, I.A., Cotter, R.J., Vinogradov, E., Perry, M.B., Haider, H., and Qureshi, N.
- 1403 (2008). Structure of a novel lipid A obtained from the lipopolysaccharide of *Caulobacter*
- 1404 crescentus. Innate Immun. 14, 25–37.

1405

- 1406 Stankeviciute, G., Guan, Z., Goldfine, H., and Klein, E.A. (2019). Caulobacter crescentus adapts
- to phosphate starvation by synthesizing anionic glycoglycerolipids and a novel
- 1408 glycosphingolipid. mBio 10, 107.

1409

- 1410 Stankeviciute, G., Tang, P., Ashley, B., Chamberlain, J.D., Hansen, M.E.B., Coleman, A.,
- 1411 D'Emilia, R., Fu, L., Mohan, E.C., Nguyen, H., et al. (2021). Convergent evolution of bacterial
- 1412 ceramide synthesis. Nat. Chem. Biol. DOI: 10.1038/s41589-021-00948-7.

1413

- 1414 Steeghs, L., Hartog, R. den, Boer, A. den, Zomer, B., Roholl, P., and Ley, P. van der (1998).
- 1415 Meningitis bacterium is viable without endotoxin. Nature 392, 449–450.

1416

- 1417 Thanbichler, M., Iniesta, A.A., and Shapiro, L. (2007). A comprehensive set of plasmids for
- 1418 vanillate- and xylose-inducible gene expression in *Caulobacter crescentus*. Nucleic Acids Res.
- 1419 35, e137.

1420

- 1421 Toh, E., Jr, H.D.K., and Brun, Y.V. (2008). Characterization of the *Caulobacter crescentus*
- 1422 holdfast polysaccharide biosynthesis pathway reveals significant redundancy in the initiating
- 1423 glycosyltransferase and polyerase steps. J. Bacteriol. 190, 7219–7131.

1424

- 1425 Velkov, T., Thompson, P.E., Nation, R.L., and Li, J. (2010). Structure-activity relationships of
- 1426 polymyxin antibiotics. J. Med. Chem. 53, 1898–1916.

1427

- 1428 Walker, S.G., Karunaratne, D.N., Ravenscroft, N., and Smit, J. (1994). Characterization of
- 1429 mutants of Caulobacter crescentus defective in surface attachment of the paracrystalline
- 1430 surface layer. J. Bacteriol. 176, 6313–6323.

- 1432 Wang, X., Ribeiro, A.A., Guan, Z., McGrath, S.C., Cotter, R.J., and Raetz, C.R.H. (2006).
- 1433 Structure and biosynthesis of free lipid A molecules that replace lipopolysaccharide in
- 1434 Francisella tularensis subsp. novicida. Biochemistry 45, 14427–14440.

Westphal, O., and Jann, K. (1965). Bacterial lipopolysaccharides extraction with phenol-water and further applications of the procedure. Methods Carbohydr. Chem. *5*, 83–91.

1438

- 1439 Wetmore, K.M., Price, M.N., Waters, R.J., Lamson, J.S., He, J., Hoover, C.A., Blow, M.J.,
- Bristow, J., Butland, G., Arkin, A.P., et al. (2015). Rapid quantification of mutant fitness in
- 1441 diverse bacteria by sequencing randomly bar-coded transposons. mBio 6, e00306–e00315.

1442

- 1443 Whitfield, C., and Trent, M.S. (2014). Biosynthesis and export of bacterial lipopolysaccharides.
- 1444 Annu. Rev. Biochem. 83, 99-128.

1445

- 1446 Wofford, J.D., Bolaji, N., Dziuba, N., Outten, F.W., and Lindahl, P.A. (2019). Evidence that a
- respiratory shield in *Escherichia coli* protects a low-molecular-mass Fe(II) pool from O<sub>2</sub>-
- dependent oxidation. J. Biol. Chem. 294, 50–62.

1449

- Yeowell, H.N., and White, J.R. (1982). Iron requirement in the bactericidal mechanism of
- streptonigrin. Antimicrob. Agents Chemother. 22, 961–968.

1452

- 1453 Yoon, S.H., Liang, T., Schneider, T., Oyler, B.L., Chandler, C.E., Ernst, R.K., Yen, G.S., Huang,
- 1454 Y., Nilsson, E., and Goodlett, D.R. (2016). Rapid lipid a structure determination via surface
- 1455 acoustic wave nebulization and hierarchical tandem mass spectrometry algorithm. Rapid
- 1456 Commun. Mass Spectrom. 30, 2555–2560.

1457

- 1458 Zhang, G., Meredith, T.C., and Kahne, D. (2013). On the essentiality of lipopolysaccharide to
- 1459 Gram-negative bacteria. Curr. Opin. Microbiol. 16, 779–785.

1460

- 1461 Zheng, S.Q., Plaovcak, E., Armache, J.P., Verba, K.A., Cheng, Y., and Agard, D.A. (2017).
- 1462 MotionCor2: anisotropic correction of bean-induced motion for improved cryo-electron
- 1463 microscopy. Nat. Methods *14*, 331–332.

- Zhou, B., Schrader, J.M., Kalogeraki, V.S., Abeliuk, E., Dinh, C.B., Pham, J.Q., Cui, Z.Z., Dill,
- 1466 D.L., McAdams, H.H., and Shapiro, L. (2015). The global regulatory architecture of transcription
- during the Caulobacter cell cycle. PLoS Genet. 11, e1004831.

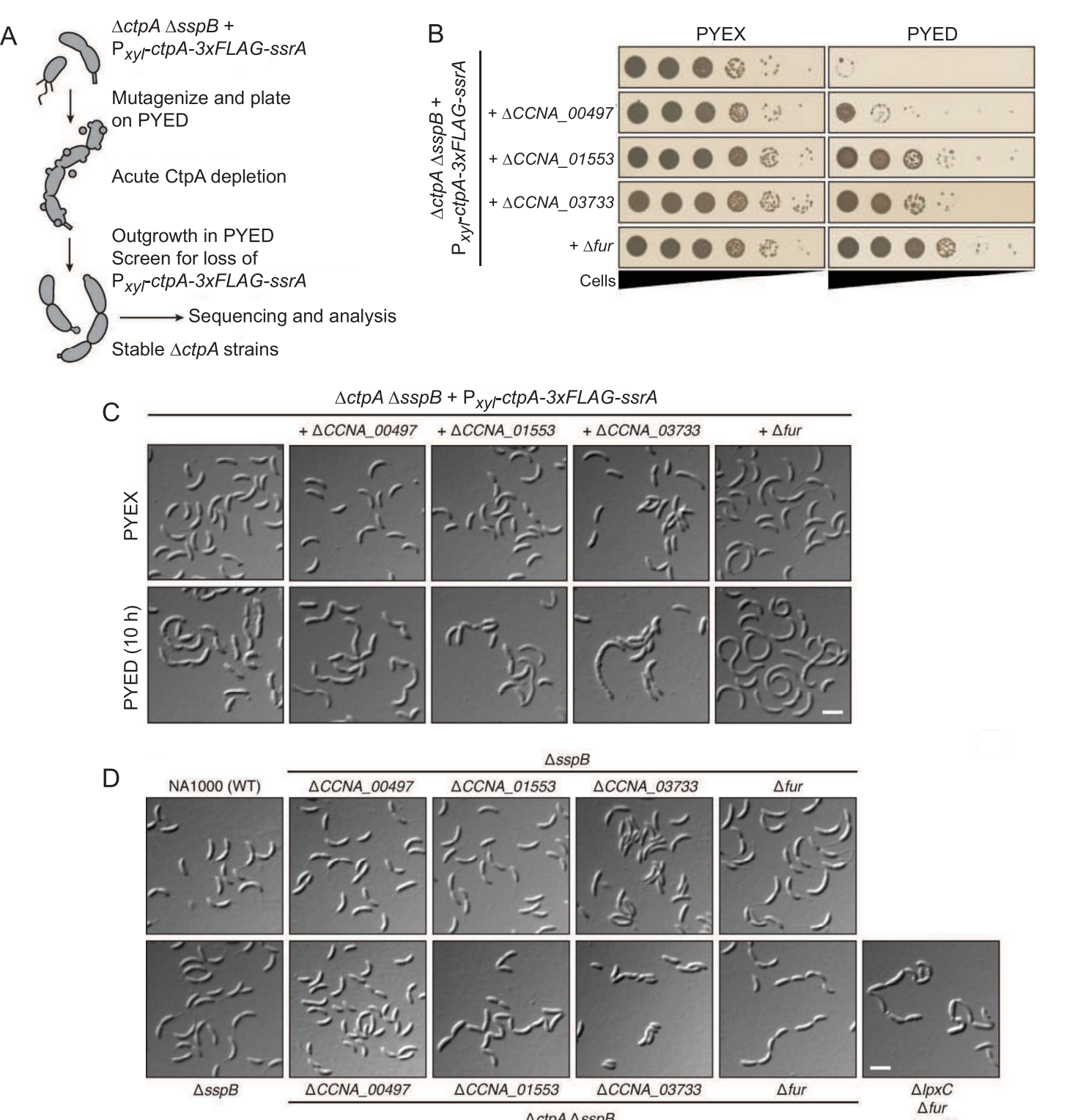
## **KEY RESOURCES TABLE**

		_
REAGENT or RESOURCE	SOURCE	IDENTIFIER
Antibodies		
rabbit α-S-LPS (recognizes smooth LPS of Caulobacter crescentus)	John Smit, University of British Columbia	Walker <i>et al.,</i> 1994
Bacterial and Virus S	trains	
RB-Tnseq library constructed in <i>Caulobacter</i> <i>crescentus</i> NA1000	Adam Deutschbauer, Lawrence Berkeley National Laboratory and Plant & Microbial Biology, UC Berkeley	Price, <i>et al.</i> 2018
Please see Table S6 for a list of strains.		
Chemicals, Peptides	, and Recombinant Proteins	
streptonigrin	Sigma-Aldrich	Cat#S1014 CAS 3930- 19-6
Q5 High-Fidelity DNA Polymerase	New England Biolabs	Cat#M0491
NEBuilder HiFi DNA Assembly Master Mix	New England Biolabs	Cat#E2621
2,2-dipyridyl	Acros Organics (now Thermo Scientific)	Cat#AC117500100 CAS 366-18-7
CHIR-090	APExBIO	Cat#A3307 CAS 728865- 23-4
Bacto Peptone	Becton Dickinson, acquired through our stockroom	Lot# 9239004 Ref#211677
Agar Granulated Bacteriological Grade	Apex BioResearch Products	Cat#20-248 Lot#AB- 2010160
PowerUp SYBR Green Master Mix	Thermo Scientific	Cat#A25777
High Capacity cDNA Reverse- Transcription Kit	Thermo Scientific	Cat#4368813
DNeasy Blood & Tissue Kit	Qiagen	Cat#69504
16.5% Mini- PROTEAN Tris- Tricine gels	Bio-Rad	Cat#4563063
RNeasy Kit	Qiagen	Cat#74004
Critical Commercial	Assays	_
Pro-Q Emerald 300 Lipopolysaccharide Gel Stain Kit	Thermo Fisher	Cat#P20495
ToxinSensor	GenScript	Cat#L00350

Deposited Data RB-Tnseq data Fitness Browser https://fit.genomics.lbl.gov  Caulobacter crescentus NA1000 library grown in PYE medium: set8IT035, aud set8IT035, audobacter crescentus NA1000 library grown in PYE medium with 2µg/ml CHIR-090: set8IT012, set8IT024, and set8IT036.  da Silva Neto et al., 2013  for Caulobacter crescentus NA1000 wild-type, Afur, and wild-type treated with 2,2-dipyridy!  Transcriptomic data for Caulobacter crescentus NA1000 wild-type, Afur, and wild-type treated with 2,2-dipyridy!  For genome resequencing accession numbers, see Table S6 Oligonucleotide sequences see Table S8 Recombinant DNA For plasmids used in this study see Table S7 Software and Algorithms Bowtie2 Langmead and Salzberg, 2013 FreeBayes Garrison and Marth, 2012 Nision-Mac BioVision Technologies ImageJ Rasband, W.S., ImageJ, U. S. National Institutes of Health, Bethesda, Maryland, USA, https://imagej.nih.gov/ij/, 1997-2018 Analyst TF1.5 Applied Biosystems		T	T
Deposited Data RB-Tnseq data Fitness Browser https://fit.genomics.lbl.gov  Caulobacter crescentus NA1000 library grown in PYE medium: set8IT031, and set8IT032, and set8IT035, Caulobacter crescentus NA1000 library grown in PYE medium: set8IT011, set8IT023, and set8IT035, Caulobacter crescentus NA1000 wild-type, Afur, and wild-type, Afur, and wild-type treated with 2,2-dipyridy!  For genome resequencing accession numbers, see Table S6 Oligonucleotides For oligonucleotides For oligonucleotides For oligonucleotides For oligonucleotides For plasmids used in this study see Table S7 Software and Algorithms Bowtie2 Langmead and Salzberg, 2013 FreeBayes Garrison and Marth, 2012  Vision-Mac BioVision Technologies ImageJ Rasband, W.S., ImageJ, U. S. National Institutes of Health, Bethesda, Maryland, U.S., https://imagej.nin.gov/lij/, 1997-2018 AMIRA Thermo Fisher Analyst TF1.5 Applied Biosystems Galaxy Afgan et al. 2016	Chromogenic LAL		
RB-Tnseq data    Fitness Browser https://fit.genomics.lbl.gov   Caulobacter crescentus NA1000 library grown in PYE medium: set8lT011, set8lT023, and set8lT021, set8lT023, and set8lT023, caulobacter crescentus NA1000 library grown in PYE medium with Jug/ml CHIR-909: set8lT012, set8lT036. Caulobacter crescentus NA1000 wild-type, Afur, and wild-type treated with 2,2-dipyridyl Transcriptomic data for Caulobacter crescentus NA1000 wild-type, Afur, and wild-type treated with 2,2-dipyridyl Transcriptomic data for Caulobacter crescentus NA1000 wild-type, Afur, and wild-type treated with 2,2-dipyridyl Transcriptomic data for Caulobacter crescentus NA1000 wild-type, Afur, and wild-type treated with 2,2-dipyridyl Transcriptomic data for Caulobacter crescentus NA1000 wild-type, Afur, and wild-type treated with 2,2-dipyridyl Transcriptomic data for Caulobacter crescentus NA1000 wild-type, Afur, and wild-type treated with 2,2-dipyridyl Transcriptomic data for Caulobacter crescentus NA1000 wild-type, Afur, and wild-type treated with 2,2-dipyridyl Transcriptomic data for Caulobacter crescentus NA1000 wild-type, Afur, and wild-type treated with 2,2-dipyridyl Transcriptomic data for Caulobacter crescentus NA1000 wild-type, Afur, and wild-type treated with 2,2-dipyridyl Transcriptomic data for Caulobacter crescentus NA1000 wild-type, Afur, and wild-type treated with 2,2-dipyridyl Transcriptomic data for Caulobacter crescentus NA1000 wild-type, Afur, and wild-type treated with 2,2-dipyridyl Transcriptomic data for Caulobacter crescentus NA1000 wild-type, Afur, and wild-type treated with 2,2-dipyridyl Transcriptomic data for Caulobacter crescentus NA1000 wild-type treated with 2,2-dipyridyl Transcriptomic data for Caulobacter crescentus NA1000 wild-type treated with 2,2-dipyridyl Transcriptomic data for Caulobacter crescentus NA1000 wild-type treated with 2,2-dipyridyl Transcriptomic data for Caulobacter crescentus NA1000 wild-type treated with 2,2-dipyridyl Transcriptomic data for Caulobacter crescentus NA1000 wild-type treated wi			
crescentus NA1000 library grown in PYE medium: set8IT021, set8IT023, and set8IT035. Caulobacter crescentus NA1000 library grown in PYE medium with 2µg/ml CHIR-090: set8IT012, set8IT024, and set8IT024, and set8IT024, and set8IT024, and set8IT024. set8IT024. and set8IT036.  Transcriptomic data for Caulobacter crescentus NA1000 wild-type, Afur, and wild-type treated with 2,2-dipyridy! Transcriptomic data for Caulobacter crescentus NA1000 wild-type, Afur, and wild-type treated with 2,2-dipyridy! For genome resequencing accession numbers, see Table S6 Oligonucleotides For oligonucleotide sequences see Table S6 Recombinant DNA For plasmids used in this study see Table S7 Software and Algorithms Bowlie2 Langmead and Salzberg, 2013 FreeBayes Garrison and Marth, 2012 IVision-Mac BioVision Technologies ImageJ Rasband, W.S., ImageJ, U. S. National Institutes of Health, Bethesda, Maryland, U.S., https://imagej.nin.gov/lyi/, 1997-2018 MotionCor2 Zheng, et al., 2017 Analyst TF1.5 Applied Biosystems Galaxy Afgan et al. 2016		C:4 D   - 44 //£:4       -     -   -	On what a net a m
for Caulobacter crescentus NA1000 wild-type, \( \text{Aftr}, \) and wild-type treated with 2,2-dipyridyl Transcriptomic data for \( \text{Caulobacter} \) crescentus NA1000 wild-type, \( \text{Aftr}, \) and wild-type, \( \text{Aftr}, \) and wild-type treated with 2,2-dipyridyl For genome resequencing accession numbers, see Table S6 Oligonucleotides For oligonucleotide sequences see Table S8 Recombinant DNA For plasmids used in this study see Table S7 Software and Algorithms Bowtie2	RB-Thiseq data	Fitness Browser https://fit.genomics.ibi.gov	crescentus NA1000 library grown in PYE medium: set8IT011, set8IT023, and set8IT035. Caulobacter crescentus NA1000 library grown in PYE medium with 2µg/ml CHIR-090: set8IT012, set8IT024, and
wild-type treated with 2,2-dipyridyl Transcriptomic data for Caulobacter crescentus NA1000 wild-type, Afur, and wild-type treated with 2,2-dipyridyl For genome resequencing accession numbers, ID PRJNA526705 See Table S6 Oligonucleotides For oligonucleotide sequences see Table S8 Recombinant DNA For plasmids used in this study see Table S7 Software and Algorithms Bowtie2 Langmead and Salzberg, 2013 FreeBayes Garrison and Marth, 2012 iVision-Mac BioVision Technologies ImageJ Rasband, W.S., ImageJ, U. S. National Institutes of Health, Bethesda, Maryland, USA, https://imagej.nih.gov/ij/, 1997-2018 MotionCor2 Zheng, et al., 2017 AMIRA Thermo Fisher Analyst TF1.5 Applied Biosystems Galaxy Afgan et al. 2016	Transcriptomic data for <i>Caulobacter</i> crescentus NA1000 wild-type. Afur. and		da Silva Neto <i>et al.</i> , 2013
for Caulobacter crescentus NA1000 wild-type, \( \Delta fur, \) and wild-type treated with 2,2-dipyridy!  For genome resequencing accession numbers, see Table S6  Oligonucleotides  For oligonucleotide sequences see Table S8  Recombinant DNA  For plasmids used in this study see Table S7  Software and Algorithms  Bowtie2 Langmead and Salzberg, 2013  FreeBayes Garrison and Marth, 2012  iVision-Mac BioVision Technologies  ImageJ Rasband, W.S., ImageJ, U. S. National Institutes of Health, Bethesda, Maryland, USA, https://imagej.nih.gov/ij/, 1997-2018  MotionCor2 Zheng, et al., 2017  AMIRA Thermo Fisher  Analyst TF1.5 Applied Biosystems  Galaxy Afgan et al. 2016	wild-type, 27th, and wild-type treated with 2,2-dipyridyl		
Archive, https://www.ncbi.nlm.nih.gov/sra, BioProject ID PRJNA526705 see Table S6 Oligonucleotides For oligonucleotide sequences see Table S8 Recombinant DNA For plasmids used in this study see Table S7 Software and Algorithms Bowtie2 Langmead and Salzberg, 2013 FreeBayes Garrison and Marth, 2012 iVision-Mac BioVision Technologies ImageJ Rasband, W.S., ImageJ, U. S. National Institutes of Health, Bethesda, Maryland, USA, https://imagej.nih.gov/ij/, 1997-2018 MotionCor2 Zheng, et al., 2017 AMIRA Thermo Fisher Analyst TF1.5 Applied Biosystems Galaxy Afgan et al. 2016	Transcriptomic data for <i>Caulobacter</i> crescentus NA1000 wild-type, Δfur, and wild-type treated with 2,2-dipyridyl		Leaden <i>et al</i> ., 2018
For oligonucleotide sequences see Table S8  Recombinant DNA  For plasmids used in this study see Table S7  Software and Algorithms  Bowtie2 Langmead and Salzberg, 2013  FreeBayes Garrison and Marth, 2012 iVision-Mac BioVision Technologies  ImageJ Rasband, W.S., ImageJ, U. S. National Institutes of Health, Bethesda, Maryland, USA, https://imagej.nih.gov/ij/, 1997-2018  MotionCor2 Zheng, et al., 2017  AMIRA Thermo Fisher  Analyst TF1.5 Applied Biosystems  Galaxy Afgan et al. 2016	For genome resequencing accession numbers, see Table S6	Archive, https://www.ncbi.nlm.nih.gov/sra, BioProject	
For oligonucleotide sequences see Table S8  Recombinant DNA  For plasmids used in this study see Table S7  Software and Algorithms  Bowtie2 Langmead and Salzberg, 2013  FreeBayes Garrison and Marth, 2012 iVision-Mac BioVision Technologies  ImageJ Rasband, W.S., ImageJ, U. S. National Institutes of Health, Bethesda, Maryland, USA, https://imagej.nih.gov/ij/, 1997-2018  MotionCor2 Zheng, et al., 2017  AMIRA Thermo Fisher  Analyst TF1.5 Applied Biosystems  Galaxy Afgan et al. 2016	Oligonucleotides		l
For plasmids used in this study see Table S7  Software and Algorithms  Bowtie2 Langmead and Salzberg, 2013  FreeBayes Garrison and Marth, 2012 iVision-Mac BioVision Technologies  ImageJ Rasband, W.S., ImageJ, U. S. National Institutes of Health, Bethesda, Maryland, USA, https://imagej.nih.gov/ij/, 1997-2018  MotionCor2 Zheng, et al., 2017  AMIRA Thermo Fisher  Analyst TF1.5 Applied Biosystems  Galaxy Afgan et al. 2016	For oligonucleotide sequences see Table S8		
in this study see Table S7  Software and Algorithms  Bowtie2 Langmead and Salzberg, 2013  FreeBayes Garrison and Marth, 2012 iVision-Mac BioVision Technologies  ImageJ Rasband, W.S., ImageJ, U. S. National Institutes of Health, Bethesda, Maryland, USA, https://imagej.nih.gov/ij/, 1997-2018  MotionCor2 Zheng, et al., 2017  AMIRA Thermo Fisher  Analyst TF1.5 Applied Biosystems  Galaxy Afgan et al. 2016	Recombinant DNA		
Bowtie2 Langmead and Salzberg, 2013  FreeBayes Garrison and Marth, 2012 iVision-Mac BioVision Technologies  ImageJ Rasband, W.S., ImageJ, U. S. National Institutes of Health, Bethesda, Maryland, USA, https://imagej.nih.gov/ij/, 1997-2018  MotionCor2 Zheng, et al., 2017  AMIRA Thermo Fisher  Analyst TF1.5 Applied Biosystems  Galaxy Afgan et al. 2016	For plasmids used in this study see Table S7		
FreeBayes  Garrison and Marth, 2012  iVision-Mac  BioVision Technologies  ImageJ  Rasband, W.S., ImageJ, U. S. National Institutes of Health, Bethesda, Maryland, USA, https://imagej.nih.gov/ij/, 1997-2018  MotionCor2  Zheng, et al., 2017  AMIRA  Thermo Fisher  Analyst TF1.5  Applied Biosystems  Galaxy  Afgan et al. 2016	Software and Algorith	T	T
iVision-Mac  BioVision Technologies  ImageJ  Rasband, W.S., ImageJ, U. S. National Institutes of Health, Bethesda, Maryland, USA, https://imagej.nih.gov/ij/, 1997-2018  MotionCor2  Zheng, et al., 2017  AMIRA  Thermo Fisher  Analyst TF1.5  Applied Biosystems  Galaxy  Afgan et al. 2016	Bowtie2	Langmead and Salzberg, 2013	
ImageJ Rasband, W.S., ImageJ, U. S. National Institutes of Health, Bethesda, Maryland, USA, https://imagej.nih.gov/ij/, 1997-2018  MotionCor2 Zheng, et al., 2017  AMIRA Thermo Fisher  Analyst TF1.5 Applied Biosystems  Galaxy Afgan et al. 2016	FreeBayes	·	
Health, Bethesda, Maryland, USA, https://imagej.nih.gov/ij/, 1997-2018  MotionCor2 Zheng, et al., 2017  AMIRA Thermo Fisher  Analyst TF1.5 Applied Biosystems  Galaxy Afgan et al. 2016	iVision-Mac		
AMIRA Thermo Fisher  Analyst TF1.5 Applied Biosystems  Galaxy Afgan et al. 2016	ImageJ	Health, Bethesda, Maryland, USA,	
Analyst TF1.5 Applied Biosystems Galaxy Afgan <i>et al.</i> 2016	MotionCor2	Zheng, <i>et al.</i> , 2017	
Galaxy Afgan <i>et al.</i> 2016	AMIRA	Thermo Fisher	
	Analyst TF1.5	Applied Biosystems	
Cutadapt Martin, 2011	Galaxy	Afgan <i>et al</i> . 2016	
	Cutadapt	Martin, 2011	

GraphPad Prism 9.3.1 for statistical analyses	GraphPad Software, LLC	
IMOD	Kremer, <i>et al,.</i> 1996	
serialEM	Mastonarde <i>et al.,</i> 2005	

Figure 1



ΔCCNA\_01553

∆ctpA ∆sspB

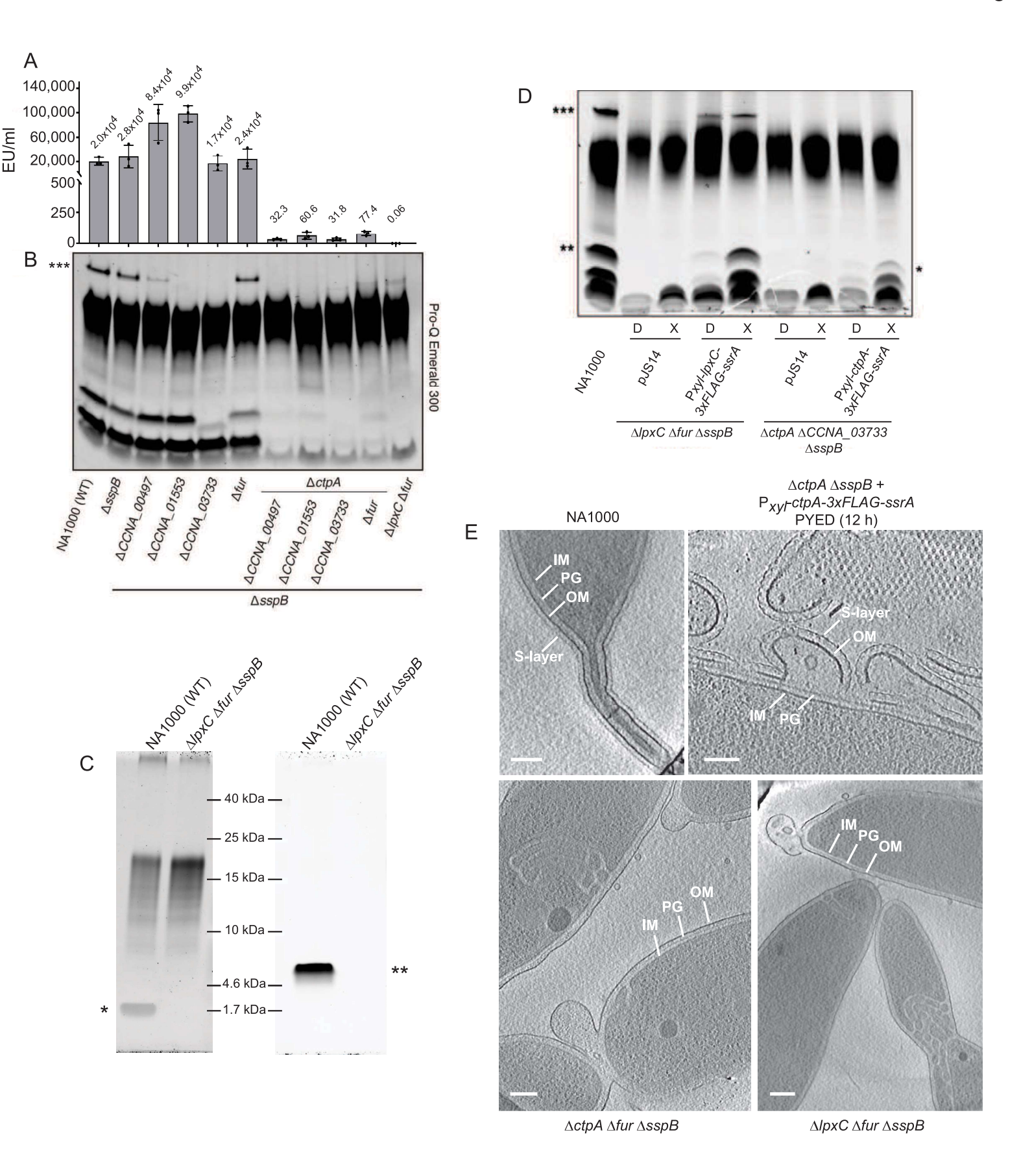
 $\Delta fur$ 

∆sspB

ΔCCNA\_00497

∆sspB

Figure 2



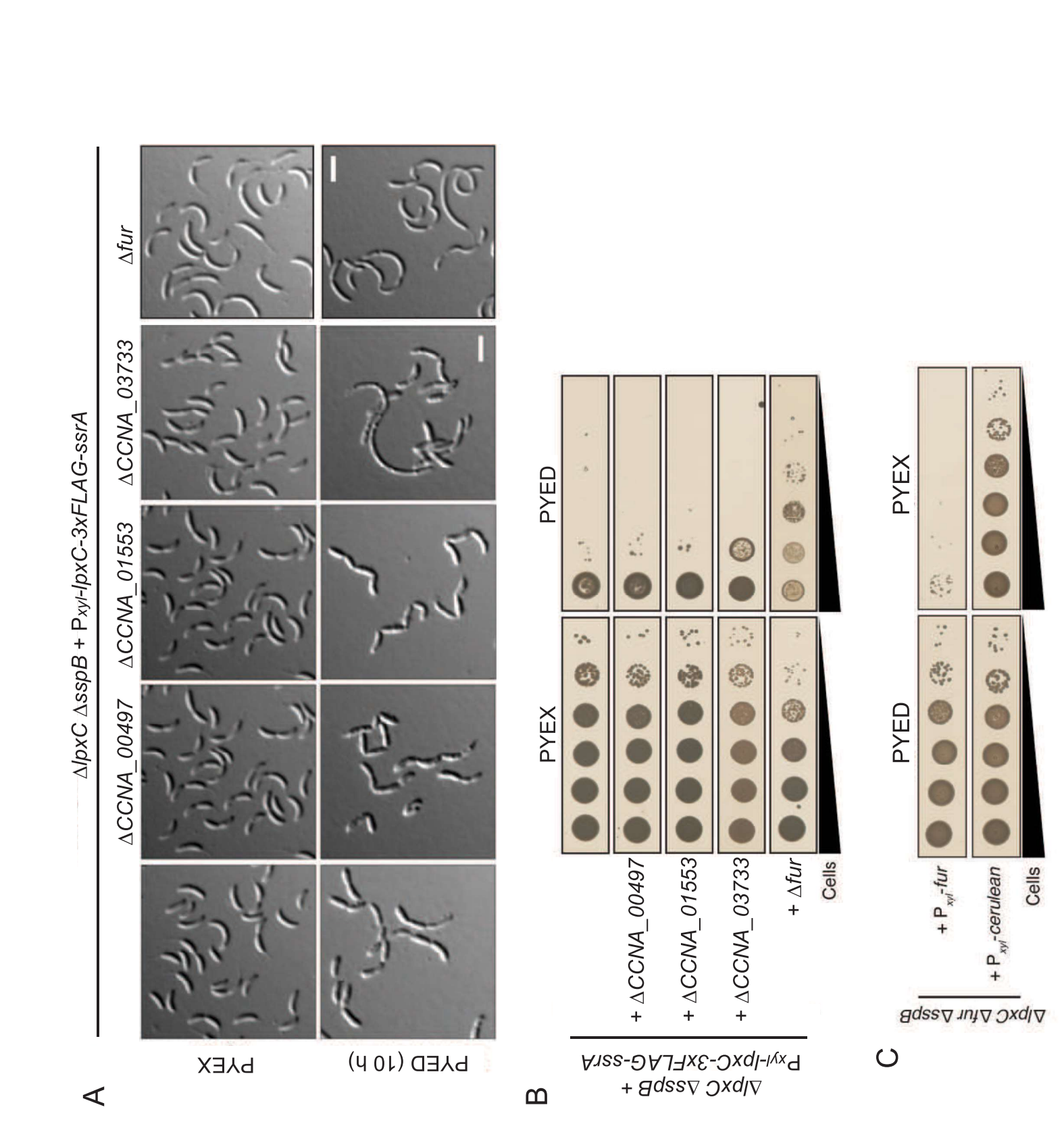
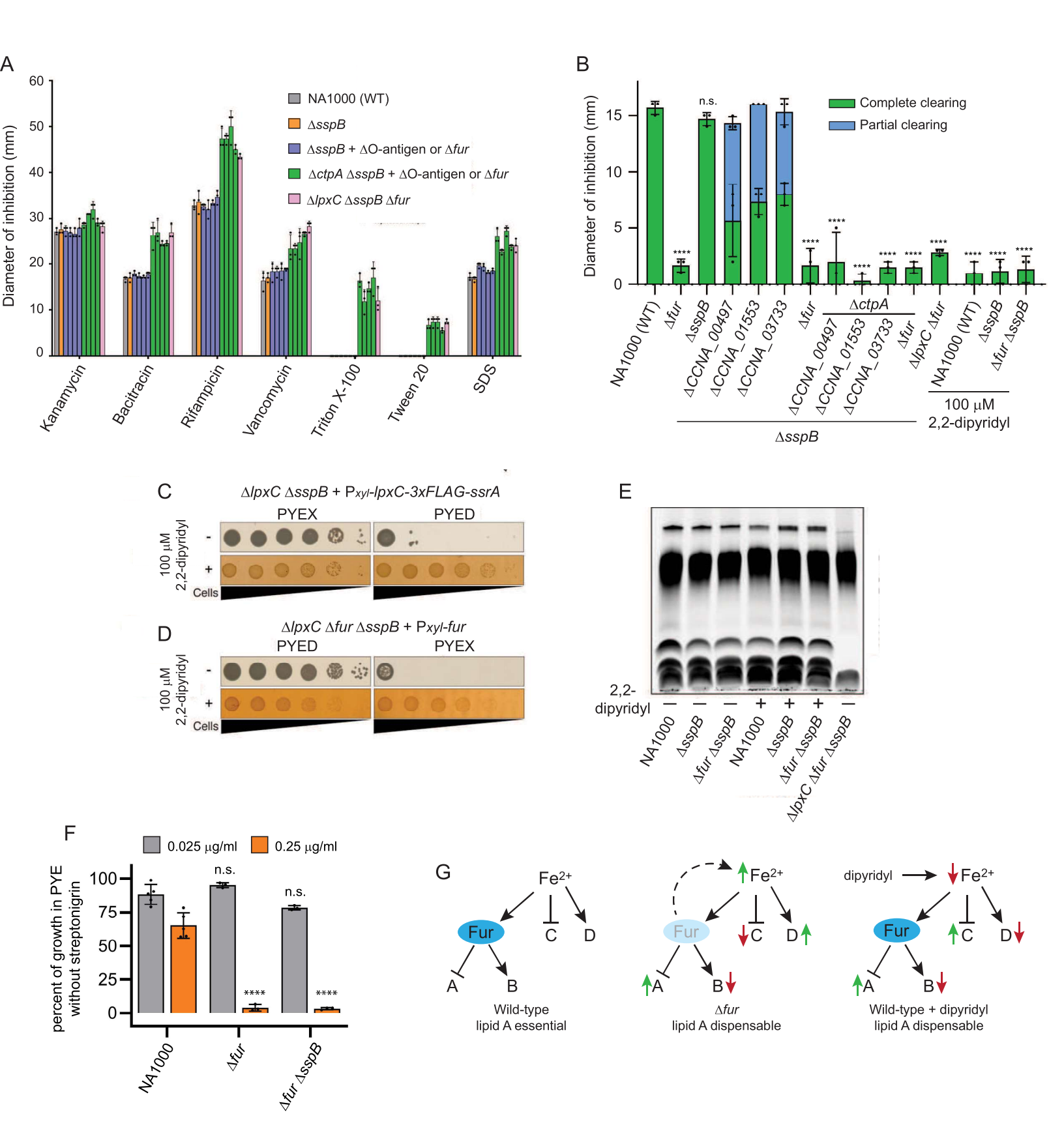
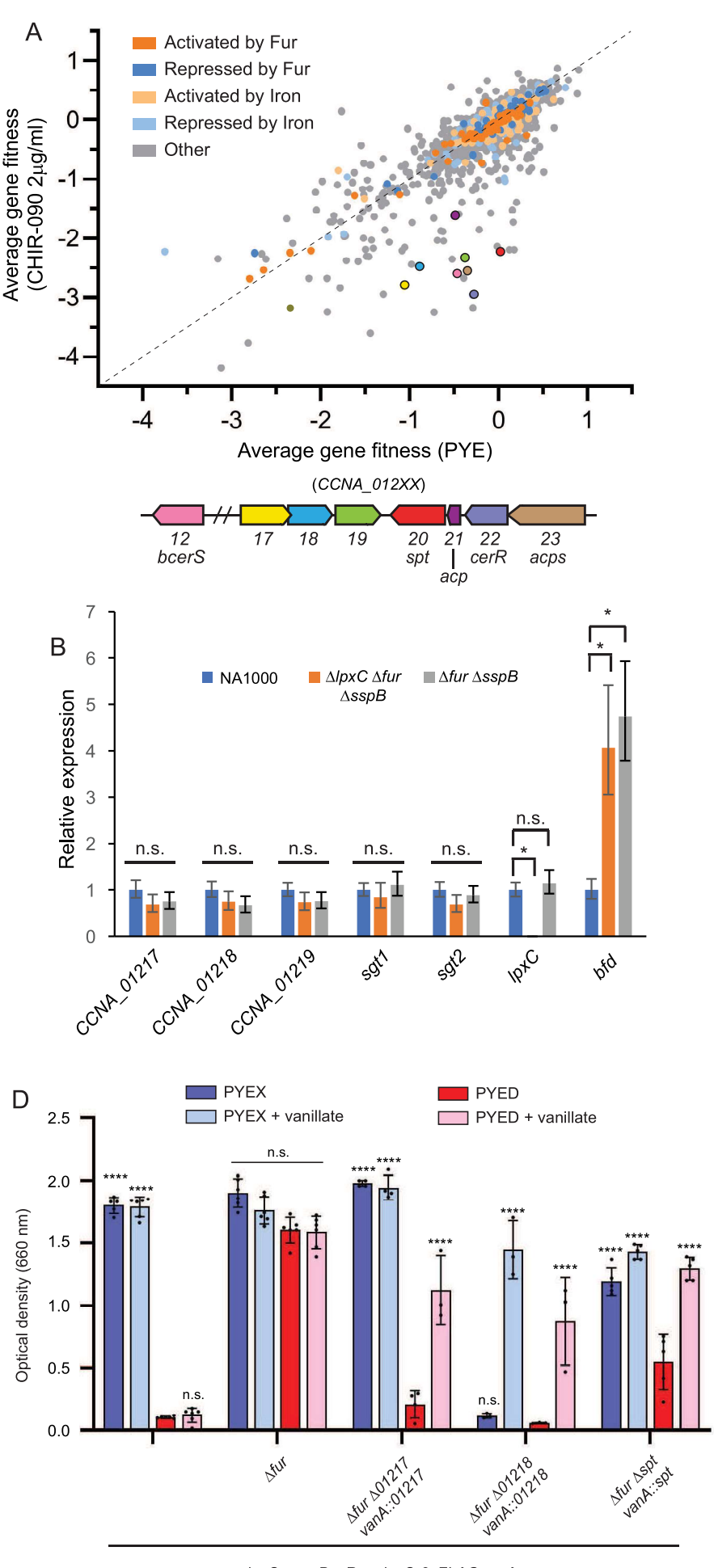
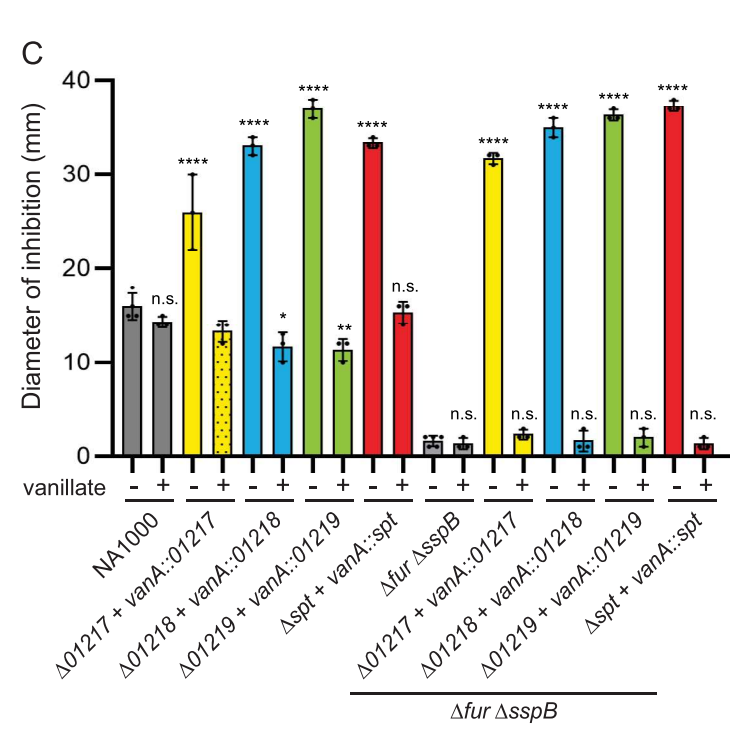
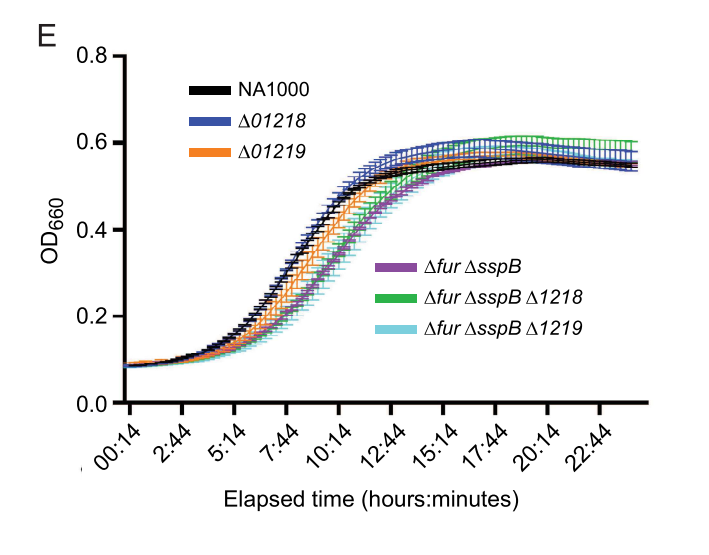


Figure 4









 $\Delta lpxC \Delta sspB + P_{xyl} - lpxC - 3xFLAG - ssrA$ 

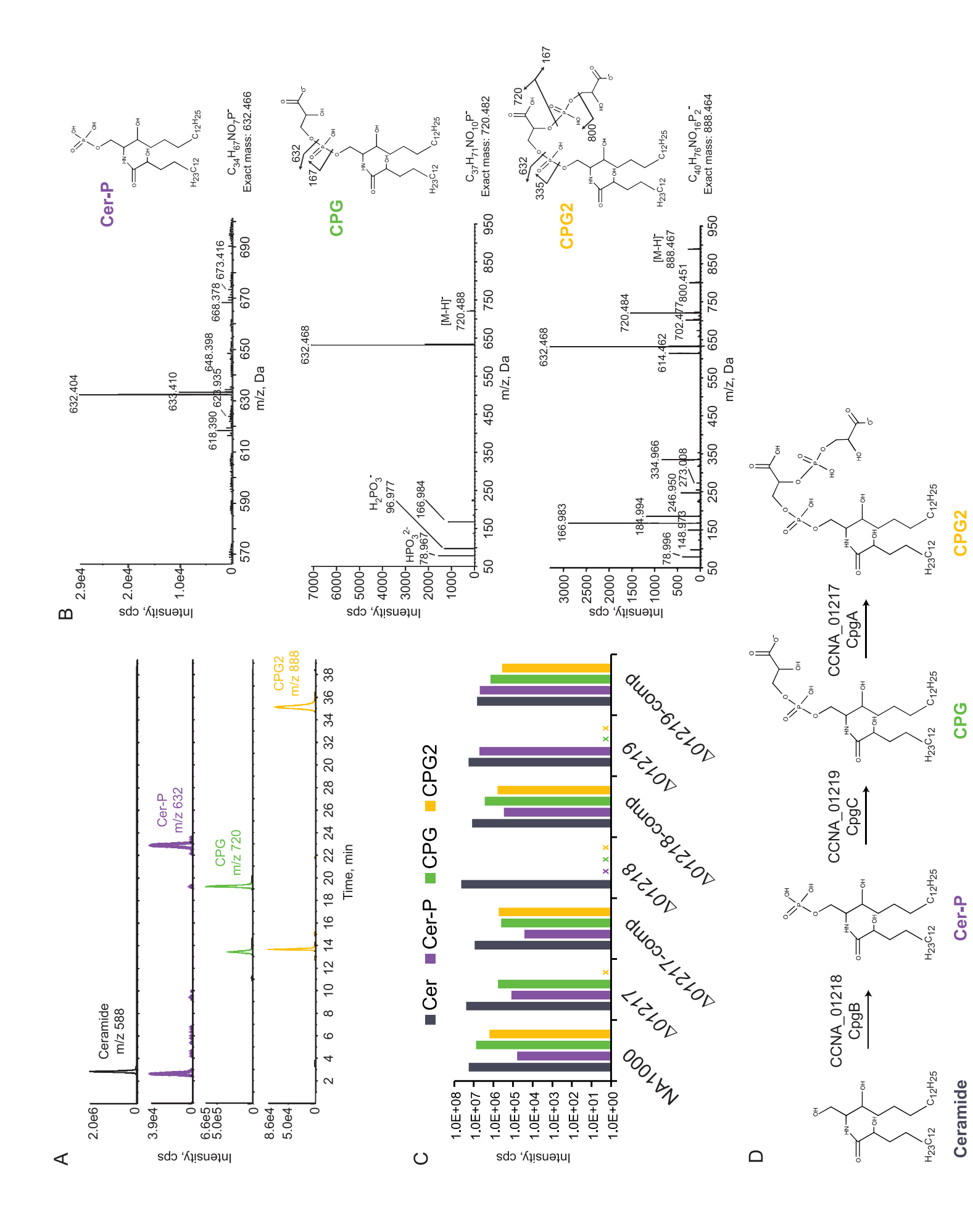
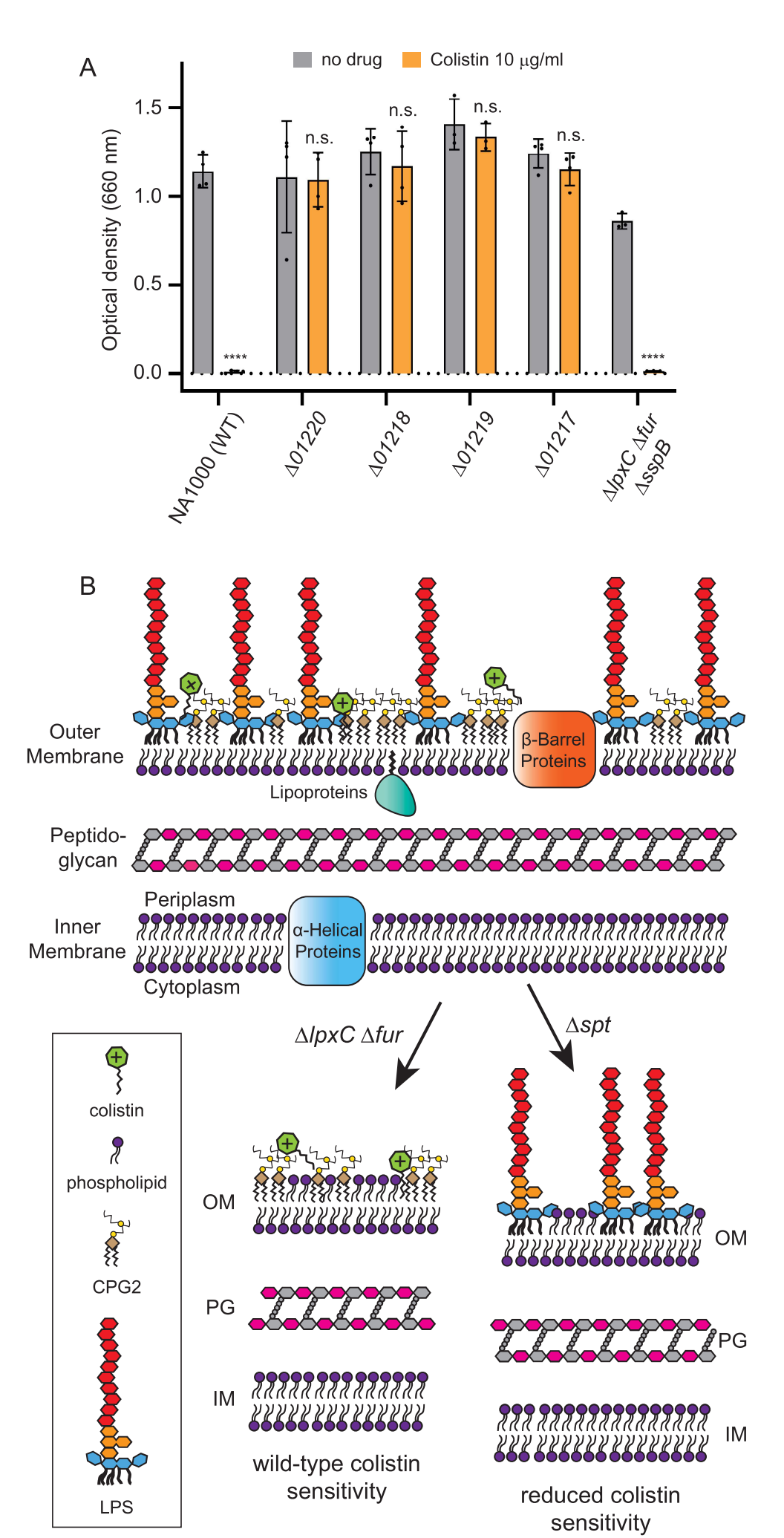
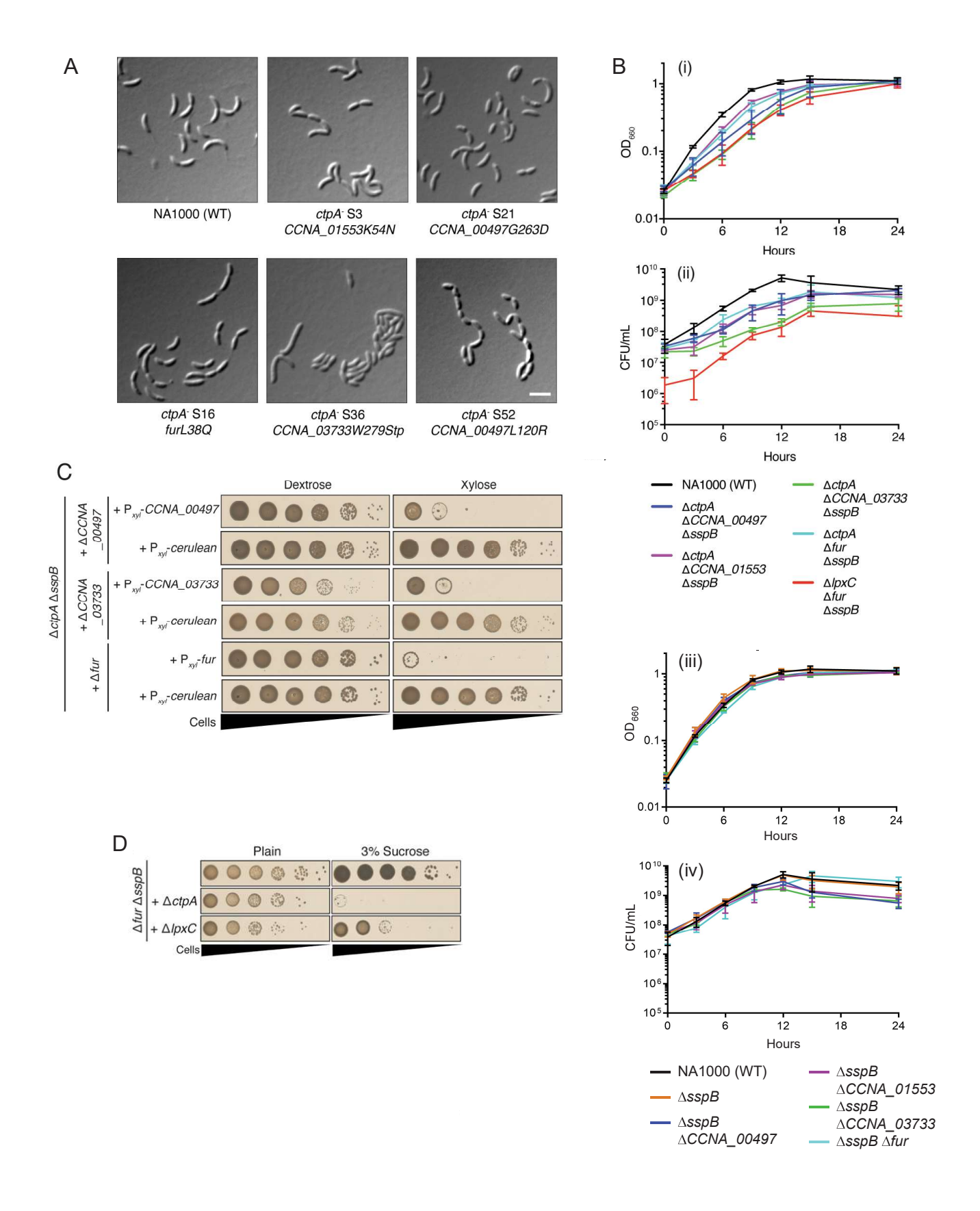
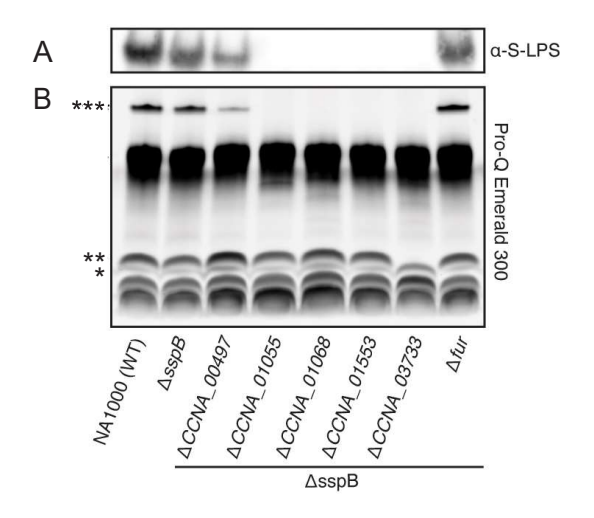


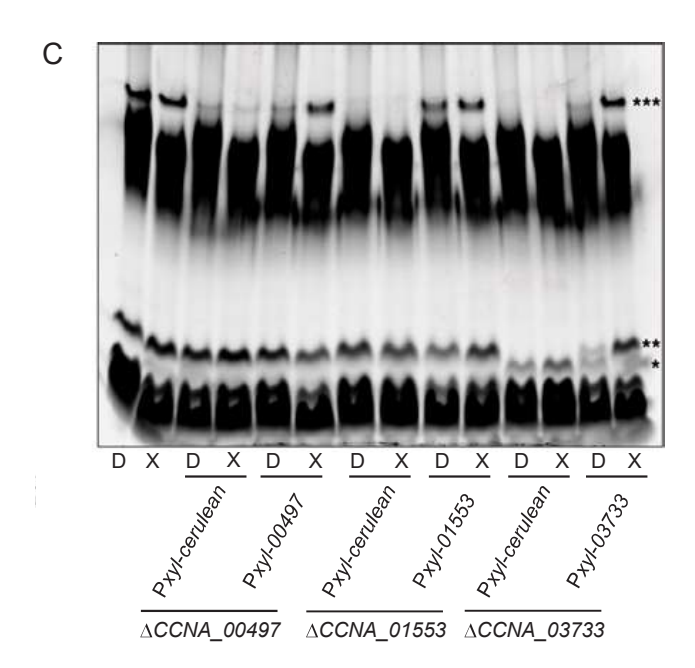
Figure 7 Figure 7



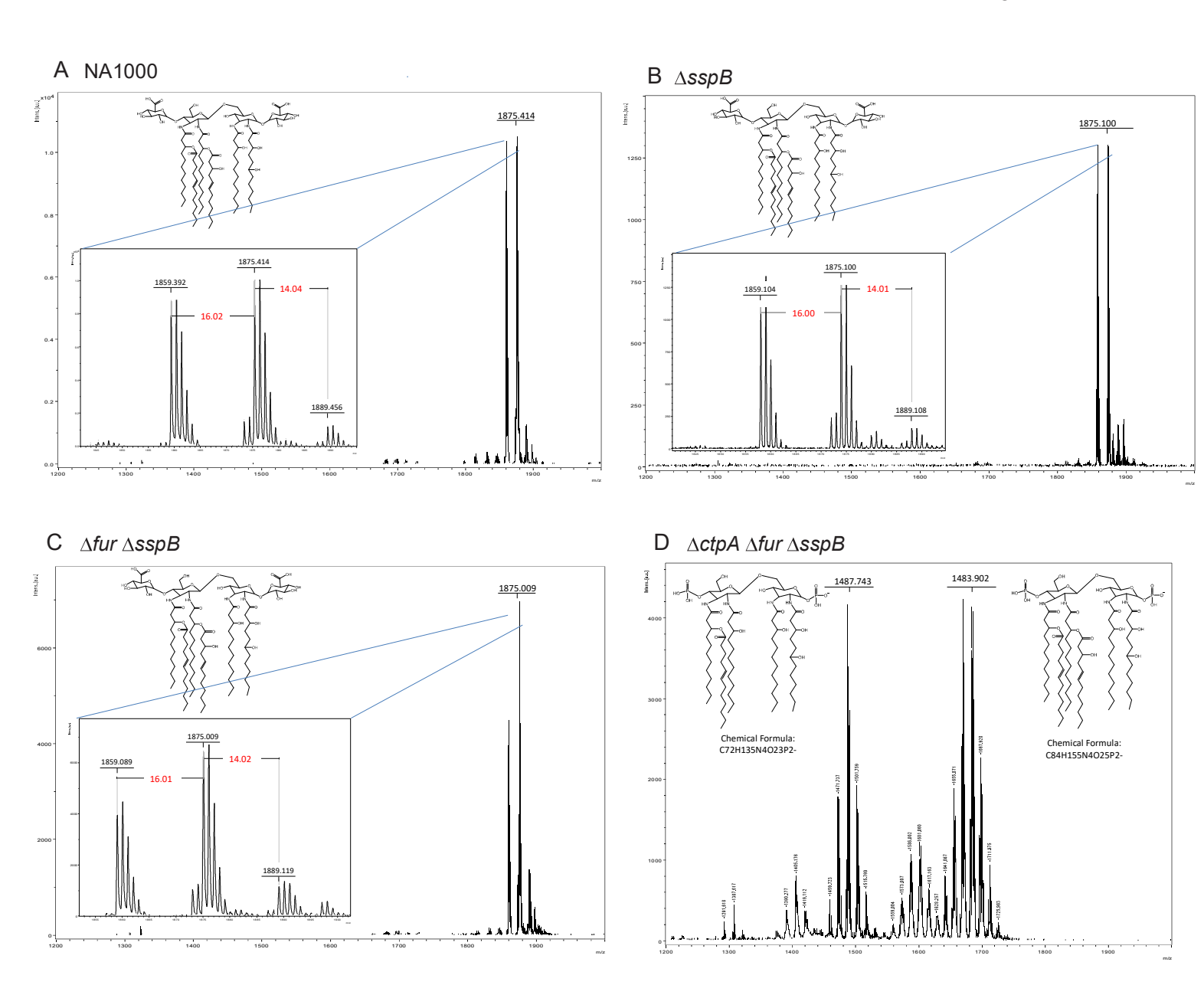


**Figure S1, related to Fig. 1:** Morphology, growth, and complementation of strains in which suppressor mutations permit the loss of ctpA. (A) Isolates from the  $\Delta ctpA$  suppressor screen show variations in morphology. DIC images of selected suppressor isolates confirmed to have lost the ctpA covering plasmid. Putative suppressor mutations identified by whole-genome resequencing are indicated. Scale bar, 3 μm. (B) Growth curves of the indicated strains in PYE showing (i or iii) OD<sub>660</sub> and (ii or iv) colony-forming units (CFU) per mL (mean ± S.D., N=3). (C) Viability assays of  $\Delta ctpA$  suppressor mutants, each harboring a vector for xylose-driven expression of the corresponding suppressor gene or the *cerulean* gene as a control. Kanamycin was included in media to retain expression vectors. (D) Viability of the indicated strains on PYE medium (Plain) or PYE medium + 3% sucrose.





**Figure S2**, **related to Fig.1**: A subset of *ctpA* suppressor mutations impair or block S-LPS production. (A) α-S-LPS-probed immunoblot and (B) Pro-Q Emerald 300-stained gel of Proteinase K-treated whole-cell lysates of the indicated strains. (C) Complementation of O-antigen biosynthesis using plasmid-borne genes driven by a xylose-inducible promoter. Pro-Q Emerald 300-stained polyacrylamide gel of Proteinase K-treated whole-cell lysates of the indicated strains grown in either PYED (D) or PYEX (X). Samples were normalized by OD660. \*\*\* = S-LPS, \*\* = putative full-length lipid A-core polysaccharide, \* = putative incomplete lipid A-core species in cells lacking *manC* activity (*CCNA\_03733*).



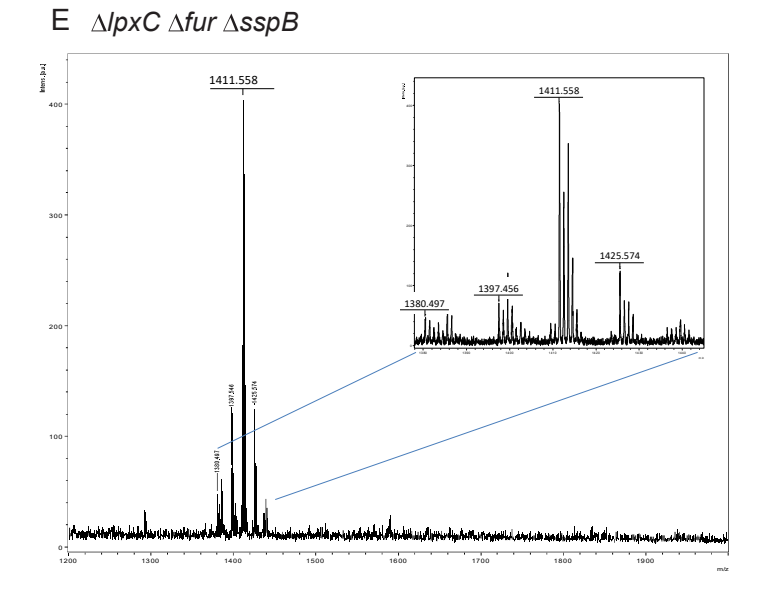
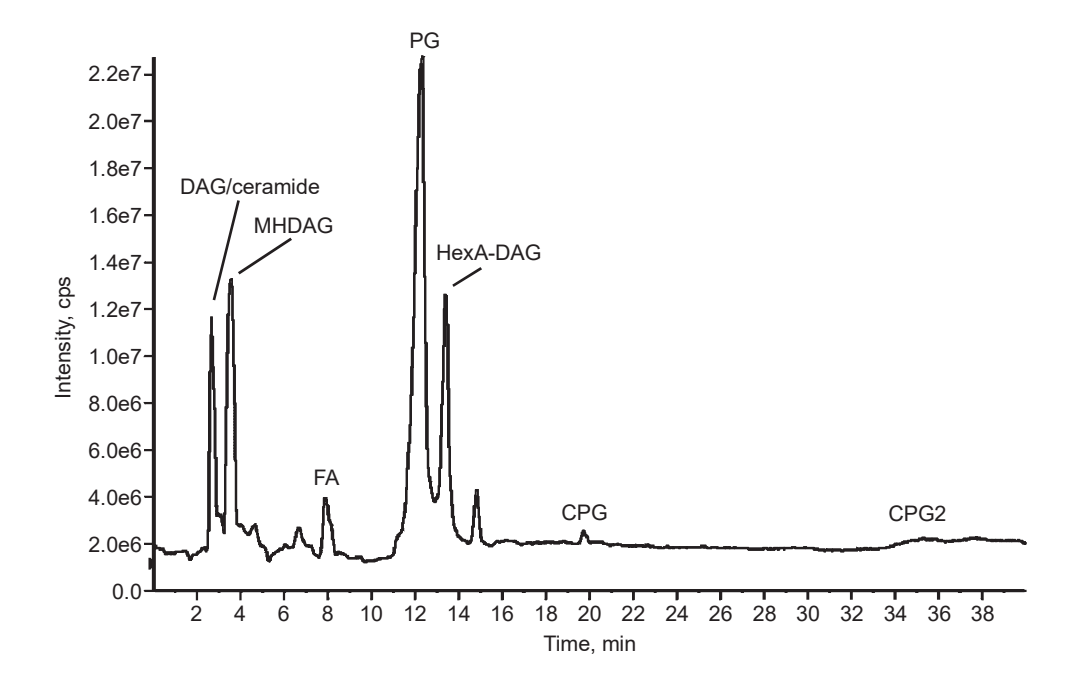
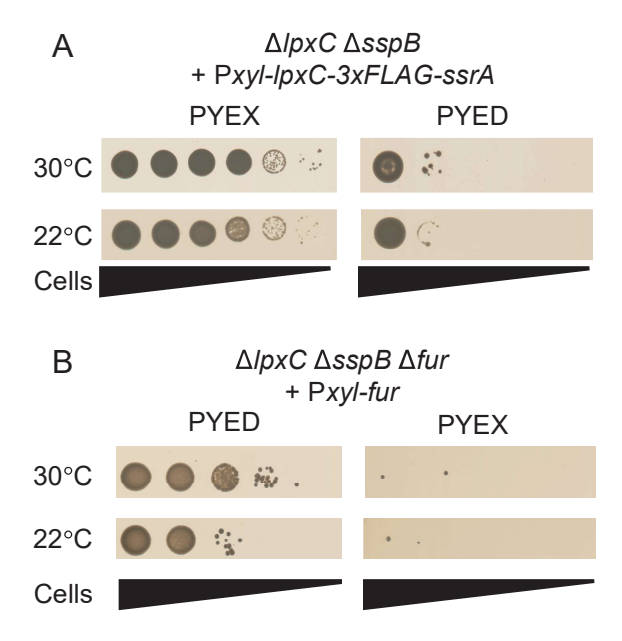


Figure S3, related to Figure 2:  $\triangle ctpA$  and  $\triangle lpxC$  strains with suppressor mutations lack wild-type lipid A. Tandem mass spectrometry (MSMS)-derived structures of lipid A from the indicated strains. Lipid extraction and MSMS analysis were performed as described in STAR Methods using the same protocols for all strains.



**Figure S4**, **related to Figure 6**: The total ion chromatogram of the *C. crescentus* lipidome shows the major lipid species present. DAG: diacylglycerol; MHDAG: mono-hexosyl diacylglycerol; FA: fatty acids; PG: phosphatidylglycerol; HexA-DAG: hexuronic acid-diacylglycerol; CPG: ceramide phosphoglycerate.



**Figure S5, related to Figure 3.** Slow growth at a reduced temperature in complex medium is insufficient for viability of ΔlpxC strains. (A) Viability of the LpxC depletion strain grown in inducing (PYEX) or depleting (PYED) conditions, at the indicated temperatures. (B) Viability of the stable  $\Delta lpxC$   $\Delta fur$   $\Delta sspB$  strain harboring a Pxyl-fur plasmid, grown in noninducing (PYED) or inducing (PYEX) conditions, at the indicated temperatures. Cells were plated from 10-fold serially diluted suspensions normalized to OD<sub>660</sub> = 0.1. Plates were incubated for 3 days (30°C) or 6 days (22°C) and are representative of at least three independent trials. Plates in B included kanamycin to retain the fur expression vector.

## Supplementary Tables Table S1, related to Figure 1: Single-nucleotide polymorphisms and indels in $\Delta ctpA$ suppressors<sup>a</sup>

Strain	Sequence	Genec	Annotation Bas		Amino Acid
	positionb		Change Substitutio		Substitution
S3	1668695	01553	Undecaprenyl-phosphate beta-N-acetyl-D- G>T K54N		K54N
			fucosaminephosphotrans-		
			ferase <sup>d</sup>		
S3	2383967	02235	SGNH hydrolase family protein	G>A	G109D
S8	3492550	03316	UDP-N-acetylglucosamine 4,6-	AG>ATG	E487Frameshift
			dehydratase/UDP-D-quinovosamine 4-		
			dehydrogenase <sup>d</sup>		
S16	58496	00055	Ferric uptake regulation protein	A>T	L38Q
S21	515085	00497	Smooth LPS biosynthesis	G>A	G263D
			glycosyltransferase <sup>d</sup>		
S21	1378399	01250	FecCD-family transporter protein	GCC>GC	A340Frameshift
S32	1157376	01056	Methyltransferase <sup>e</sup>	A>AG	S31Framshift
S32	2164248	02016	nuoMNADH-quinone oxidoreductase chain M	C>T	M7I
S32	2949436	02792	TonB-dependent outer membrane receptor	A>G	S516G
S36	3901011	03733	Mannose-1-phosphate guanylyltransferased	C>T	W279Stop
S38	726779	00669	Glycosyltransferase family 99 protein WbsX <sup>d</sup>	CTG>CG	Q476Frameshift
S40	378822	00362	Zinc uptake regulation protein	A>T	C156S
S40	2868272	-	-	G>C	-
S40	3913883	03744	dTDP-glucose 4,6-dehydratase <sup>d</sup>	T>A	I269F
S43	1377138	01249	ABC-transporter substrate binding protein	C>T	A169V
S43	1668861	01553	Undecaprenyl-phosphate beta-N-acetyl-D-	CC>GA	P110E
			fucosaminephosphotransferased		
S43	2976030	02820	TadG-family protein	C>T	Silent
S44	727833	00669	Glycosyltransferase family 99 protein WbsX <sup>d</sup>	A>C	L125R
S47	537654	00524	Conserved hypothetical cytosolic protein	A>AG	L369Frameshift
S47	1173251	01068	Glycosyltransferased	GCC>GC	R293Frameshift
S52	514656	00497	Smooth LPS biosynthesis	T>G	L120R
			glycosyltransferased		
S52	810384	00752	3-hydroxybutyryl-CoA dehydrogenase	T>A	Stop>Y
S52	3797776	-	-	T>C	-

S53	58379	00055	Ferric uptake regulation protein	G>T	S77Stop
S53	1778110	01656	Endonuclease/exonuclease/phosphatase	A>C	L4R
			family protein		
S53	3900664	03733	Mannose-1-phosphate guanylyltransferased	G>A	Q395Stop
S54	1377127	01249	ABC-transporter substrate binding protein	CGG>CG	G166Frameshift
S54	3492771	03316	UDP-N-acetylglucosamine 4,6-	G>A	E561K
			dehydratase/UDP-D-quinovosamine 4-		
			dehydrogenase <sup>d</sup>		
S57	1492703	01378	Protein-L-isoaspartate O-methyltransferase	G>GC	G59Frameshift
S57	2487074	02347	Phosphomannomutase/	G>A	G266D
			phosphoglucomutased		
S111	295119	00283	2,3,4,5-tetrahydropyridine-2,6-dicarboxylate	A>T	L284Q
			N-succinyltransferase		
S111	1173965	01068	Glycosyltransferased	TGC>T	R55Frameshift
S112	311705	00297	Two-component response regulator	C>T	W64Stop
S112	315570	00301	Phosphotransferase family protein	T>G	I319S
S112	2487307	02347	Phosphomannomutase/	G>A	E344K
			phosphoglucomutased		
S112	3569520	03399	Flavin prenyltransferase UbiX	C>T	A159T

<sup>&</sup>lt;sup>a</sup>In addition to the indicated mutations, each strain is also  $\Delta ctpA$   $\Delta sspB$ .

<sup>&</sup>lt;sup>b</sup>Sequence positions refer to the genome of *Caulobacter crescentus* NA1000 (NC\_011916.1).

<sup>&</sup>lt;sup>c</sup>The prefix for each gene number is *CCNA*\_.

<sup>&</sup>lt;sup>d</sup>Genes known or predicted to be involved in O-antigen synthesis.

<sup>&</sup>lt;sup>e</sup>We speculate that the frameshift in *CCNA\_01056* affects the expression of the downstream gene *CCNA\_01055*, annotated as a GT1 family glycosyltransferase.

Table S2, related to Figure 3: Single-nucleotide polymorphisms and indels identified in  $\Delta lpxC$  suppressors<sup>a</sup>

Strain	Sequence	Genec	Annotation	Base	Amino Acid
	position <sup>b</sup>			Change	Substitution
S1	58446	00055	Ferric uptake regulation protein Fur	A>T	Y55N
	4000704	03835	3-oxoacyl-(Acyl-carrier-protein) synthase	C>T	G396S
S5	58436	00055	Ferric uptake regulation protein Fur	A>T	V58E

<sup>&</sup>lt;sup>a</sup>In addition to the indicated mutations, each strain is also  $\Delta lpxC \Delta sspB \Delta 00497$ .

<sup>&</sup>lt;sup>b</sup>Sequence positions refer to the genome of *Caulobacter crescentus* NA1000 (NC\_011916.1).

<sup>&</sup>lt;sup>c</sup>The prefix for each gene number is *CCNA*\_.

Table S3, related to Fig. 2: Fur or iron regulation of genes predicted to participate in lipid synthesis.

Genea	Name <sup>b</sup>	Regulation by Fur and/or iron <sup>c</sup>
CCNA_00363	рдрВ	None
CCNA_01382	fadD	None
CCNA_01431	plsX	None
CCNA_01432	fabH	None
CCNA_01746	fabD	None
CCNA_01747	fabG	None
CCNA_01750	fabF	None
CCNA_01932	plsC	None
CCNA_01960	ассВ	None
CCNA_01961	accC	Downregulated by iron limitation only (Leaden, et al., 2018)
CCNA_01977	plsB	None
CCNA_01989	fabZ	None
CCNA_01995	cdsA	None
CCNA_02001	рдрС	None
CCNA_02040	рдрС	None
CCNA_02302	plsC	None
CCNA_03002	pgsA	None
CCNA_03090	accA	None
CCNA_03656	accD	Upregulated by iron limitation only (Leaden, et al., 2018)
CCNA_03833	fabl	Downregulated by iron limitation only (Leaden, et al., 2018)
CCNA_03835	fabB	None
CCNA_03836	fabA	None

<sup>&</sup>lt;sup>a</sup>Gene numbers refer to the genome of *Caulobacter crescentus* NA1000 (NC\_011916.1).

<sup>&</sup>lt;sup>b</sup>Names are derived from annotations in NCBI associated with NC\_011916.1 or from BLAST or PSI-BLAST searches of the *Caulobacter crescentus* NA1000 genome initiated with the indicated *E. coli* amino acid sequence ((Altschul, 1997; Altschul et al., 1990).

<sup>&</sup>lt;sup>c</sup>Gene regulation was assessed by inspection of results (Leaden et al., 2018; da Silva Neto et al., 2013).

Table S4, related to Figure 5: Genes whose average fitness scores were lower in CHIR-090-treated cultures than in control cultures by >1.

Gene <sup>a</sup>	Average fitness PYE <sup>b</sup>	Average fitness PYE + 2 µg/ml CHIR-090°	Net average fitness <sup>d</sup>	Annotation
CCNA 03609	-0.287	-3.176	-2.889	Outer membrane protein
CCNA_01222	-0.290	-2.953	-2.662	NADH-ubiquinone oxidoreductase (cerR)
CCNA_03983	-0.726	-3.246	-2.520	HicA-related toxin-antitoxin protein
CCNA_01060	0.175	-2.191	-2.365	Type I protein secretion ATP-binding protein,
				RsaD
CCNA_01638	0.122	-2.195	-2.317	Beta-lactamase family protein
CCNA_01162	-0.391	-2.668	-2.277	Beta-D-glucoside glucohydrolase
CCNA_01220	0.019	-2.222	-2.240	BioF-family ceramide biosynthesis protein
				CcbF (spt)
CCNA_01223	-0.354	-2.549	-2.195	Acyl-CoA synthetase (acps)
CCNA_03026	-1.443	-3.605	-2.162	Two-component response regulator, PetR
CCNA_01817	-0.016	-2.139	-2.123	Nitrogen assimilatory regulatory protein, NtrX
CCNA_01212	-0.470	-2.589	-2.120	dATP pyrophosphohydrolase (bcerS)
CCNA_01219	-0.383	-2.337	-1.955	Putative cytosolic protein (cpgC)
CCNA_01067	0.164	-1.730	-1.894	Type I secretion outer membrane protein RsaFa
CCNA_00252	-0.523	-2.345	-1.822	Multimodular transpeptidase-transglycosylase
				PbpX
CCNA_01217	-1.063	-2.808	-1.746	Phosphatidylglycerophosphate synthase (cpgA)
CCNA_02127	0.155	-1.521	-1.676	Bifunctional lysylphosphatidylglycerol
				flippase/synthetase MprF
CCNA_00525	-1.296	-2.941	-1.645	Prolipoprotein diacylglyceryl transferase
CCNA_03027	-0.219	-1.855	-1.636	Two-component sensor histidine kinase
CCNA_03321	0.202	-1.390	-1.593	VanZ superfamily protein
CCNA_01218	-0.894	-2.458	-1.564	Sphingosine kinase/diacylglycerol kinase-related
				protein (cpgB)
CCNA_03864	-0.087	-1.572	-1.485	DUF3576 domain-containing protein
CCNA_00001	-0.980	-2.436	-1.456	Pyruvate, phosphate dikinase regulatory protein
CCNA_01427	-0.619	-2.040	-1.421	Beta-barrel assembly machine protein BamE
CCNA_03876	0.509	-0.880	-1.389	Transcription termination factor rho
CCNA_00512	-0.689	-2.035	-1.345	GTP-binding protein, probable translation factor
CCNA_00050	-1.925	-3.242	-1.317	Apolipoprotein N-acyltransferase Lnt

CCNA_00190	-0.624	-1.885	-1.261	Acyl-CoA hydrolase
CCNA_02386	-0.650	-1.875	-1.225	O-antigen ligase related enzyme
CCNA_00080	0.341	-0.862	-1.203	LexA-related transcriptional repressor
CCNA_00924	0.373	-0.813	-1.186	MarR/EmrR family transcriptional regulator
CCNA_00354	-0.212	-1.384	-1.172	NIpC/P60 CHAP domain amidase protein
CCNA_00027	0.109	-1.045	-1.154	2OG-Fe(II) oxygenase
CCNA_01324	-0.445	-1.588	-1.143	LSU ribosomal protein L30P
CCNA_01226	-1.084	-2.210	-1.126	OstA family protein
CCNA_01221	-0.499	-1.623	-1.124	acyl carrier protein (acp)
CCNA_00851	0.073	-1.030	-1.103	periplasmic multidrug efflux lipoprotein precursor
CCNA_03782	-1.055	-2.153	-1.098	cytochrome c biogenesis ATP-binding export
				protein CcmA
CCNA_03336	-3.118	-4.188	-1.071	Tol-Pal system periplasmic component YbgF
CCNA_03820	-1.783	-2.837	-1.055	LolA-family outer membrane lipoprotein carrier
				<u>protein</u>
CCNA_03260	0.243	-0.810	-1.054	queuosine biosynthesis protein QueD
CCNA_00850	0.065	-0.980	-1.045	cation/multidrug efflux pump acrB2
CCNA_02081	0.006	-1.013	-1.019	Sec-independent protein translocase protein tatB
CCNA_00735	0.361	-0.644	-1.005	beta-barrel assembly machine protein BamF

<sup>&</sup>lt;sup>a</sup>Gene numbers refer to the genome of *Caulobacter crescentus* NA1000 (NC\_011916.1).

<sup>&</sup>lt;sup>b</sup>Average fitness in PYE was calculated from fitness values in set8IT011, set8IT023, and set8IT035.

 $<sup>^{</sup>c}\text{Average}$  fitness in PYE + 2  $\mu\text{g/ml}$  CHIR-090 was calculated from fitness values in set8IT012, set8IT024, and set8IT036.

<sup>&</sup>lt;sup>d</sup>Net average fitness = (Average fitness PYE + 2 μg/ml CHIR-090)-(Average fitness PYE).

Table S5, related to Figure 3: Growth rates in PYE medium at 22°C.

	Doubling time +/- standard				
	deviation (hours) <sup>a</sup>				
Strain	PYE 30°C	PYE 22°C			
NA1000	1.61 +/- 0.04	2.50 +/- 0.17			
ΔsspB	1.51 +/- 0.04	2.44 +/- 0.09			
Δfur ΔsspB	1.77 +/- 0.08	3.16 +/- 0.21			

<sup>&</sup>lt;sup>a</sup>Doubling times were calculated from optical density measurements (660 nm) during exponential growth.

Table S6, related to STAR Methods: Strains used in this study.

Strain	Description <sup>a</sup>	NCBI BioSample	Reference
Number	·	Accession <sup>b</sup> or Note	
KR4000	Wild-type Caulobacter NA1000		(Evinger and
			Agabian,
			1977)
KR3180	NA1000 pJS14		This study
KR1499	ΔsspB::aadA		(Shapland et
L/D0077	A CONTA - 00407-16-19		al., 2011)
KR3877	\( \triangle CCNA_00497::hyg		This study
KR4198	ΔCCNA_00497::hyg pJS14		This study
KR3871	\( \Delta CCNA_01553::hyg \)		This study
KR4197	ΔCCNA_01553::hyg pJS14		This study
KR4076	\( \Delta fur::hyg \)		This study
KR4199	Δfur::hyg pJS14		This study
KR3953	ΔCCNA_00497::hyg ΔsspB::aadA		This study
KR4115	ΔCCNA_01055::hyg ΔsspB::aadA		This study
KR4116	ΔCCNA_01068::hyg ΔsspB::aadA		This study
KR3954	ΔCCNA_01553::hyg ΔsspB::aadA		This study
KR3955	ΔCCNA_03733::hyg ΔsspB::aadA		This study
KR4077	Δfur::hyg ΔsspB::aadA		This study
KR4153	ΔsspB::aadA pXCERN-2		This study
KR4154	ΔCCNA_00497::hyg ΔsspB::aadA pXCERN-2		This study
KR4155	ΔCCNA_01553::hyg ΔsspB::aadA pXCERN-2		This study
KR4156	ΔCCNA_03733::hyg ΔsspB::aadA pXCERN-2		This study
KR4157	Δfur::hyg ΔsspB::aadA pXCERN-2		This study
KR4158	ΔCCNA_00497::hyg ΔsspB::aadA pZIK172		This study
KR4159	ΔCCNA_01553::hyg ΔsspB::aadA pZIK173		This study
KR4160	ΔCCNA_03733::hyg ΔsspB::aadA pZlK174		This study
KR4161	Δfur::hyg ΔsspB::aadA pZIK175		This study
KR4269	Δfur::hyg ΔsspB::aadA pZIK197		This study
KR3906	ΔctpA::tetAR ΔsspB::aadA pAB6	Restock of KR2423	(Shapland et
		from Shapland	al., 2011)
		2011	
KR4111	ΔctpA::tetAR ΔsspB::aadA ΔCCNA_00497::hyg pAB6	SAMN12568762	This study
KR4112	ΔctpA::tetAR ΔsspB::aadA ΔCCNA_01553::hyg pAB6	SAMN12568763	This study
KR4092	ΔctpA::tetAR ΔsspB::aadA ΔCCNA_03733::hyg pAB6	SAMN12568761	This study
KR4090	ΔctpA::tetAR ΔsspB::aadA Δfur::hyg pAB6	SAMN12568759	This study
KR4007	ΔlpxC::tetAR ΔsspB::aadA pZIK133		This study
KR4008	ΔlpxC::tetAR ΔsspB::aadA ΔCCNA_00497::hyg pZIK133		This study
KR4223	ΔlpxC::tetAR ΔCCNA_00497::hyg pZIK133		This study
KR4009	ΔlpxC::tetAR ΔsspB::aadA ΔCCNA_01553::hyg pZIK133		This study
KR4010	ΔlpxC::tetAR ΔsspB::aadA ΔCCNA_03733::hyg pZIK133		This study
KR4091	ΔlpxC::tetAR ΔsspB::aadA Δfur::hyg pZlK133	SAMN12568760	This study

KR4113	ΔctpA::tetAR ΔsspB::aadA ΔCCNA_00497::hyg	SAMN12568767	This study
KR4114	ΔctpA::tetAR ΔsspB::aadA ΔCCNA_01553::hyg	SAMN12568768	This study
KR4104	ΔctpA::tetAR ΔsspB::aadA ΔCCNA_03733::hyg	SAMN12568766	This study
KR4102	ΔctpA::tetAR ΔsspB::aadA Δfur::hyg	SAMN12568764	This study
KR4103	ΔlpxC::tetAR ΔsspB::aadA Δfur::hyg	SAMN12568765	This study
KR4176	ΔctpA::tetAR ΔsspB::aadA Δfur::hyg pZIK175		This study
KR4270	ΔctpA::tetAR ΔsspB::aadA Δfur::hyg pZIK197		This study
KR4177	ΔctpA::tetAR ΔsspB::aadA Δfur::hyg pXCERN-2		This study
KR4178	ΔlpxC::tetAR ΔsspB::aadA Δfur::hyg pZIK175		This study
KR4271	ΔlpxC::tetAR ΔsspB::aadA Δfur::hyg pZIK197		This study
KR4179	ΔlpxC::tetAR ΔsspB::aadA Δfur::hyg pXCERN-2		This study
KR4180	ΔctpA::tetAR ΔsspB::aadA ΔCCNA_03733::hyg pZIK174		This study
KR4181	ΔctpA::tetAR ΔsspB::aadA ΔCCNA_03733::hyg pXCERN-2		This study
KR4182	ΔctpA::tetAR ΔsspB::aadA ΔCCNA_00497::hyg pZIK172		This study
KR4183	ΔctpA::tetAR ΔsspB::aadA ΔCCNA_00497::hyg pXCERN-2		This study
KR4148	ΔlpxC::tetAR ΔsspB::aadA Δfur::hyg pZIK133		This study
	Plasmid re-introduced for complementation		-
KR4149	ΔlpxC::tetAR ΔsspB::aadA Δfur::hyg pJS14		This study
KR4150	ΔctpA::tetAR ΔsspB::aadA ΔCCNA_03733::hyg pAB6		This study
	Plasmid re-introduced for complementation		
KR4151	ΔctpA::tetAR ΔsspB::aadA ΔCCNA_03733::hyg pJS14		This study
KR4264	NA1000 pZIK200		This study
KR4147	NA1000 pZIK171		This study
KR4170	NA1000 pZIK179		This study
KR4489	ΔCCNA_01217		This study
KR4549	ΔCCNA_01217 vanA::01217::FLAG	pKR438 integrated	This study
KR4450	ΔCCNA_01218		This study
KR4505	ΔCCNA_01218 vanA::01218::FLAG	pKR435 integrated	This study
KR4430	ΔCCNA_01219		This study
KR4501	ΔCCNA_01219 vanA::01219::FLAG	pKR436 integrated	This study
EK720	ΔCCNA_01220 also known as KR4431		(Stankeviciute
			et al., 2019)
KR4530	ΔCCNA_01220 vanA::01220::FLAG	pKR437 integrated	This study
KR4517	Δfur::hyg ΔsspB::aadA ΔCCNA_01217		This study
KR4551	Δfur::hyg ΔsspB::aadA ΔCCNA_01217 vanA::01217::FLAG	pKR438 integrated	This study
KR4442	Δfur::hyg ΔsspB::aadA ΔCCNA_01218		This study
KR4503	Δfur::hyg ΔsspB::aadA ΔCCNA_01218 vanA::01218::FLAG	pKR435 integrated	This study
KR4438	Δfur::hyg ΔsspB::aadA ΔCCNA_01219		This study
KR4513	Δfur::hyg ΔsspB::aadA ΔCCNA_01219 vanA::01219::FLAG	pKR436 integrated	This study
KR4439	Δfur::hyg ΔsspB::aadA ΔCCNA_01220		This study
KR4532	Δfur::hyg ΔsspB::aadA ΔCCNA_01220 vanA::01220::FLAG	pKR437 integrated	This study
KR4509	ΔlpxC::tetAR ΔsspB::aadA Δfur::hyg ΔCCNA_01217		This study
	pZIK133		

KR4555	ΔlpxC::tetAR ΔsspB::aadA Δfur::hyg ΔCCNA_01217 vanA::01217::FLAG pZIK133	pKR438 integrated	This study
KR4451	ΔlpxC::tetAR ΔsspB::aadA Δfur::hyg ΔCCNA_01218 pZlK133		This study
KR4527	ΔlpxC::tetAR ΔsspB::aadA Δfur::hyg ΔCCNA_01218 vanA::01218::FLAG pZIK133	pKR435 integrated	This study
KR4441	ΔlpxC::tetAR ΔsspB::aadA Δfur::hyg ΔCCNA_01220 pZIK133		This study
KR4545	ΔlpxC::tetAR ΔsspB::aadA Δfur::hyg ΔCCNA_01220 vanA::01220::FLAG pZIK133	pKR437 integrated	This study
KR4205	ΔctpA::tetAR ΔsspB::aadA suppressor isolate #3	SAMN11107060	This study
KR4206	ΔctpA::tetAR ΔsspB::aadA suppressor isolate #8	SAMN11107061	This study
KR4207	ΔctpA::tetAR ΔsspB::aadA suppressor isolate #16	SAMN11107062	This study
KR4208	ΔctpA::tetAR ΔsspB::aadA suppressor isolate #21	SAMN11107063	This study
KR4209	ΔctpA::tetAR ΔsspB::aadA suppressor isolate #32	SAMN11107064	This study
KR4210	ΔctpA::tetAR ΔsspB::aadA suppressor isolate #36	SAMN11107065	This study
KR4211	ΔctpA::tetAR ΔsspB::aadA suppressor isolate #38	SAMN11107066	This study
KR4212	ΔctpA::tetAR ΔsspB::aadA suppressor isolate #40	SAMN11107067	This study
KR4213	ΔctpA::tetAR ΔsspB::aadA suppressor isolate #43	SAMN11107068	This study
KR4214	ΔctpA::tetAR ΔsspB::aadA suppressor isolate #44	SAMN11107069	This study
KR4215	ΔctpA::tetAR ΔsspB::aadA suppressor isolate #47	SAMN11107070	This study
KR4216	ΔctpA::tetAR ΔsspB::aadA suppressor isolate #52	SAMN11107071	This study
KR4217	ΔctpA::tetAR ΔsspB::aadA suppressor isolate #53	SAMN11107072	This study
KR4218	ΔctpA::tetAR ΔsspB::aadA suppressor isolate #54	SAMN11107073	This study
KR4219	ΔctpA::tetAR ΔsspB::aadA suppressor isolate #57	SAMN11107074	This study
KR4220	ΔctpA::tetAR ΔsspB::aadA suppressor isolate #111	SAMN11107075	This study
KR4221	ΔctpA::tetAR ΔsspB::aadA suppressor isolate #112	SAMN11107076	This study
KR4224	ΔlpxC::tetAR ΔsspB::aadA suppressor isolate #1	SAMN11107077	This study
KR4225	ΔlpxC::tetAR ΔsspB::aadA suppressor isolate #5	SAMN11107078	This study

<sup>&</sup>lt;sup>a</sup> For all strains designated "suppressor isolate," additional genotype information is available in Table S1 or Table S2.

<sup>&</sup>lt;sup>b</sup>BioSample Accession numbers refer to genome resequencing data for the indicated strains in the Sequence Read Archive at <a href="https://www.ncbi.nlm.nih.gov/sra">https://www.ncbi.nlm.nih.gov/sra</a>, under BioProject ID PRJNA526705

Table S7, related to STAR Methods: Plasmids used in this study.

Name	Description	Reference
pJS14	Broad host range cloning vector; high copy; chlor <sup>R</sup> ; pBBR1MCS derivative	(J. Skerker,
	with unique EcoRI site	unpublished)
pNPTS138	kan <sup>R</sup> ; sacB-containing integration vector	(M.R. Alley,
		unpublished)
pXCERN-2	For integration at P <sub>xy/X</sub> ; encodes xylose-inducible <i>cerulean</i> that can be	(Thanbichler et
	exhcanged for gene of interest; kan <sup>R</sup>	al., 2007)
pMCS-2	For integration at locus specified by insert sequence; kan <sup>R</sup>	(Thanbichler et
		al., 2007)
pAB6	pJS14-P <sub>xy/x</sub> -ctpA-3xFLAG-ssrA	(Shapland et
		al., 2011)
pZIK133	pJS14-P <sub>xy/x</sub> -lpxC-3xFLAG-ssrA	This study
pZIK172	pXCERN-2-P <sub>xylX</sub> -CCNA_00497	This study
pZIK173	pXCERN-2-P <sub>xylX</sub> -CCNA_01553	This study
pZIK174	pXCERN-2-P <sub>xy/X</sub> -CCNA_03733	This study
pZIK175	pXCERN-2-P <sub>xy/X</sub> -CCNA_00055 (fur)	This study
pZIK78	pNPTS138-CCNA_00497::hyg; for replacing CCNA_00497 with	This study
	hygromycin resistance cassette	
pZIK82	pNPTS138-CCNA_01055::hyg; for replacing CCNA_01055 with	This study
	hygromycin resistance cassette	
pZIK81	pNPTS138-CCNA_01068::hyg; for replacing CCNA_01068 with	This study
	hygromycin resistance cassette	
pZIK73	pNPTS138-CCNA_01553::hyg; for replacing CCNA_01553 with	This study
	hygromycin resistance cassette	
pZIK80	pNPTS138-CCNA_03733::hyg; for replacing CCNA_03733 with	This study
	hygromycin resistance cassette	
pZIK161	pNPTS138-CCNA_00055::hyg; for replacing fur with hygromycin resistance	This study
	cassette	
pZIK134	pNPTS138-CCNA_02064::tetAR; for replacing lpxC with tetracycline	This study
	resistance cassette	
pHP45Ω-hyg	For isolating <i>hyg</i> fragment; hyg <sup>R</sup> ; amp <sup>R</sup>	(Blondelet-
		Rouault et al.,
		1997)
pKOC3	Contains <i>tetAR</i> flanked by EcoRI sites; amp <sup>R</sup> ; tet <sup>R</sup>	(Skerker et al.,
		2005)
pVMCS-4	For amplification of <i>aacC1</i> ; gent <sup>R</sup>	(Thanbichler et
		al., 2007)
pMCS-4	For single integration to disrupt genomic loci; gent <sup>R</sup>	(Thanbichler et
		al., 2007)
pVGFPC-2	Complementation vector for expressing target genes from <i>vanA</i> locus; kan <sup>R</sup>	(Thanbichler et
		al., 2007)

pVGFPC-4	Complementation vector for expressing target genes from <i>vanA</i> locus;	(Thanbichler et
	gent <sup>R</sup>	al., 2007)
pVCHYC-5	Complementation vector for expressing target genes from <i>vanA</i> locus; tet <sup>R</sup>	(Thanbichler et
		al., 2007)
pFLGC-1	Vector for adding FLAG tag to the C-terminus of open reading frames;	(Thanbichler et
	spec <sup>R</sup>	al., 2007)
pGS74	pNPTS138-based plasmid for markerless deletion of CCNA_01217	This study
pEK406	pVCHYC-5-based complementing vector, vanA::CCNA_01217-FLAG	This study
pKR438	pVGFPC-4-based complementing vector, vanA::CCNA_01217-FLAG	This study
pKR429	pNPTS138-based plasmid for markerless deletion of CCNA_01218	This study
pKR432	CCNA_01218::FLAG in pFLGC-1	This study
pKR435	pVGFPC-2-based complementation vector, vanA::CCNA_01218-FLAG	This study
pGS76	pNPTS138-based plasmid for markerless deletion of CCNA_01219	This study
pKR433	CCNA_01219::FLAG in pFLGC-1	This study
pKR436	pVGFPC-2-based complementation vector, vanA::CCNA_01219-FLAG	This study
pEK722	pNPTS138-based plasmid for markerless deletion of CCNA_01220	(Stankeviciute
		et al., 2019)
pKR434	CCNA_01220::FLAG in pFLGC-1	This study
pKR437	pVGFPC-2-based complementation vector, vanA::CCNA-01220-FLAG	This study
pKR438	pVGFPC-4-based complementation vector, vanA::CCNA-01217-FLAG	This study

Table S8, related to STAR Methods: Primers used in this study.

Name	Sequence (5'-3')
pJS14-PxylX	AGAACTAGTGGATCCTCACATGGTCTCGAA
PxylX-lpxC R	ACCCGAAGCCGACACGGCGTCGTCTCCCCA
PxylX-lpxC F	TGGGGAGACGCCGTGTCGGCTTCGGGT
lpxC-3xFLAG R	GTAGTCCATGGATCCAACCGCTTCTGCAAG
lpxC-3xFLAG F	CTTGCAGAAGCGGTTGGATCCATGGACTAC
ssrA-pJS14	CTTGATATCGAATTCTCACGCAGCGACGGC
pVCERN-2 00497 F	ACGCATATGAACAGCATTCTCCCG
pVCERN-2 00497 R	CCGGAGCTCCTAGATCGGCCGGCC
pVCERN-2 01553 F	ACGCATATGAAGCGTATGTTTGAT
pVCERN-2 01553 R	CCGGAGCTCCTAACGGGTGACGCC
pVCERN-2 03733 F	ACGCATATGGCTGCGATCTATCCG
pVCERN-2 03733 R	CCGGAGCTCTCAACGCGGCTTCGT
Pvan-fur	GAGGAAACGCATATGGATCGACTCGAAAAG
fur-pVCERN	AATTCTCCGGAGCTCTTACTCCTCCAGCGG
3xFLAG-F	cgccggcggatccatggactacaaag
3xFLAG-JS14	CTTGATATCGAATTCTCACTTGTCATCGTCATC
00497::hyg UpF	CTCACTAGTAGGACGCCCATA
00497::hyg UpR	ATCCCCGGGGCAAGGGTCGAGAC
00497::hyg DownF	ATCCCCGGGCGCCCGCTGTGG
00497::hyg DownR	AGCGAATTCACCGAGGATTTGGTT
01055::hyg UpF	CTCACTAGTGCTGGCAAGA
01055::hyg UpR	ACCGGATCCTTGAGCGCCATGGGC
01055::hyg DownF	ACCGGATCCGATGGACGAGCGCAG
01055::hyg DownR	AGCGAATTCTACGATGACGAGTCG
01068::hyg UpF	CTCACTAGTGCGCGAGGACACCGT
01068::hyg UpR	ACCGGATCCGACGCCTGGGTGGCG
01068::hyg DownF	ACCGGATCCCAGGCGCCCATAT
01068::hyg DownR	AGCGAATTCTTGACCTGCTTGAGC
01553 UpF	AAAACTAGTATCGAGCAGGGCGTC
01553 UpR	GGCCCCGGGATCAAACATACGCTT
01553 DownF	ATCCCCGGGCCGGTGCTGACCGCA
01553 DownR	AAAGAATTCTATGCCGCCAAGCT
03733::hyg UpF	CTCACTAGTGACGCTGGCCCTTGT
03733::hyg UpR	ACCGGATCCGAAGGCGTGATCGAG

03733::hyg DownF	ACCGGATCCGCCACACAGGAT
03733::hyg DownR	AGCGAATTCATGCTCAAGGACCTC
fur UpF	CTCACTAGTAAGAGGGTGACCTCG
fur UpR	ACCGGATCCGAGCTCTACGGGATG
fur DownF	ACCGGATCCTTCGATACAGGCCTT
fur DownR	AGCGAATTCTATATGCAGGCCTTC
lpxC KO F	CTTCGAAACGCCGATGATG
lpxC KO R	GATCAACACGCCGATGACG
lpxC UpF	CTCACTAGTTCAGATAGGCTTCGA
lpxC UpR	CATGAATTCCTCAATAACGCCGTG
lpxC DownF	CTTGAATTCCGTGTGCTGAAAATA
lpxC DownR	GACGCATGCTGGCCGCAAGCCGCG
aacC1 EcoRI F	CGCGAATTCgaattgacataagcc
aacC1 EcoRI R	GGGGAATTCgaattggccgcggcg
ctpA KO F	GAAGAAGCGCGGGATCAAGA
ctpA KO R	GTTGCCATGCTTGATGTGCA
EK897	AAGCTTGGCGCCAGCCGG
EK898	GAATTCGCTAGCTTCGGC
EK1047	gctggcgccaagcttAGGCGCTCGATCTGATCTTG
EK1048	caggaagatCGGCCCTTTTTGAACTTCAC
EK1049	aagggccgATCTTCCTGGCCCTCTTC
EK1050	cgaagctagcgaattcCTTGATCGTCGGGTTCTC
EK1055	gctggcgccaagcttGGCTTCTTCCACAACTTTG
EK1056	accttgagGAGGACCCCGGACATATC
EK1057	gggtcctcCTCAAGGTCTGGAGAGAG
EK1058	cgaagctagcgaattcCGTCATCTGTCGTCCCTAC
01218 up_fwd	attgaagccggctggcgccaTGGCACGGCCATTTCGGC
01218 up_rev	tgagcccaaaGCCGTCGATCACCAGCAAG
01218 down_fwd	gatcgacggcTTTGGGCTCAAGCCGTTCG
01218 down_rev	cgtcacggccgaagctagcgGCCGTTCGACAAGCCGCG
EK1357	tactcatATGAGTAGTGAAGTTCAAAAAGGGCCG
EK1358	tactgctagcTTActtgtcatcgtcatccttgtagtcTTTCGCCAGCCAGGACTGG
EK S216	ACCCCGTCTGATAAGGCTTC
EK S217	GCGAGACCGTGATCGACT
EK S238	GTAGGCAGGGTCCGACAGT
EK S239	ACCGCAAAGTTGTGGAAGAA

EK S240	ATGACCTTCCTCGACACG			
EK S241	GAGTCGATCACGGTCTCG			
EK S242	AGGGCTTCTTTGGCATT			
EK S243	ACTTCATCGTCGGCACCTT			
RecUni-1	ATGCCGTTTGTGATGGCTTCCATGTCC	3		
RecVan-2	CAGCCTTGGCCACGGTTTCGGTACC			
Nde-01218	TATATTCATATGCTTCGTCGTGCACGC	CATCC		
01218-Mlu	ATTATACGCGTTCCGACCAGGAACCG	CAAGGC		
Nde-01219	TATATTCATATGAGCCGCCTGCGCGG	ССТС		
01219-Mlu	TAATAACGCGTTGCGGCTTGCCGCCG	СТСТС		
Nde-01220	TATATTCATATGGGGCTATTTGATAAG	CACCTGGCC		
01220-Mlu	AATAACGCGTGGCGCGCGCTTGAG			
01217-FLAG F	CCACGATGCGAGGAAACGCATATGAGTAGTGAAGTTCAAAAAG			
01217-FLAG R	AATTAAGGCGCCTGCAGGCAGCTAGC	TCACTTGTCATC		
01218-FLAG F	CCACGATGCGAGGAAACGCATATGCTTCGTCGTGCACG			
01218-FLAG R	AATTAAGGCGCCTGCAGGCAGCTAGCTTACTTGTCATCGTC			
01219-FLAG F	CCACGATGCGAGGAAACGCATATGAGCCGCCTGCGCGG			
01219-FLAG R	AATTAAGGCGCCTGCAGGCAGCTAGCTTACTTGTCATCGTCATCCTTGTAG			
01220-FLAG F	CCACGATGCGAGGAAACGCATATGGGGCTATTTGATAAG			
01220-FLAG R	AATTAAGGCGCCTGCAGGCAGCTAGCTTACTTGTCATC			
The following prime	The following primer pairs were used for qRT-PCR analyses of the indicated genes.			
Gene	Forward primer (5'-3')  Reverse primer (5'-3')			
CCNA_03142 rpoD	CTCTATGCGATCAACAAGCG	ATAGGCCTTGAGGAACTCGC		
CCNA 03372 bfd	GTCTGCAACTGTAACGGCATC	CAGCCCTTGTGACGGAAG		
CCNA_00793 sgt1	AGCCTTTGTCAGGACCAGAA	CACCACCTCGTCGAGAATTT		
CCNA _00792 sgt2	CCACGAGCTGTTCGTCATC	TGTAGTAGTTGGCGTCAAACG		
CCNA _01217 cpgA	GTCACCTTCATCGGCTTTGT	CGAGGAAGGTCATGATCCAG		
CCNA _01218 cpgB	GAGAGAACCCGACGATCAAG	CAGGTTGGTGGCCTTCAC		
CCNA _01219 cpgC	CCGGGGTCCTCGACTACTAC	CCGTGCTCAAACTCGTGATA		
CCNA _02064 lpxC	TTGTTGATCACCGTGCCGAG	CCGACATGGGGATCGTCTTT		